133p.

SUMMARY REPORT
RESEARCH AND DEVELOPMENT OF S-1C HEAT SHIELD HONEYCOMB PANELS

ER-764

For

GEORGE C. MARSHALL SPACE FLIGHT CENTER
HUNTSVILLE, ALABAMA

CNASA Contract No. NAS8-5221
Request No. TP-385154

Period of Performance January 29, 1963 to January 29, 1964, Inclusive

Submitted by:

AERONCA MANUFACTURING CORPORATION
MIDDLETOWN, OHIO

00 48 512

Prepared by:

DONALD Y. POTTER and
GEORGE W. SOMERS

28 Jan 1964 133p rezer

MSFC Technical Supervisor
James O. Lysaght

January 28, 1964

ABSTRACT

17765

A

This report describes the work accomplished on Research and Development of S-1C Heat Shield Panels utilizing brazed stainless steel honeycomb sandwich construction for the period January 29, 1963, to January 29, 1964, inclusive.

The principal effort in this program was the stress, thermal and design analysis of two S-1C heat shield panel designs which differed by virtue of the panel mounting system. As a consequence of this analytical study and the NASA S-1C Heat Shield Panel Tests conducted at Wylie Laboratories, either panel design appears to satisfy the S-1C requirements provided the M-31 insulation is retained on the panel by deformation of the honeycomb insulation reinforcement.

Additional items investigated include:

1. Application of Beryllium Sheet to S-1C Heat Shield Panels.
2. Deflection Characteristics of M-31 Insulation with Deformed Stainless Steel Honeycomb Reinforcement.
3. Analysis of Braze Defects, Braze Quality Standards and Repair Methods.
4. Analysis of Holes in Heat Shield Panels and Experimental Measurements of Stresses at Hole Boundaries.
5. Design Recommendations for Heat Shield Panels.

AUTHOR

TABLE OF CONTENTS

LIST OF TABLES

LIST OF TABLES (Cont'd)

LIST OF ILLUSTRATIONS

LIST OF ILLUSTRATIONS (Cont'd)

LIST OF ILLUSTRATIONS (Cont'd)

LIST OF ILLUSTRATIONS (Cont'd)

SECTION I

TRANSIENT THERMAL ANALYSIS

FOR S-1C HEAT SHIELD PANELS

Introduction

Presented in this section are the transient heat transfer analyses of the Saturn base heat shield panel for design drawing Nos. 30M12571 and SK 60B-20001 and shown in Figure 1, page 2. All analyses are three dimensional in nature and are based on heating rates and surface temperatures derived from NASA Huntsville data*. Included are the maximum temperature profiles of the edge attachment schemes for the two panel designs. The temperature profiles presented are for the condition of 100% brazing alloy node flow in the honeycomb support structure. All other assumptions and ground rules which govern the analysis are presented in "Methods of Analysis".

In addition to the thermal analyses of the two panel concepts, a set of parametric curves is presented illustrating the temperature differentials across the honeycomb support structure as a function of brazing node flow size, cell dimensions and M-31 reinforcement honeycomb dimensions. While these parametric studies are confined to the dimensions bounded for the most part by the dimensions of the panel considered, they do present the possible trade-offs that could be considered for possible panel design optimization from thermal considerations.

Methods of Analysis

Aeronca has developed a digital computer program which has general applicability to thermal analysis of high temperature structures. For purposes of analysis the structure is represented by a set of spatially distributed points or nodes. The temperature of each node is determined by solving the generalized heat balance equation in finite difference form:

$$T_j' - T_j = \frac{\Delta\tau}{\rho V C_p} \left[\dot{Q}_j''' + \dot{Q}_j'' - \sum_{i=1}^{n} U_{ij} (T_j' - T_j) \right] \qquad (1)$$

T_j' and T_j represent the temperatures at the end and beginning of the time step, respectively. The parameters $\dot{Q}_j'''$ and $\dot{Q}_j''$ represent volumetric heating and incident surface flux, respectively. U_{ij} is the thermal conductance between the adjacent nodes i and j. The program does an iteration for T' and re-evaluates temperature dependent functions (radiation coefficient, etc.) on the temperature at the midpoint of the time step. This is the so-called Implicit Method.

*MSFC Memorandum, "Estimated Temperatures for S-1C Heat Shield Attachment", dated 2/11/63, M-P&VE PH 26-63. See Figure 2.

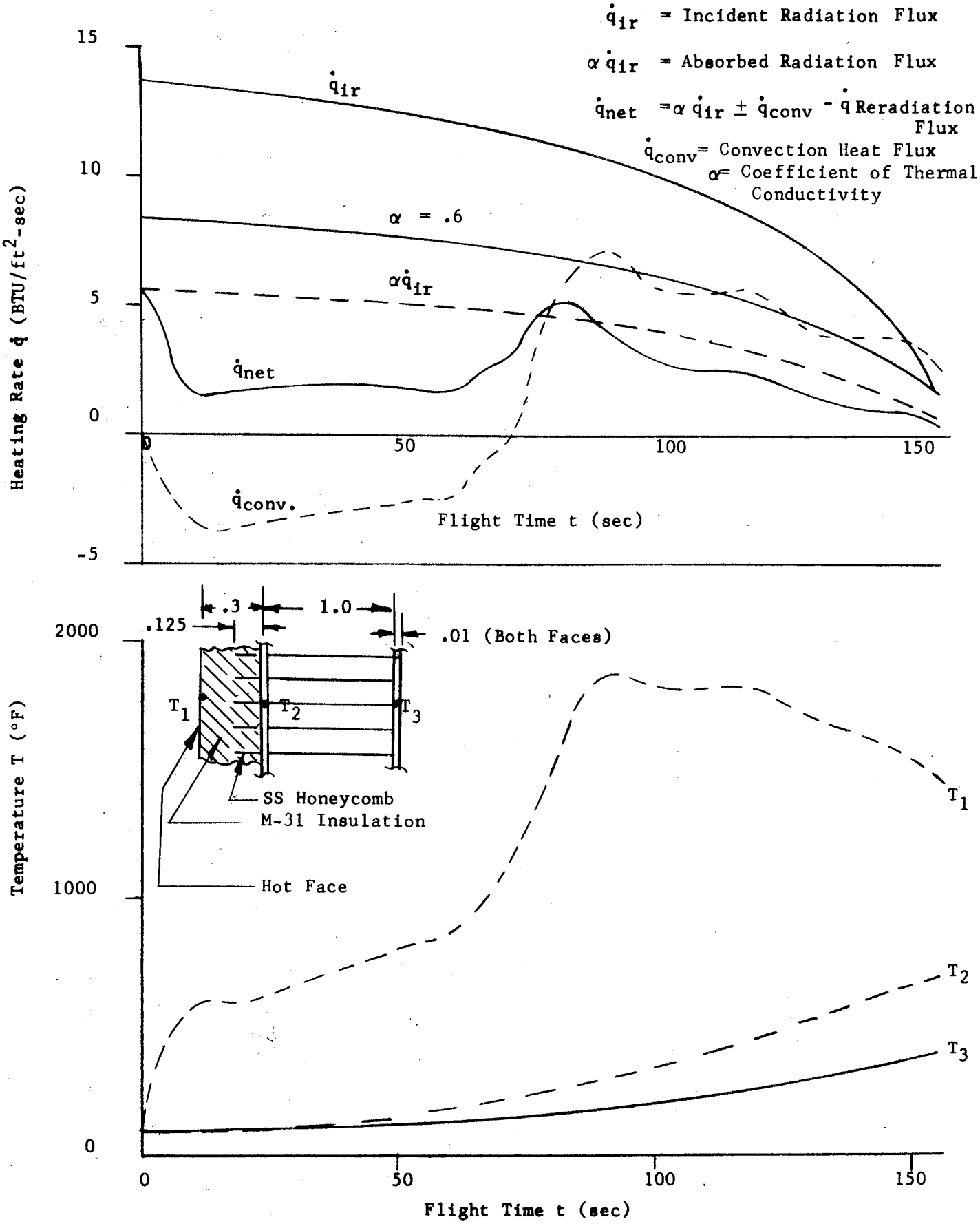

Figure 1 Typical S-1C Heat Shield Heating Rates & Surface Temperature As a Function of Flight Time (NASA supplied data 2-11-63)

The program can use the Explicit Method, in which T_j' and T_j are the same as in the Implicit Method. The heat balance equation will become explicit in T_j'

$$T_j' - T_j = \frac{\Delta\tau}{\rho V C_p} \left[\dot{Q}_j''' + \dot{Q}_j'' - \sum_{i=1}^{n} U_{ij} (T_j - T_i) \right] \qquad (2)$$

There is now a limit on the length of time step $\Delta\tau$ which the program calculates and is given by $\Delta\tau = \rho V C_p / U_{ij}$ and taken so that the expression $\rho V C_p / U_{ij}$ is a minimum for the entire nodal system. Here, n is the total number of thermal connections.

The expression used to evaluate zero-volume nodes (surface) and steady-state calculations is

$$\sum_{i=1}^{n} U_{ij} (T_j - T_i) - \dot{Q}_j''' - \dot{Q}_j'' = 0 \qquad (3)$$

The parameters $\dot{Q}_j'''$ and $\dot{Q}_j''$ are the same as defined previously.

The thermal conductance term, U_{ij}, is used in three basic forms: (1) solid to solid conduction, with contact coefficient; (2) solid to solid radiation, with radiation coefficient; and (3) solid to fluid, with conduction and film coefficient.

There are several important features in this computer program. The amount of data necessary to run a problem is quite large and would include such things as: (1) time, boundary temperature tables; (2) time, rate tables; (3) Nusselt number correlation tables; (4) material property tables; (5) node description data for each node; and (6) connection data for each node. Although a large amount of input data is necessary, the engineer requires little or no knowledge of computer programming or techniques to use the program. Use of stacked storage is employed rather than the bulkier reserved storage, so that problems with greater than 1000 nodes can be run.

The program is divided into five chains: Chain 1 accepts data in a form which is easy for the user to prepare and stores it for further processing--in other words, Chain 1 is just to input the problem; Chain 2 processes data from Chain 1 into a form which the program can use; Chain 3 takes this processed data and performs the computation of Equations (1) or (2); Chain 4 is an editing chain which will (1) give a time-temperature history if requested, and (2) if the run is pulled for time, punch the current temperature distribution or decimal cards so that the run can be restarted; Chain 5 sets up change cases. A more detailed description of the program is presented in Ref. 1*.

*Ref. 1 - Niehaus, W. R., Criss, R., Cannizzaro, R., "A Transient Heat Transfer Computer Analysis for Space Vehicle Application", Aeronca Manufacturing Corporation, ER-638, February 1963.

A second method of heat transfer which was employed was to assemble "n" heat balance equations, one for each temperature point in the panel and for given time intervals and time dependent boundary conditions use the Gauss-Seidel iteration method to determine the unknown temperatures.

This process is repeated for each time interval until the desired transient analysis is complete.

The general form of the heat balance equation for one point in the panel for a single time interval is given below.

Thermal Storage = Convection + Conduction +

$$\frac{\rho VC}{\Delta \mathcal{T}} (T-T') = \sum_{n=1}^{6} \frac{A_n}{\frac{\Delta X_n}{K} + \frac{\Delta X_n}{K_h} + \frac{1}{h_n} + \frac{1}{h_c}} (T_n - T) +$$

Fluid flow input +

$(W_t/W)WC\ (T_n-T)$ +

Surface Flux +

$A_h \dot{Q}_F$ +

Solid Radiation +

$$\sum_{h=1}^{3} \sum_{i=1}^{3} \sigma A_h F_i \epsilon_1 \epsilon_2 \left[T_h^4 - T'^4\right]$$

Basically, the transient analysis was one of using the finite difference technique of dividing the panel geometry into a three-dimensional network of nodes. Each node had a finite volume enclosed by a maximum of six sides. Material properties and states were considered to be uniform within a given node and correspond to the temperature at the center of the node.

Design Point Analysis

Z-Type Edge Panel (Dwg. 30M12571):

The temperature histories at various levels throughout the panel are given in Figure 2 and are based on the effective thermal properties of the various layers as given in Table 1. The temperature histories at various points on the Z-type edge attachment are given in Figure 3.

Cup-Type Panel (Dwg. SK 60B20001):

The temperature histories at various levels throughout the panel are given in Figure 4 and are based on the effective thermal properties of the various layers given in Table 1.

The temperature histories at various points on the cup-type edge attachment are given in Figure 5.

Assumptions Made in the Preceding Analysis:

The following assumptions and/or ground rules were made and incorporated in the transient heat transfer analysis:

1. When composite layers existed in the heat shields (i.e., where parallel heat transfer paths exist), an effective thermal conductivity and density were used. The effective thermal conductivity is equal to the sum of the parallel conductances divided by the total panel heat flow area.

2. The temperature differential across the honeycomb support structure facings was considered small and the unit conductance (k/x) was substituted as a contact coefficient to account for thermal conductance through them. The volumetric heating was neglected.

3. Node flow was included in the thermal conductance of the honeycomb support panel. Two (2) braze nodes per honeycomb cell were considered having an effective cross sectional area equal to that of an equilateral triangle of side 0.010 inch. This dimension was based on measurements of the node flow width made from 30M12571 panel X-rays.

4. The cold face surface was adiabatic.

5. The radiation exchange and natural convection were both considered negligible in the honeycomb cells.

6. The contact coefficients between the panel edges and the attachment bolts were based on a nominal air gap of 0.001".

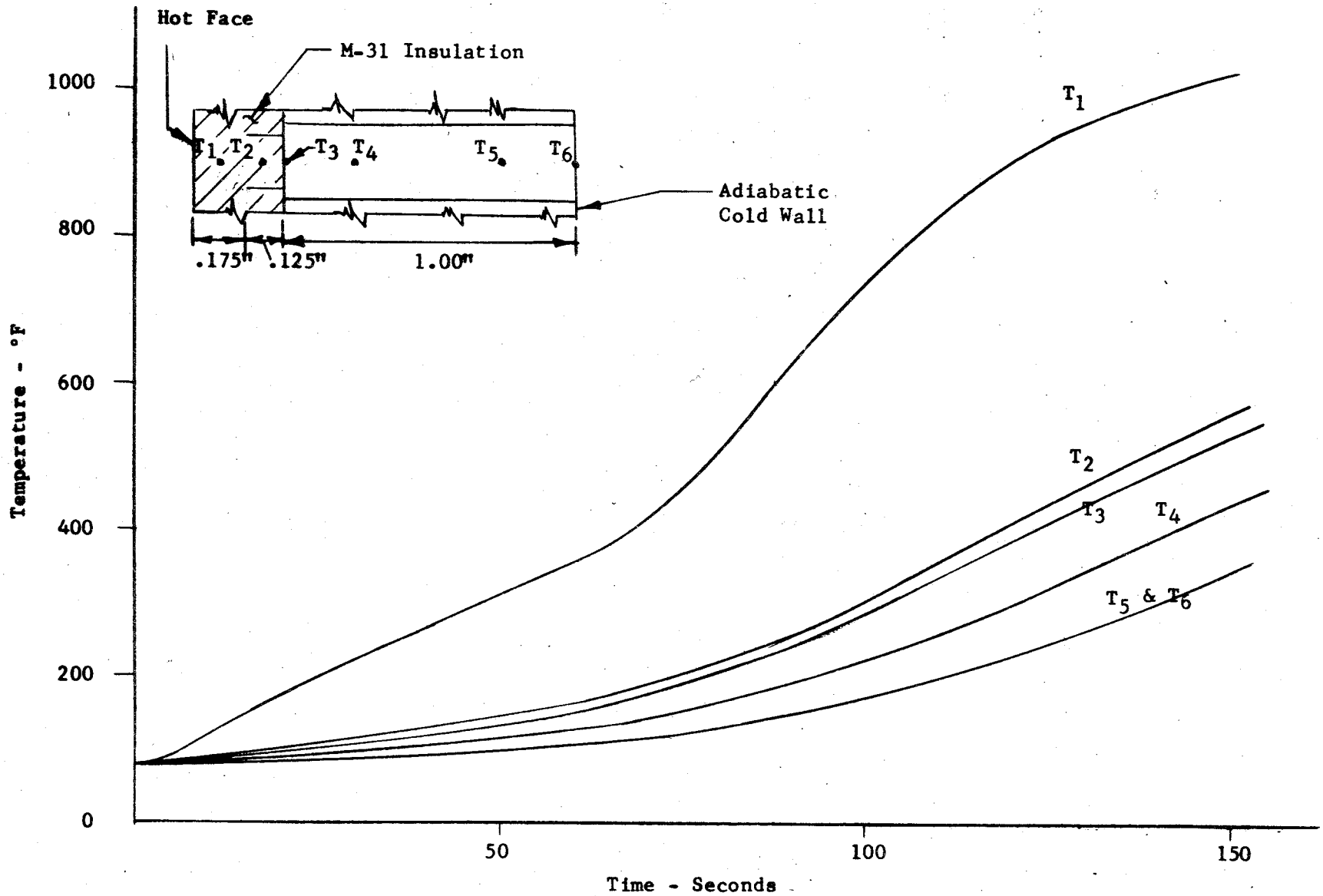

Figure 2 Temperature Profile for Heat Shield Panel 30M12571
100% Node Flow (.010 inch width)

TABLE 1

THERMAL ANALYSIS,
EFFECTIVE MATERIAL PROPERTIES
BASED ON HOMOGENEOUS LAYERS

	Material Layer	T-°F	$K_{Effective}$ BTU/Hr/Ft/°F	Specific Heat C_p BTU/#/°F	Density-ρ Lbs/Cu.Ft.
1.	Honeycomb Structure (4-15) Cell Size PH15-7Mo	0	.228	.11	7.19
		800	.265	.11	7.19
2.	M-31 Plus Honeycomb Support	0	.130	.31	50.1
		800	.152	.31	50.1
3.	M-31		.083	.31	47.0
		3000	.083	.31	47.0

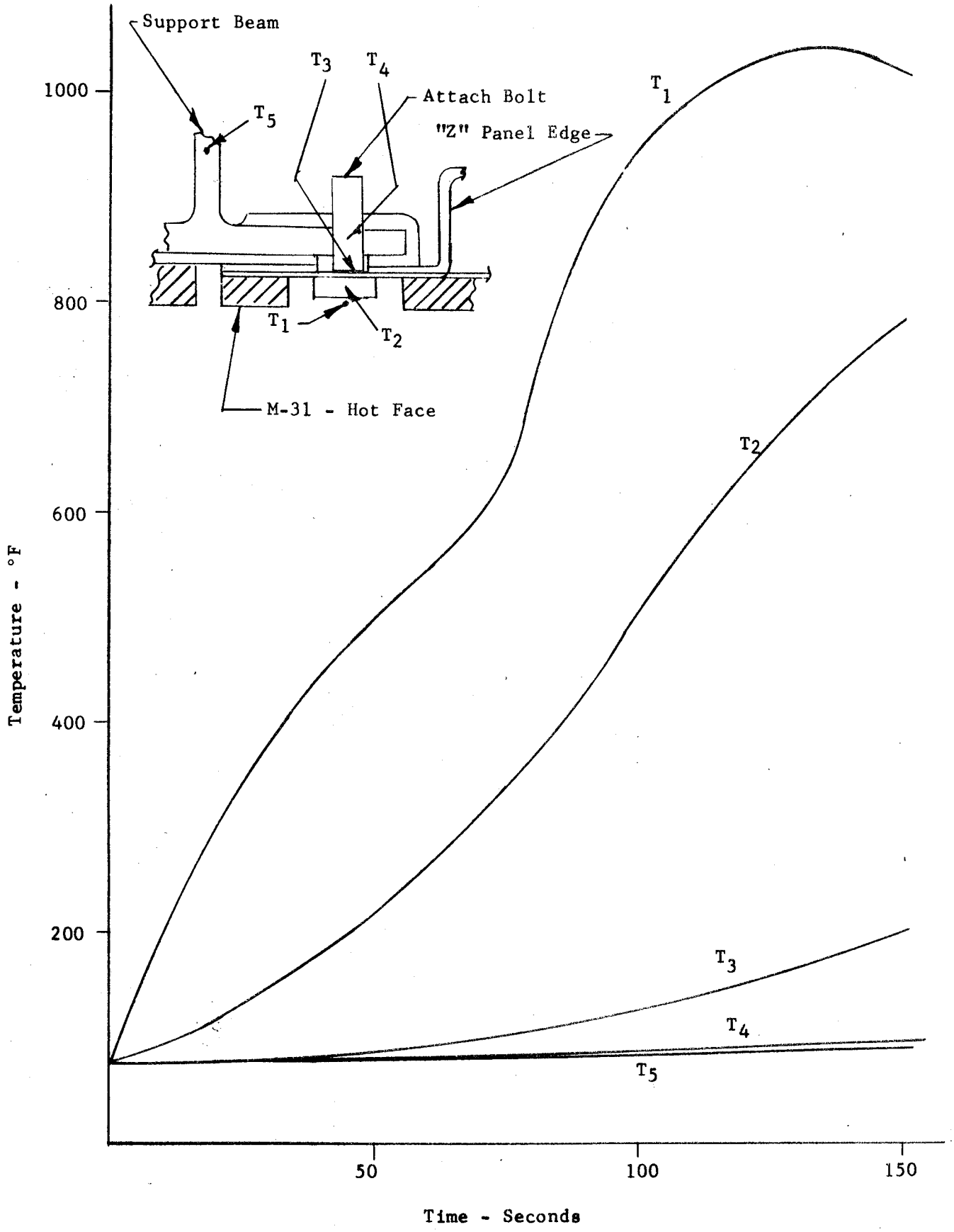

Figure 3 Temperature Profile - "Z" Type Panel Attachment Panel 30M12571

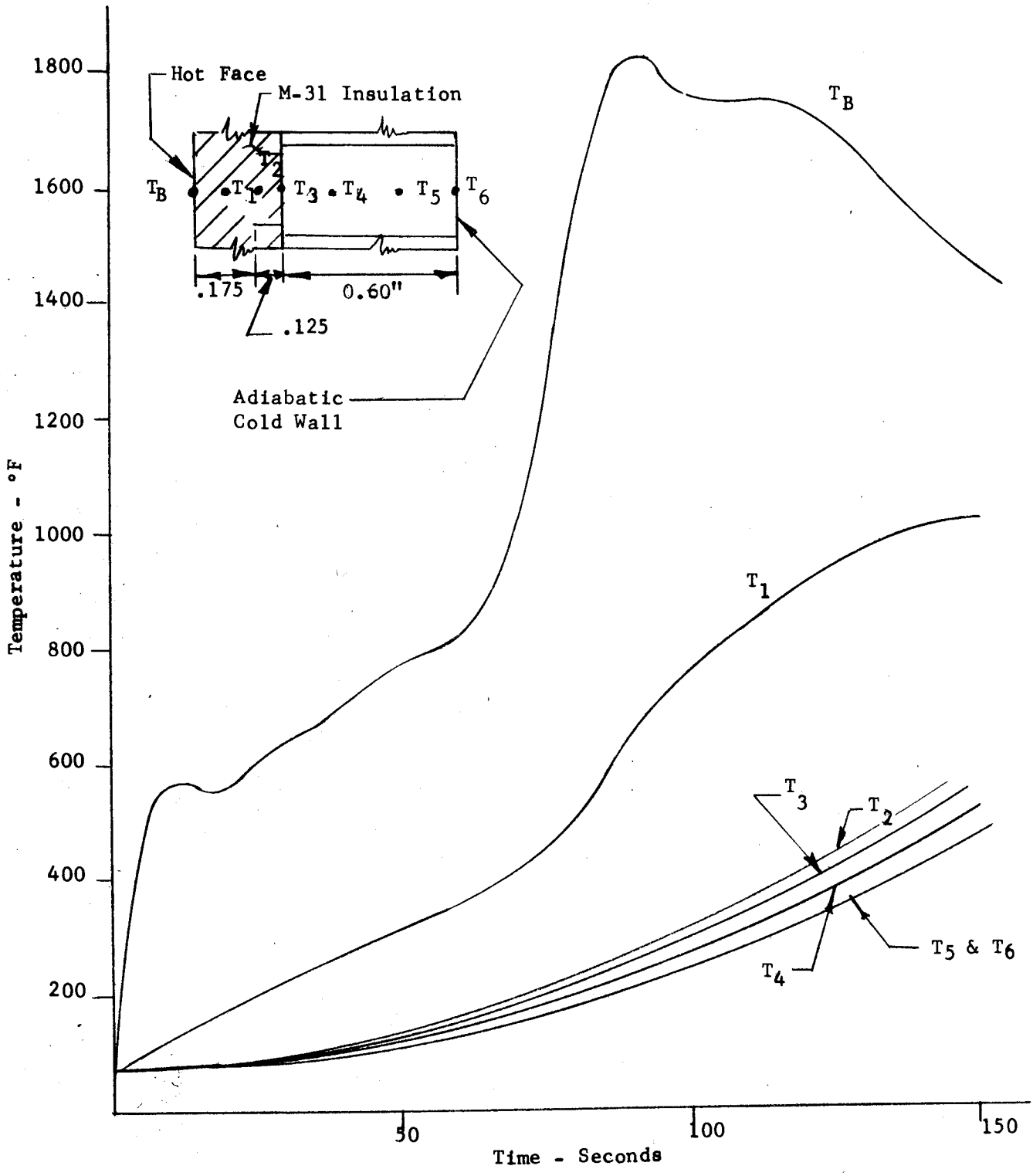

Figure 4 Temperature Profile for Heat Shield Panel SK 60B20001 with 100% Node Flow (.010 inch width)

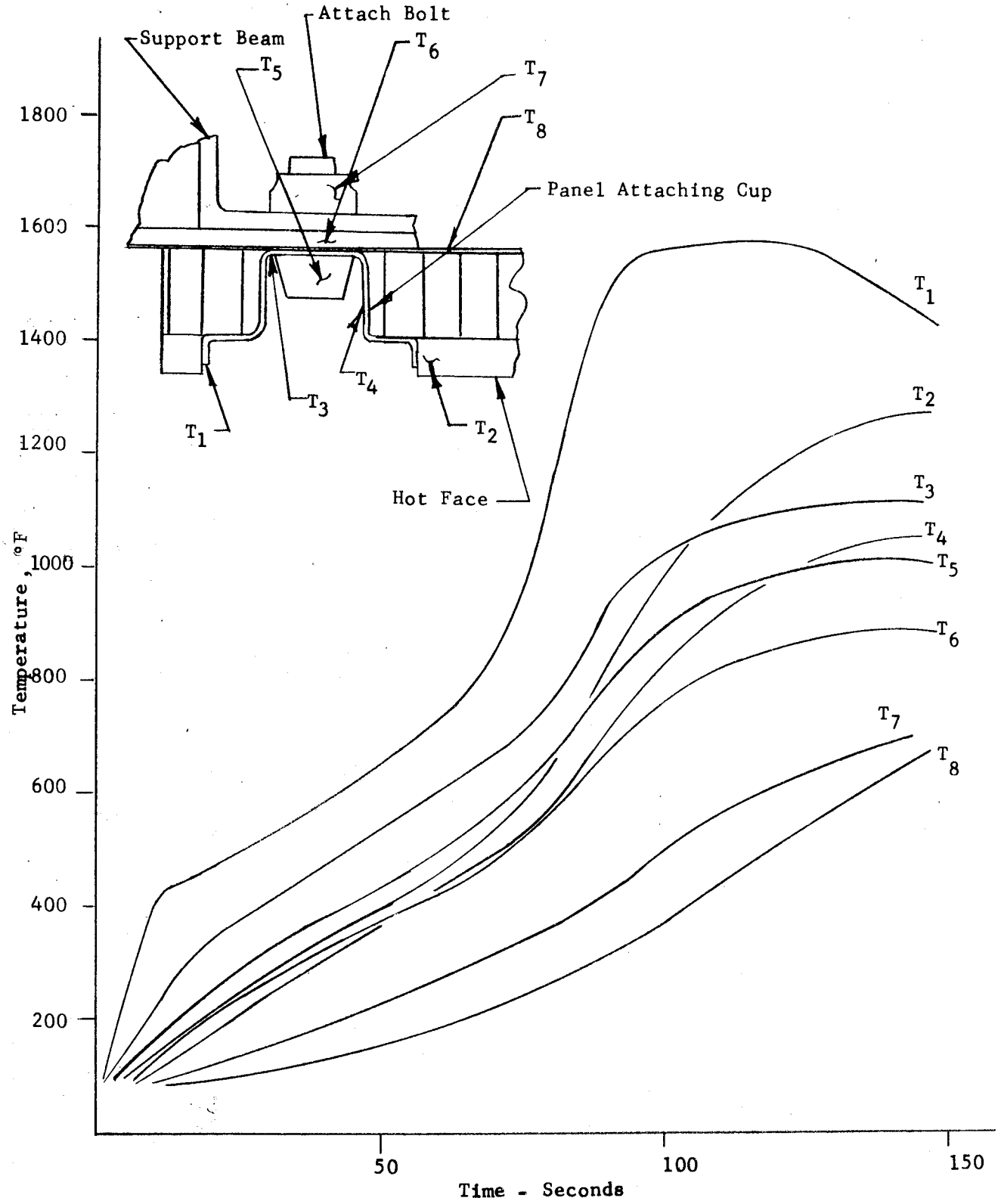

Figure 5 Temperature Profile - Cup-Type Panel Edge Attachment

Design Point Temperatures

The maximum temperature differentials to be used for design purposes across the brazed honeycomb sandwich panels are as follows:

Panel Configuration	Silver Braze Alloy Node Flow Condition	ΔT°F	Time Duration Seconds
SK60B20001 0.6" Thick Core	Complete--0.010" Width	80	155
30M12571 1.0" Thick Core	Zero	320	155
30M12571 1.0" Thick Core	Complete--0.005"	280	155
30M12571 1.0" Thick Core	Complete--0.010" Width	180	155

The beneficial effect of brazing alloy node flow in the load bearing honeycomb core, reducing the temperature difference and the resultant thermal stress, is shown for the 30M12571 heat shield panel design by the above data.

Parametric Analysis

As a result of the thermal analysis performed on the two heat shield panel concepts, a parametric analysis was made which considered the effects of node flow width, cell dimensions, and M-31 reinforcing honeycomb effects on the transient temperature differentials across the honeycomb support structure.

A careful review of the thermal analyses of honeycomb panels in the past has indicated that the presence of good node flow with the use of high thermal conductivity brazing alloy is the probable cause of the high rate of heat conductance through honeycomb panels.

The term "node flow" refers to the phenomenon of the formation of fillets of braze alloy which connect the panel faces, in the corners of the honeycomb core cells. Such metal "bridges" offer conduction paths between the panel faces which are orders of magnitude better than that in the air gap within the cells and which, at reasonably low temperature levels, transfer considerably more thermal energy between panel faces than is transferred by thermal radiation. If the thermal conductivity of the node-flow metal approaches that of silver, which is on the order of 20 times that of a high-nickel-content brazing alloy, the node-flow conductance path will be by far the dominating factor in the transmission of heat through the panel.

Reference 2* presents an analysis of sample test data wherein it is shown, on the basis of a reasonable set of assumptions, that of the total heat passing through the test panel, 5.2% was by radiation between the panel faces, 17.0% was by conduction through the core foil, and the remaining 77.8% was by conduction through the high-silver-content brazing alloy. While the exact magnitude of the numbers may be subject to some questions on the basis of the assumptions used in calculating them, the relative magnitudes are felt to be quite correct.

The parametric analyses presented here are intended to furnish in a limited way the trade-offs to be made in designing a heat shield panel from thermal considerations. The range of honeycomb cell dimension considered brackets the dimensions of the two design panels. As such the material discussed in this section and the feasible trade-offs that can be derived from the curves apply only in the neighborhood of the dimensions and environments of the previously mentioned design panels.

Node Flow Effect

Figures 6 to 8 show the effects of node flow width on the effective thermal conductivity of the honeycomb, the weight of the honeycomb panel, and the temperature differentials across the honeycomb panel.

Figure 6 shows that in doubling the cell width the effective conductivity of the panel is reduced by a factor of from 2 - 2½ for node flow widths of about 0.010". Also, it is evident that for a node flow width above 0.010" the effective conductivity increases rapidly. However, with this increase in thermal conductivity, which is desirable from a thermal stress standpoint, there is an increase in panel weight. Figure 7 shows the trade-off between effective honeycomb density and increase in effective conductivity as a function of cell width and node flow width. For a node flow width of 0.010", the per cent increase in density of a honeycomb having a 3-15 cell (.188" cell width, .0015" foil width) when such a braze node flow is added is 21% of the original density with no node flow. The per cent increase in thermal conductivity, however, is 118%. In values of density the increase would go from 8.3 to 10.03 lb/ft^3 while the conductivity would increase from .136 BTU/Hr-Ft-°F to .387 BTU/Hr-Ft-°F.

Figure 8 gives the effect of node flow width and cell width on the temperature differentials across a 1.0" thick honeycomb panel (Panel No. 30M12571). The temperature differential decreases with an increase in both cell width and node flow width. This is to be expected since an increase in either of these increases the effective thermal conductivity across the panel.

*Reference 2 - ASD-TR--7-845 (II) Page 367

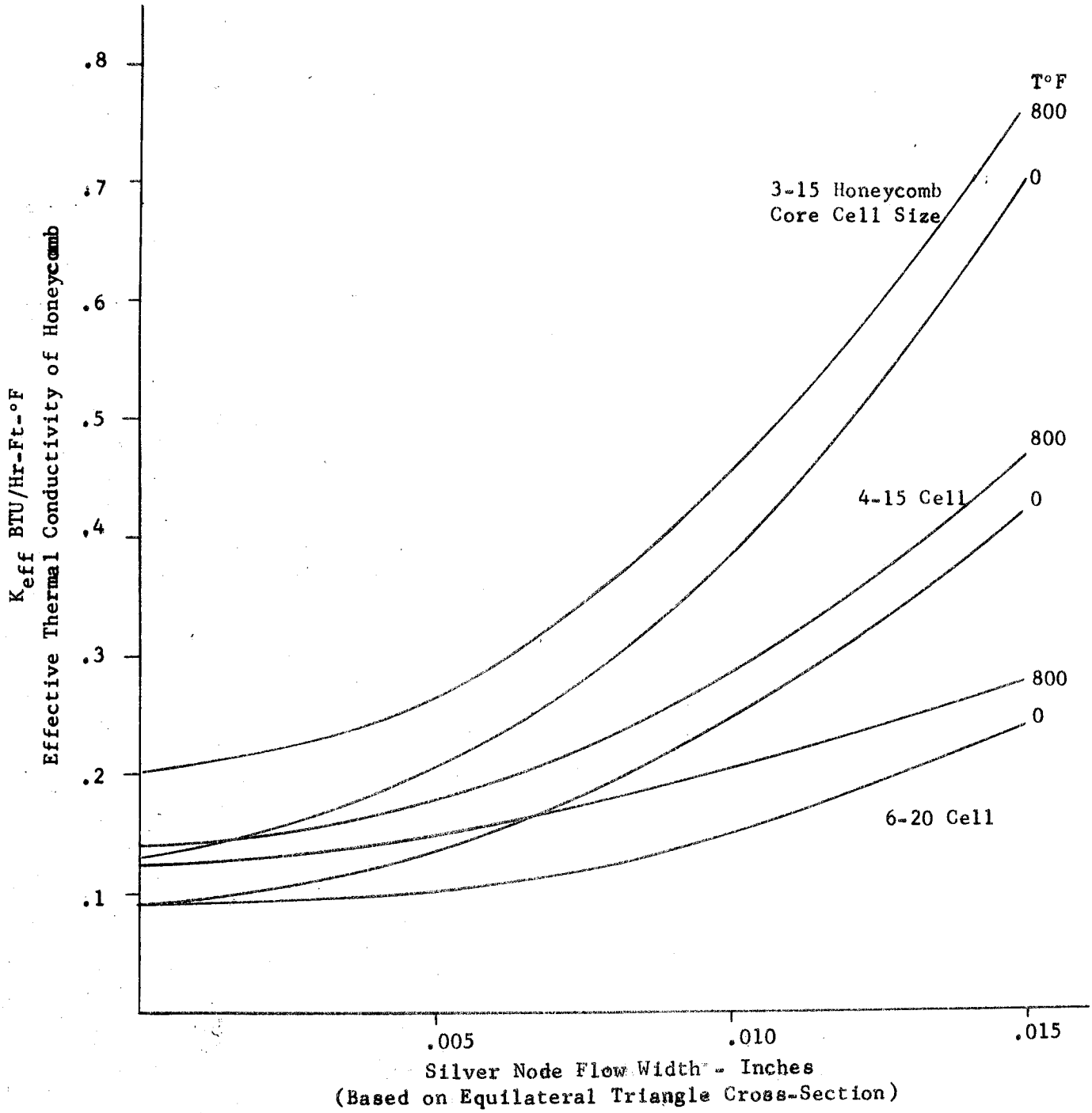

Figure 6 Thermal Conductivity of Heat Shield Panel Vs. Cell Width and Node Flow Width

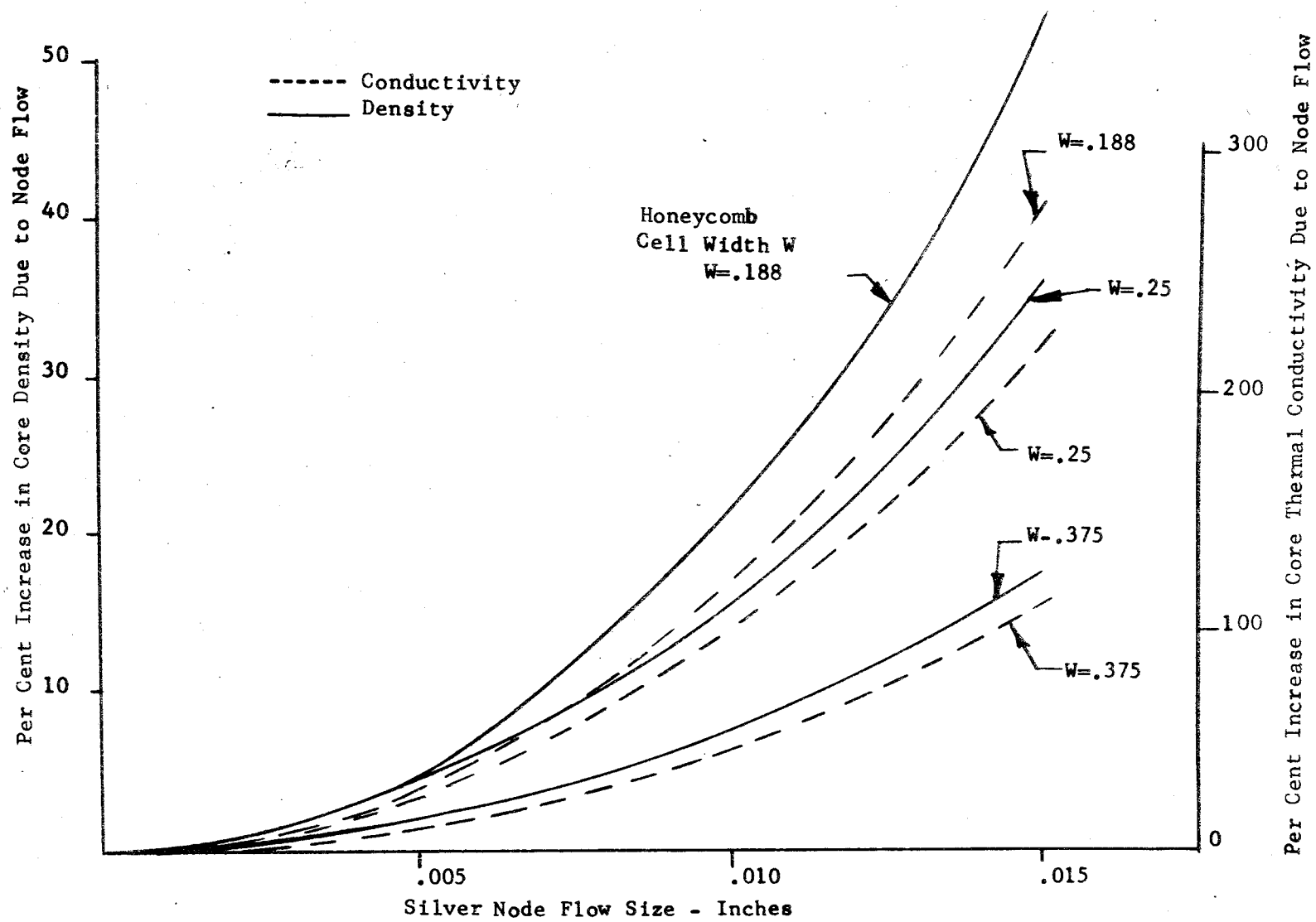

Figure 7 Effect of Node Flow Size on Panel Unit Weight & Thermal Conductivity

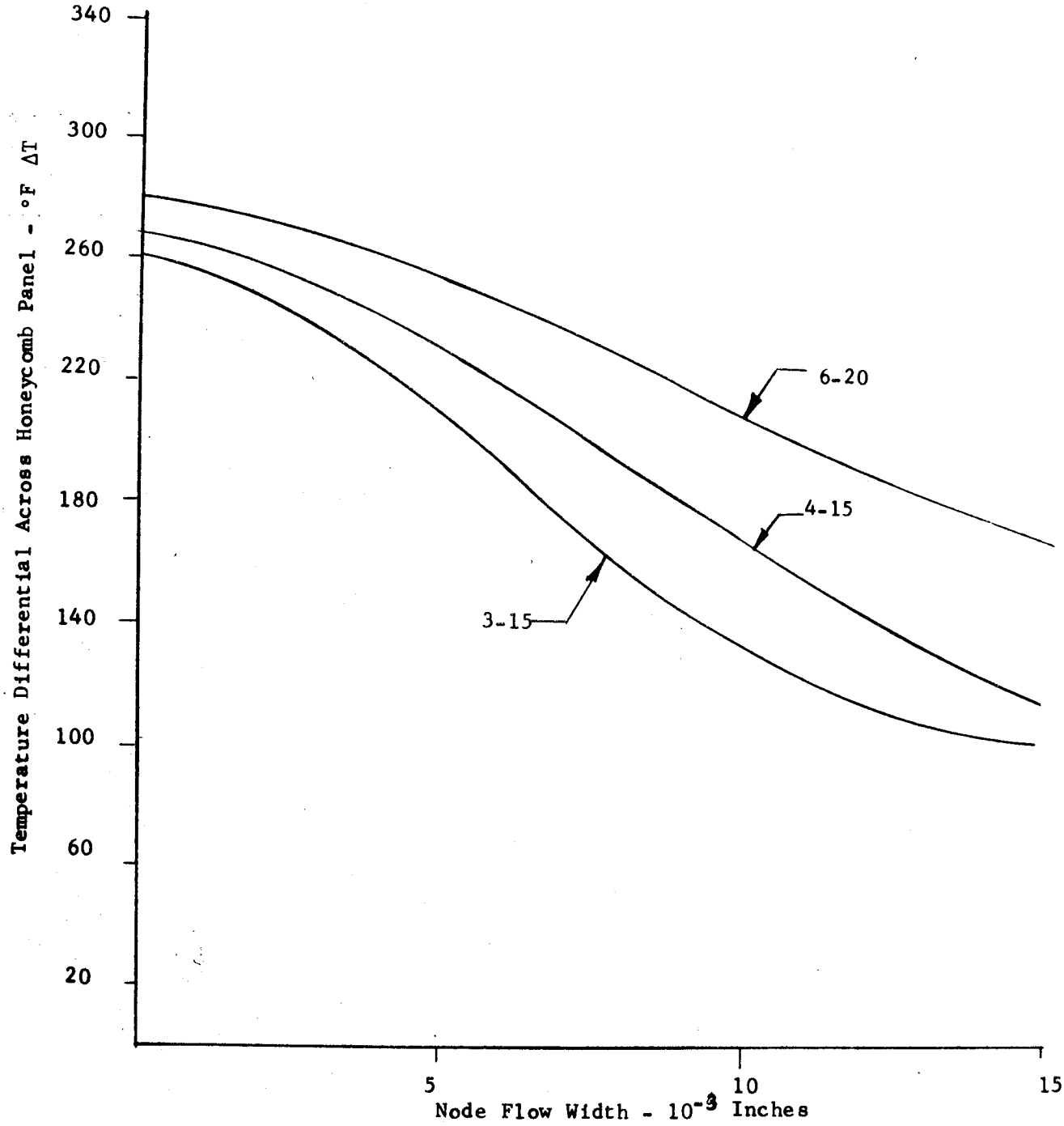

Figure 8 Effect of Node Flow Width & Cell Size on Temperature Differentials Across the 30M12571 Panel Design for Three Different Load Bearing Core Sizes

Cell Depths

In Figure 9, the adiabatic temperature differentials are given across the honeycomb core as a function of cell depth and node flow width for a constant cell size of 4-15 (¼" wide and 0.0015" foil thickness). It is quite evident that for any one cell depth, the temperature drop across the honeycomb decreases with an increase in node flow width. Also, for a constant node flow width the ΔT approaches zero as the cell depth is decreased, as would be expected.

It should be pointed out here that holding all parameters constant and decreasing the cell depth for the adiabatic case increases the back face (cold side) temperature of the honeycomb panel. This is due largely to the fact that the boundary conditions are the same so that there is less total mass to absorb the same amount of heat.

M-31 Reinforcing Honeycomb Effects

Figure 10 gives the temperature profiles for the heat shield panel No. 30M-12571 as a function of variable M-31 reinforcement cell width. The cell size was varied from 8-15 to 4-15, respectively. As is evident from the curves there was no noticeable effect on the temperature distribution in the honeycomb structure. Although not shown on the curves, a slight variance was noted in the temperatures T_1 and T_2, but was of such a magnitude ($\pm$ 10°) as to make it negligible.

Supplementary Information Relating to Parametric Studies

The temperature profiles given in Figures 11 to 23 were the basis for the preceding parametric analyses. Table 2 shows in tabular form the characteristics of the three honeycomb panels that served as the models for the parametric analyses.

Discussion

The methods of thermal analysis and the design point analysis presented here have been discussed previously (Ref. 1) and have been given to consolidate the thermal analysis and its results into a single unit for reference.

In reference to the information given in the section on the parametric analyses, it should be pointed out that the curves can be used most accurately in predicting the trend or trade-offs that occur for any one set of cell dimensions. This is especially so when predicting the effect of node flow width on temperature differentials across the honeycomb panel. It is quite evident from the curves that the node flow size is of prime consideration.

It should also be noted here that the ΔT (168°F) for the 4-15 cell having 0.010" node flow width in Figure 8 differs from the ΔT given in the section "Design Point Temperatures" for the design point (180°F). The difference is due to a refinement in the effective thermal conductivity of the honeycomb panel which was made for the parametric analyses. However, since the design point value was conservative, it was not changed.

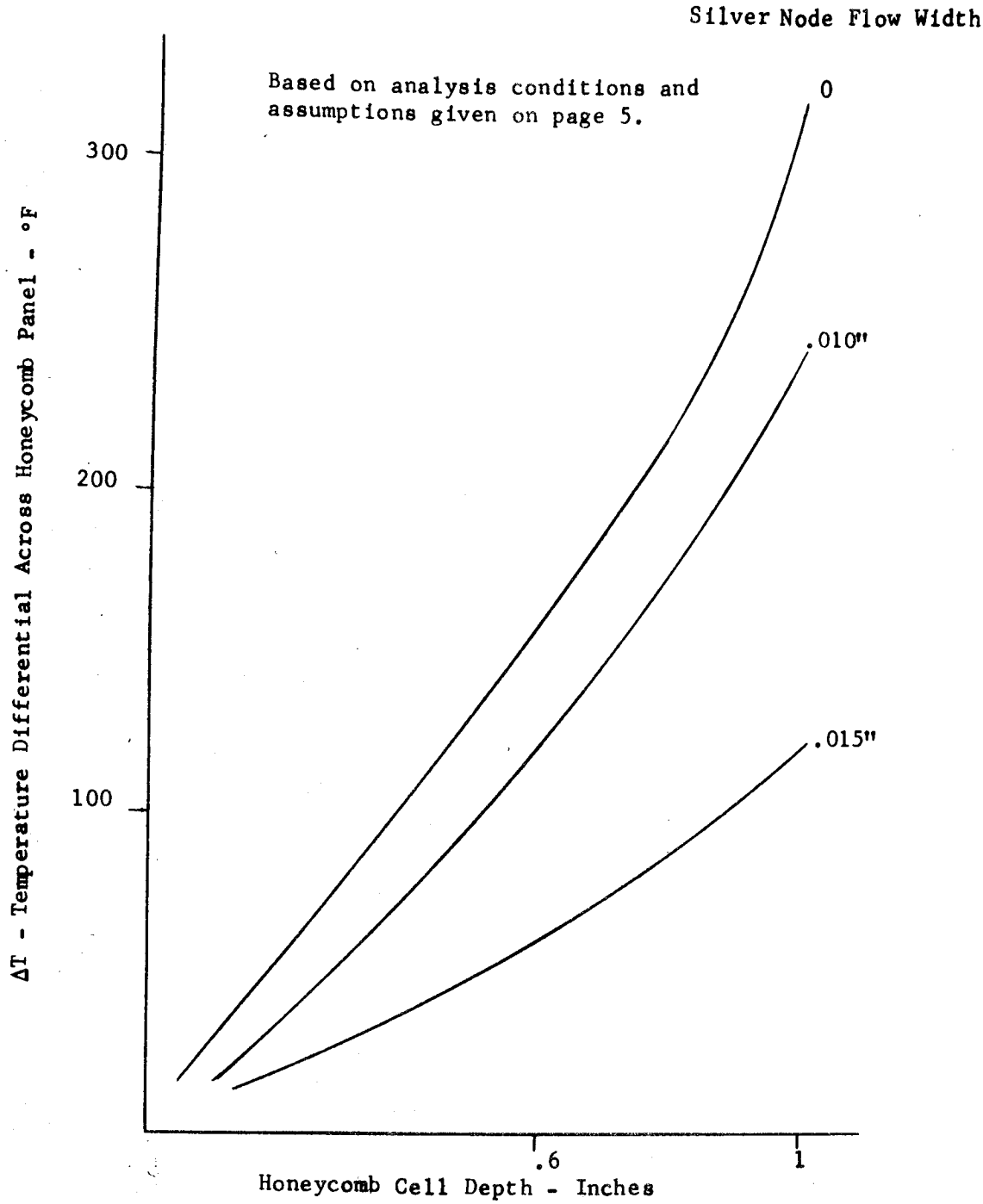

Figure 9 Temperature Differentials Across the Honeycomb As Function of Cell Depth and Node Flow Width. Core Size 4-15

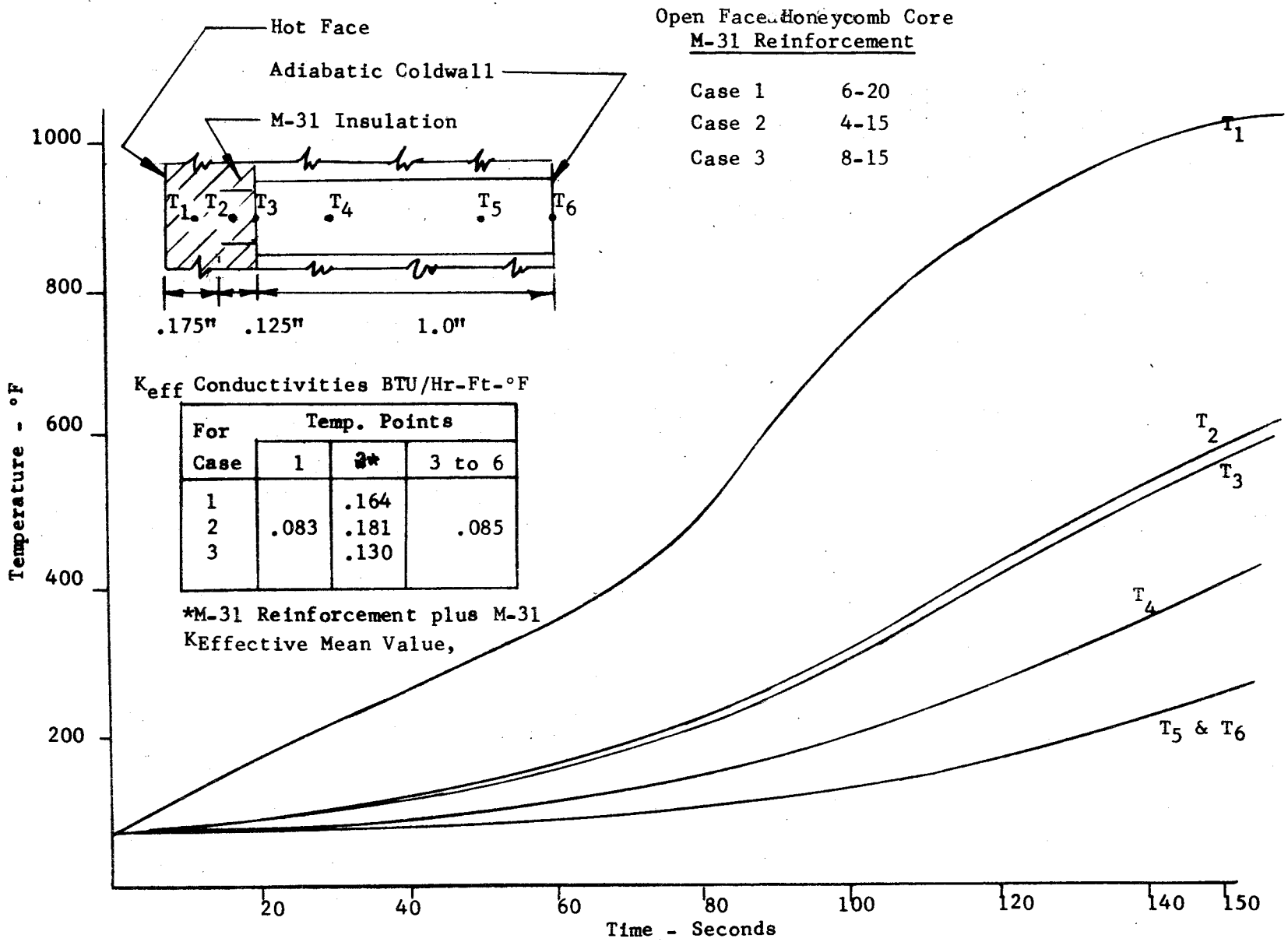

Figure 10 Temperature Profiles in Heat Shield Panel No. 30M12571
Zero Node Flow--Cell Size 4-15, Variable M-31 Reinforcement

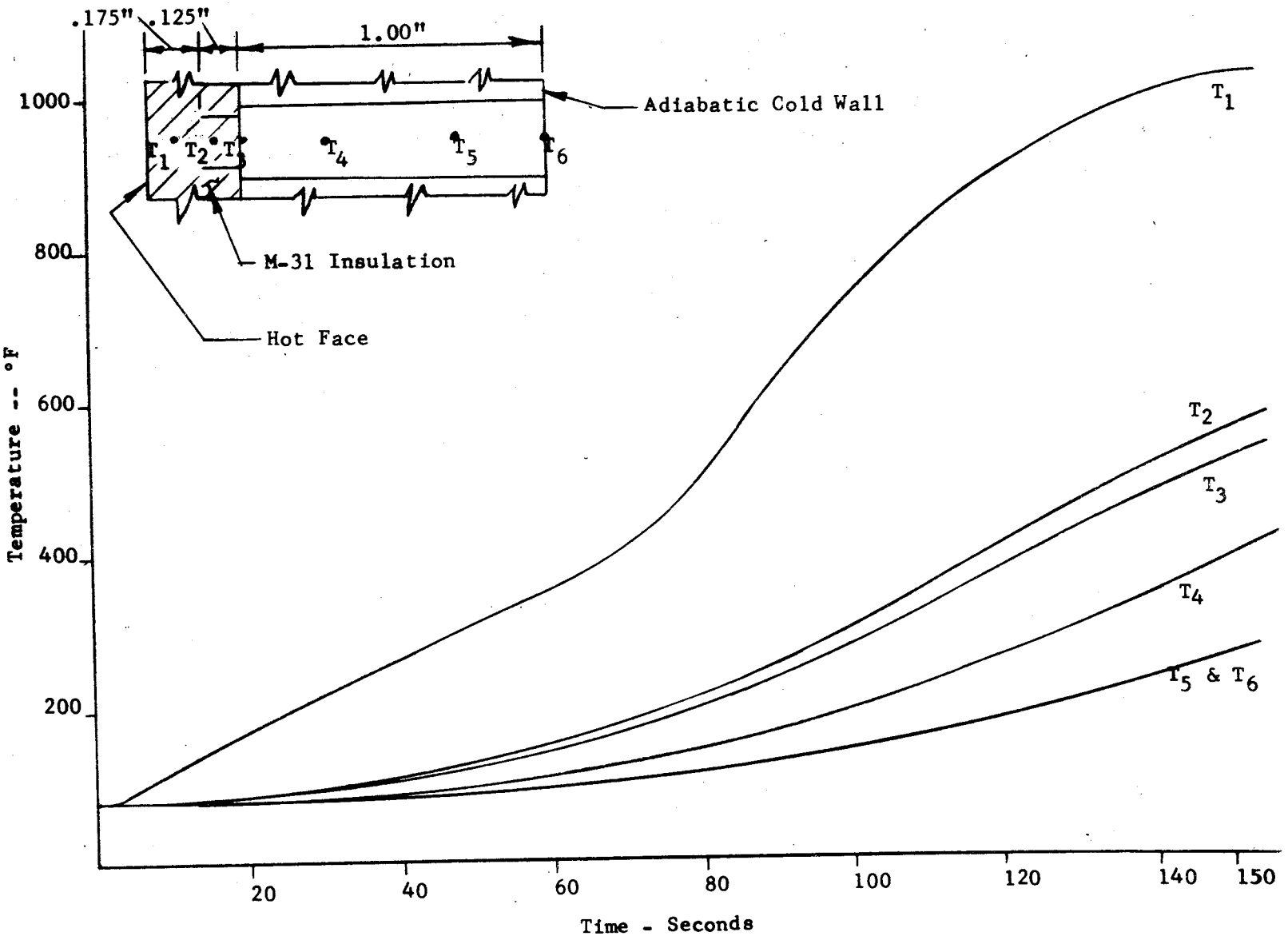

Figure 11 Temperature Profiles, Panel No. 30M12571
Zero Node Flow - Cell Size 3-15
Open Core Size, 8-15

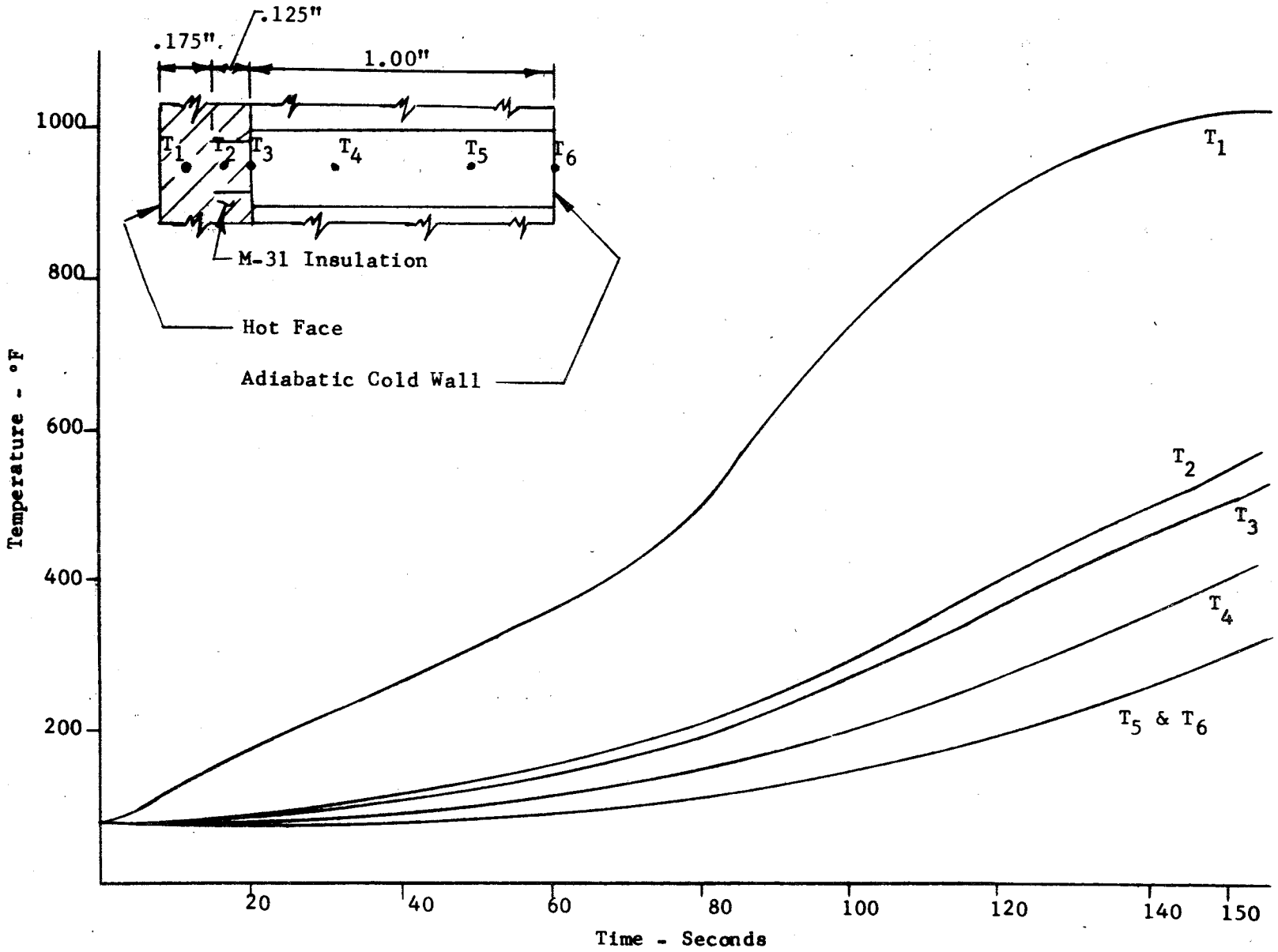

Figure 12 Temperature Profiles, Panel No. 30M12571
.005 Inch Node Flow Width - Cell Size 3-15
Open Core Size, 8-15

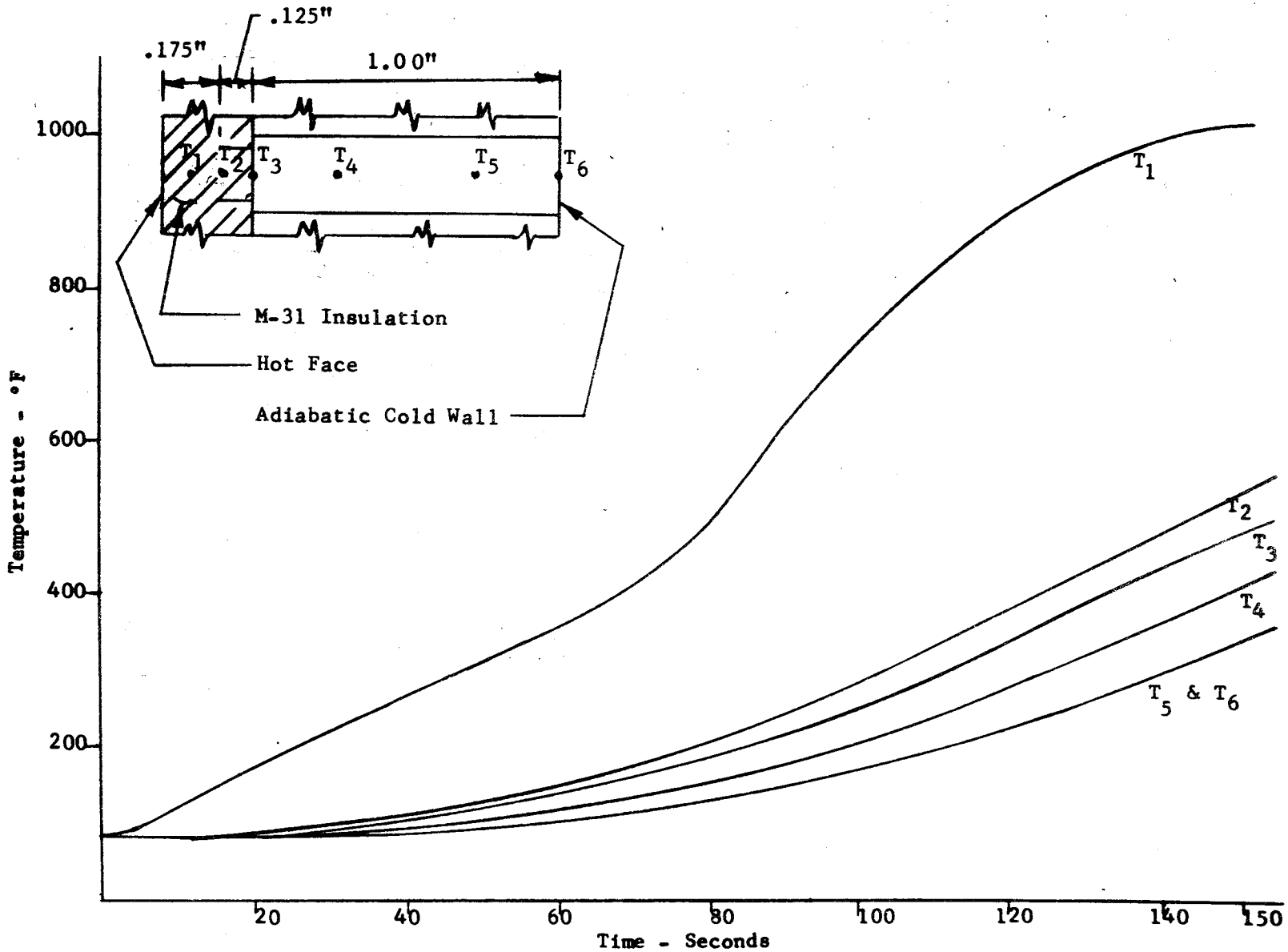

Figure 13 Temperature Profiles, Panel No. 30M12571
.010 Inch Node Flow Width - Cell Size 3-15
Open Core Size, 8-15

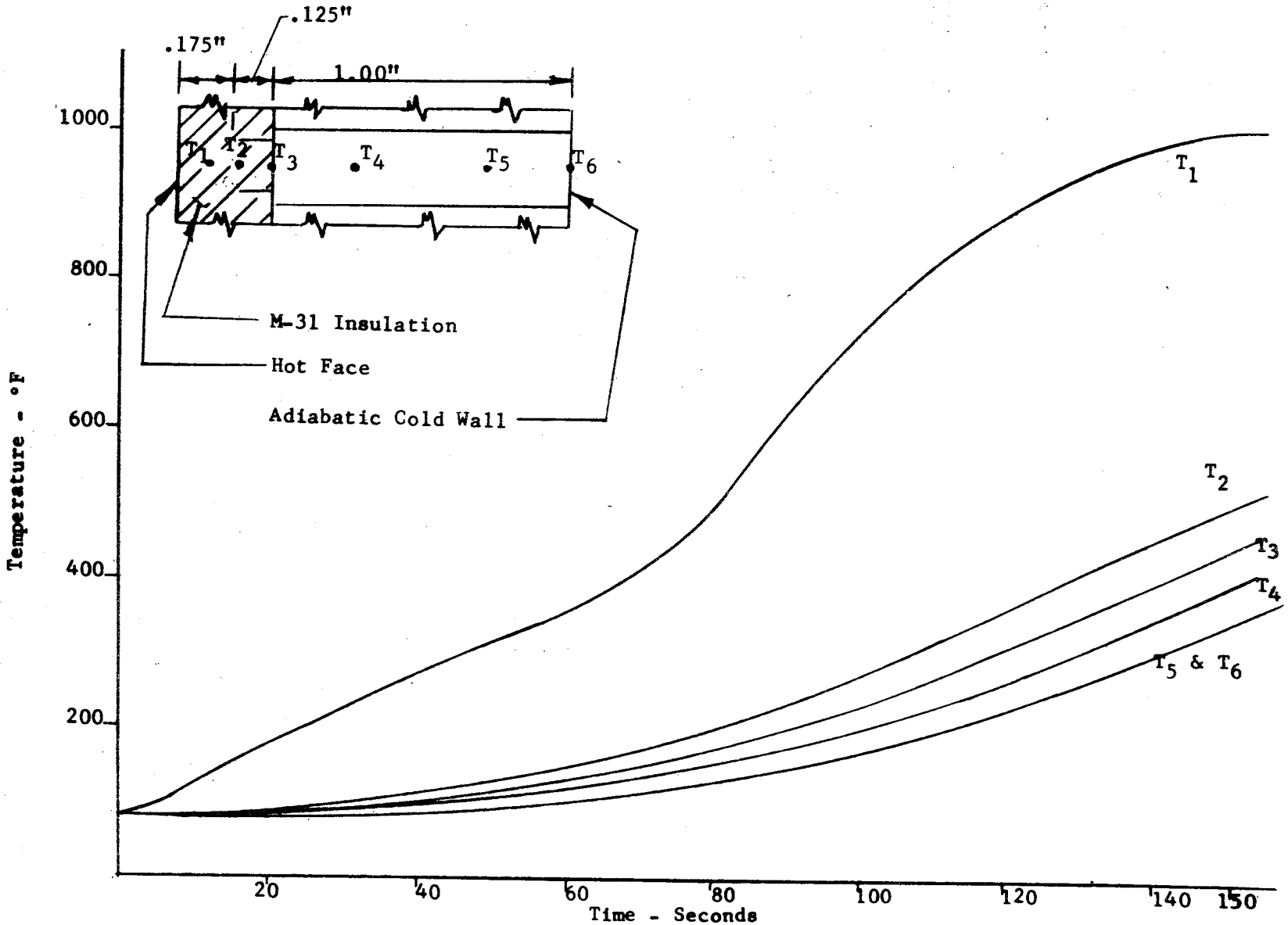

Figure 14 Temperature Profiles, Panel No. 30M12571
.015 Inch Node Flow Width - Cell Size 3-15
Open Core Size, 8-15

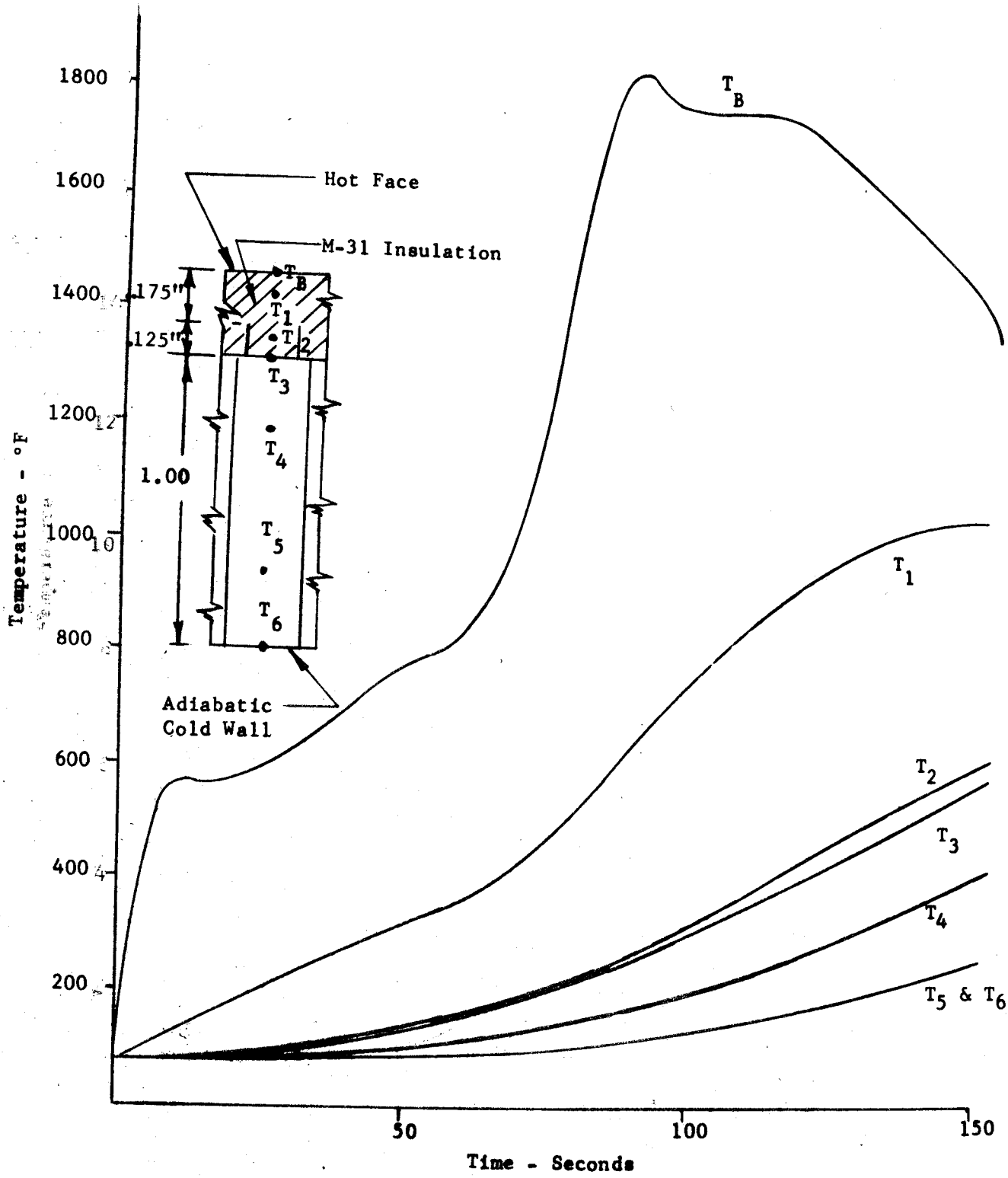

Figure 15 **Temperature Profiles - Panel No. 30M12571**
Zero Node Flow - Cell Size 4-15
Open Core Size, 8-15

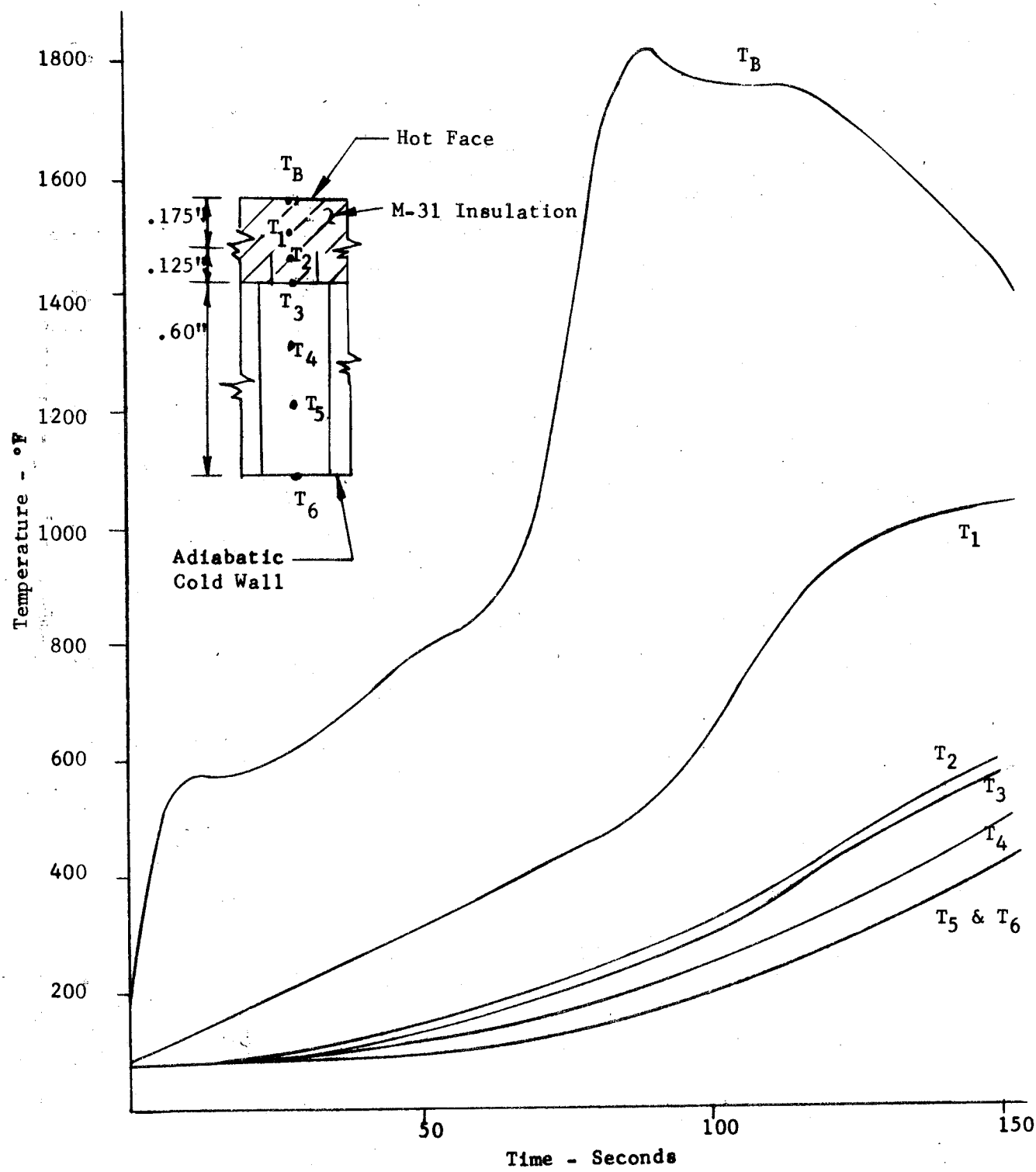

Figure 16 Temperature Profiles - Panel No. SK 60B20001
Zero Node Flow - Cell Size 4-15
Open Core Size, 8-15

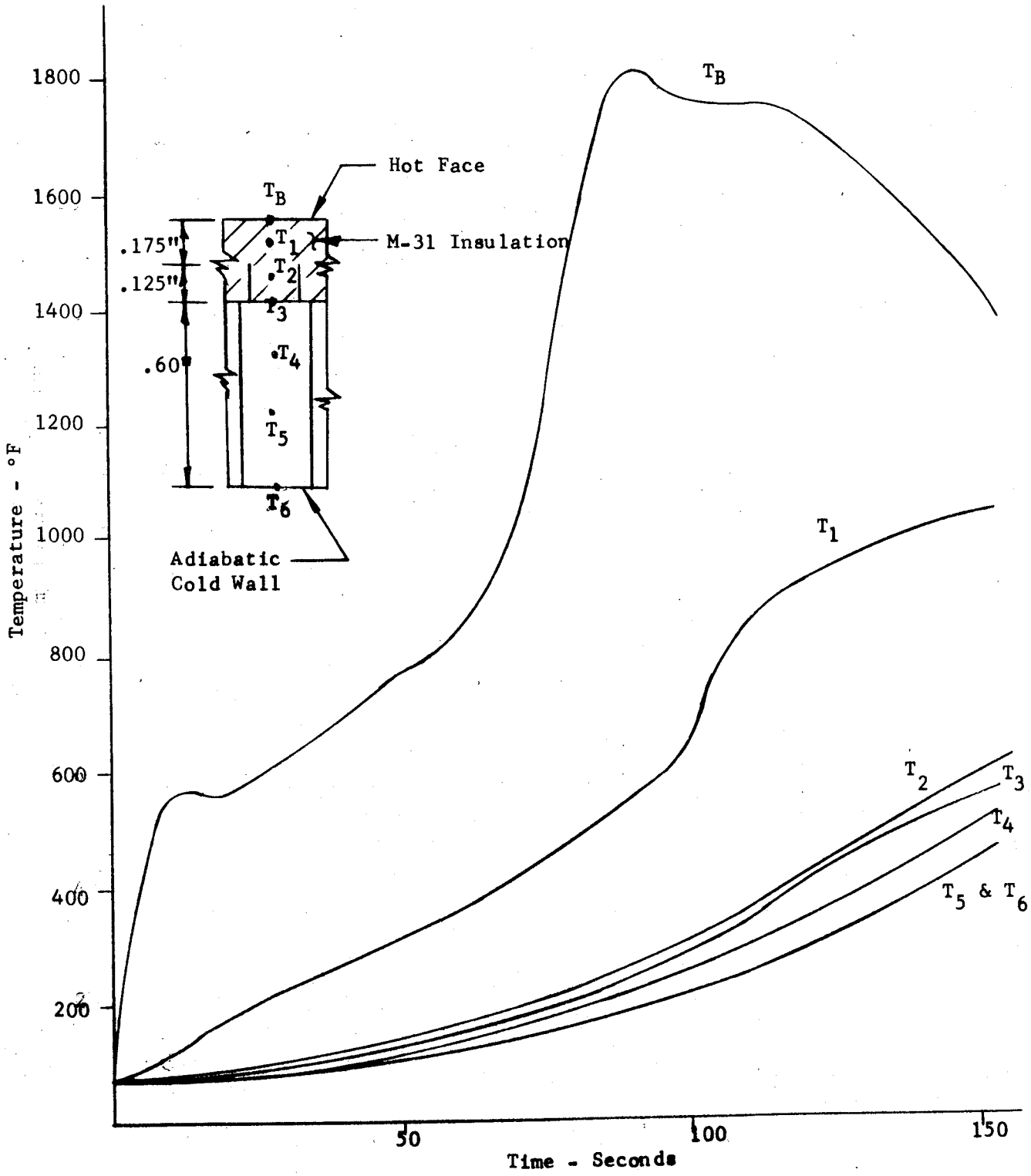

Figure 17 Temperature Profiles - Panel No. SK 60B20001
.005 Inch Node Flow Width - Cell Size 4-15
Open Core Size, 8-15

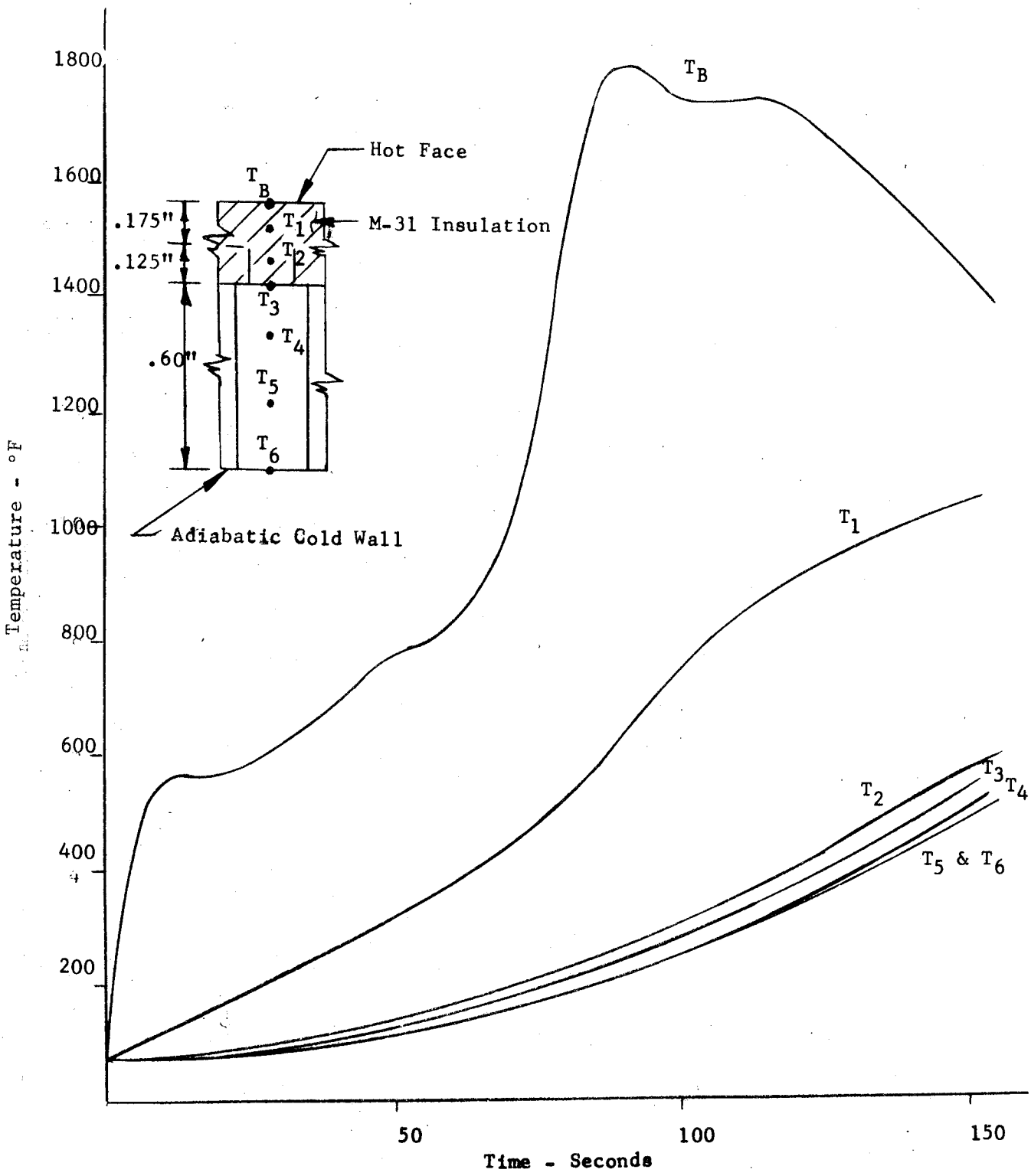

Figure 18 Temperature Profiles -- Panel Sk 60B20001
.015 Inch Node Flow Width - Cell Size 4-15
Open Core Size, 8-15

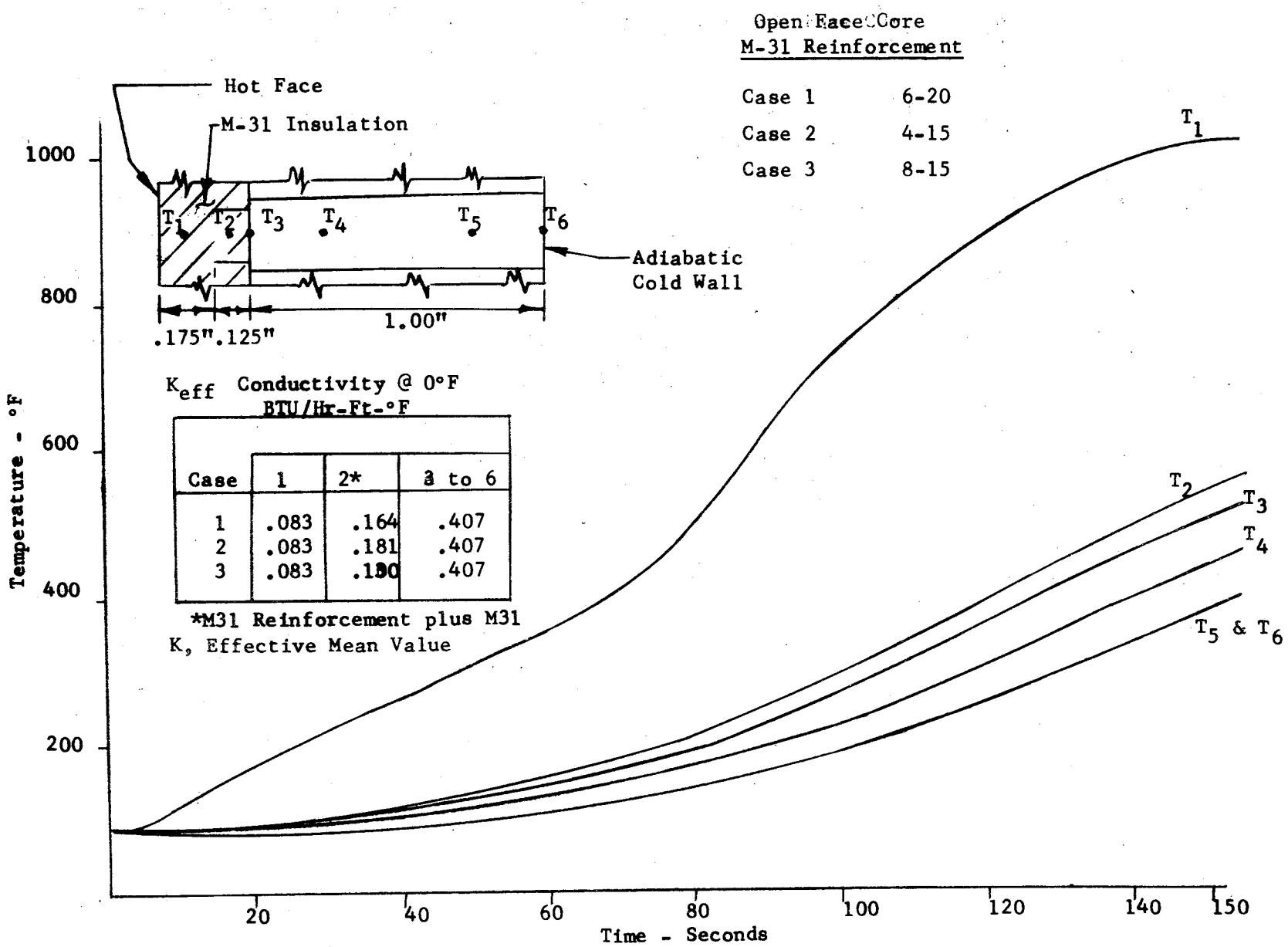

Figure 19 Temperature Profiles in Heat Shield Panel No. 30M12571
.015 Inch Node Flow Width - Cell Size 4-15
Variable M-31 Reinforcement

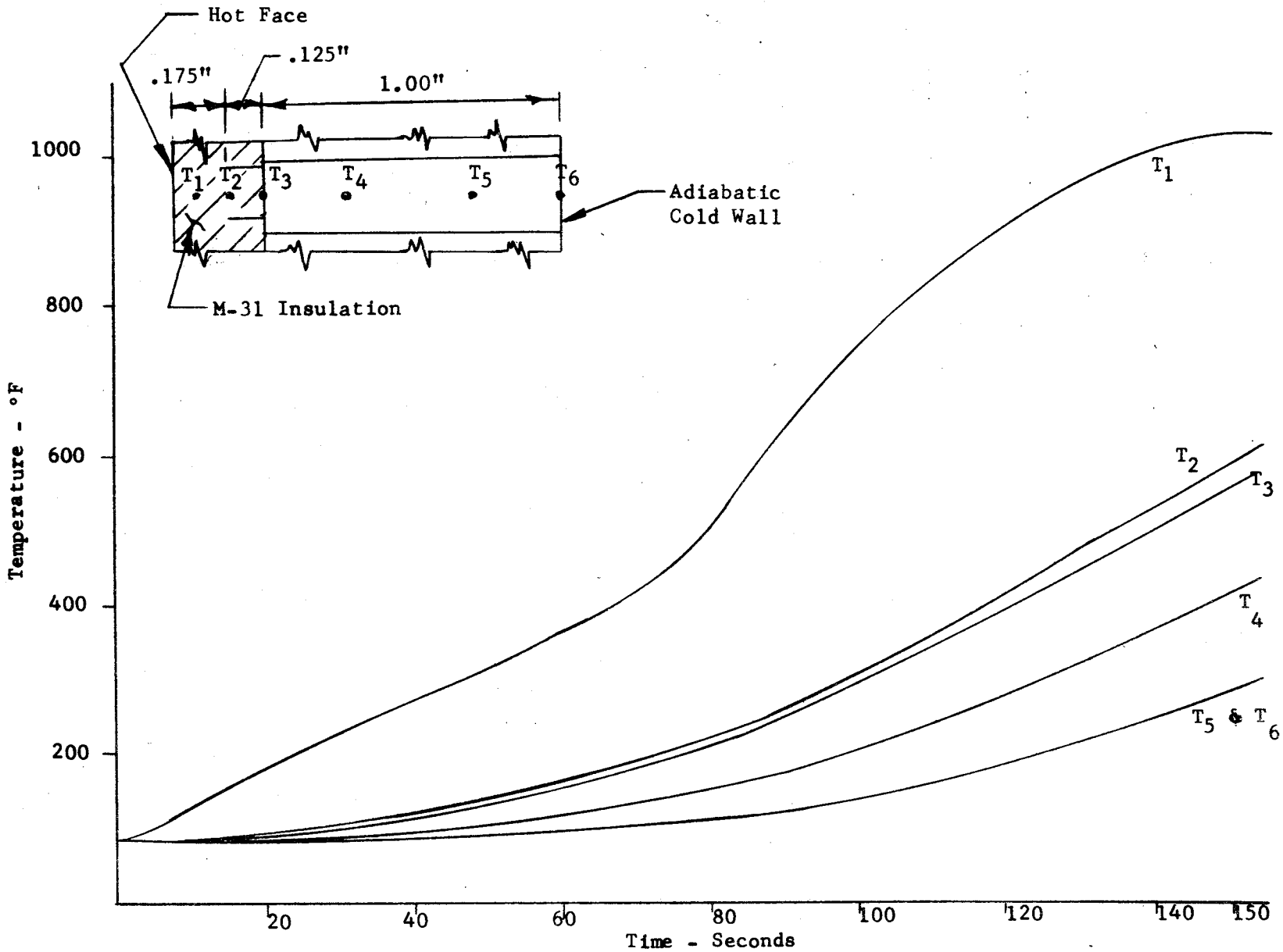

Figure 20 Temperature Profiles Panel No. 30M12571
Zero Node Flow - Cell Size 6-20
Open Core Size, 8-15

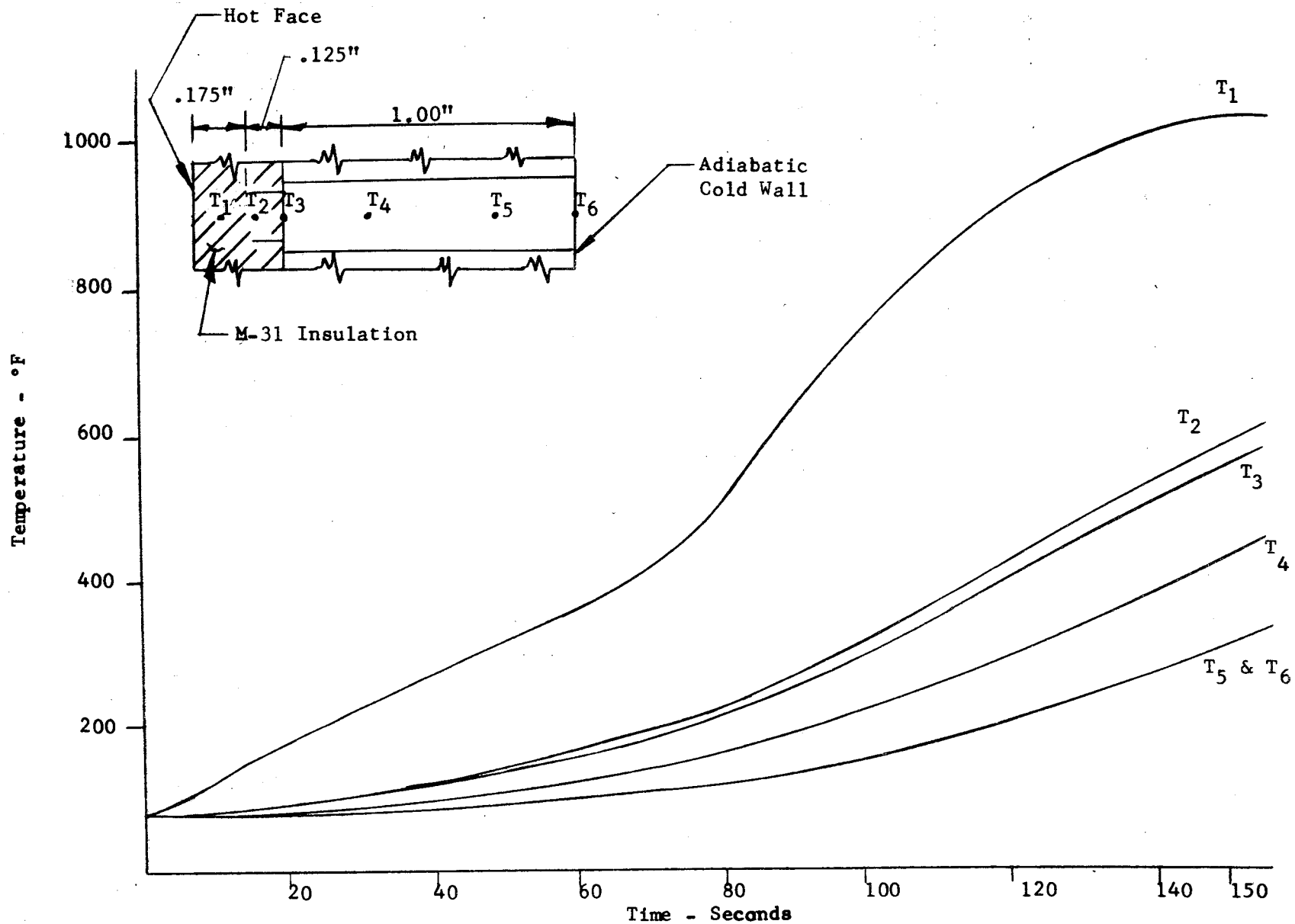

Figure 21 Temperature Profiles - Panel No. 30M12571
.005 Inch Node Flow Width - Cell Size 6-20
Open Core Size, 8-15

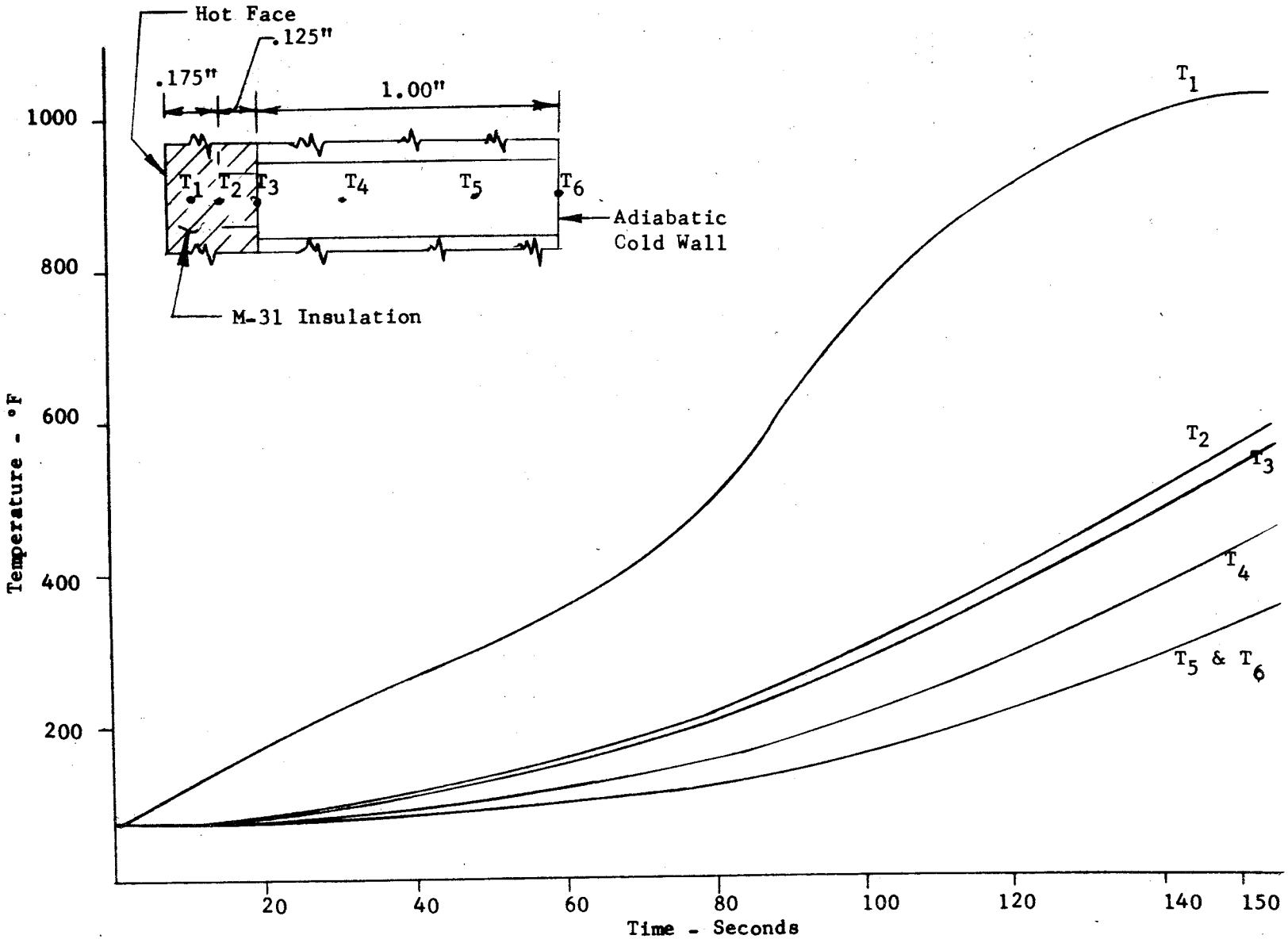

Figure 22 Temperature Profiles - Panel No. 30M12571
.010 Inch Node Flow Width - Cell Size 6-20
Open Core Size, 8-15

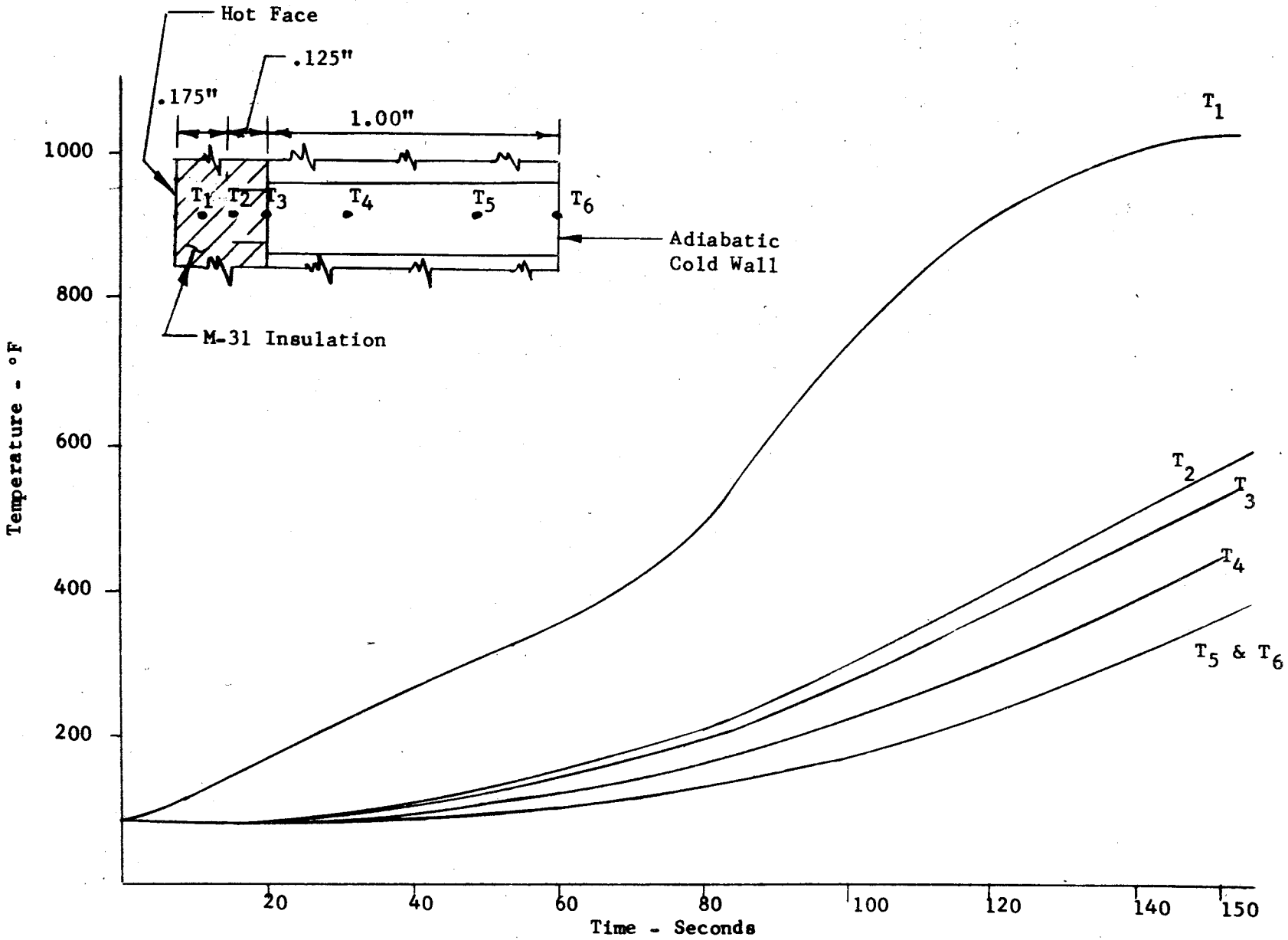

Figure 23 Temperature Profiles - Panel No. 30M12571
.015 Inch Node Flow Width - Cell Size 6-20
Open Core Size, 6-20

TABLE 2

PANEL DIMENSIONS AND THERMAL CONDUCTIVITIES FOR PARAMETRIC STUDY

Honeycomb Cell Dimensions		Area of Honeycomb Cells	Honeycomb Foil Area	Node Flow Area A_{NF} (ft^2)			Core Density O_{NF}*	Node Flow Density NF #/ft^3			Effective Conductivity K			Temp.
				Node Flow Width				Node Flow Width			Node Flow Width			
Width	Foil Thick.	Ft^2	Sq. Ft.	.005	.01	.015	#/ft^3	.005	.01	.015	.005	.01	.015	T°F
.25	.0015	2304	.012	.0004	.0016	.0036	6.2	.248	.99	2.23	.138	.245	424	0
(Type 4-15 Honeycomb Core)											.182	.289	.468	800
.188	.0015	4096	.016	.0007	.0028	.0064	8.3	.433	1.73	3.960	.199	.387	.709	0
(Type 3-15 Honeycomb Core)											.258	.446	.768	800
.375	.002	2048	.011	.0002	.0007	.0016	5.6	.124	.43	.990	.112	.157	.237	0
(Type 6-20 Honeycomb Core)											.152	.197	.277	800

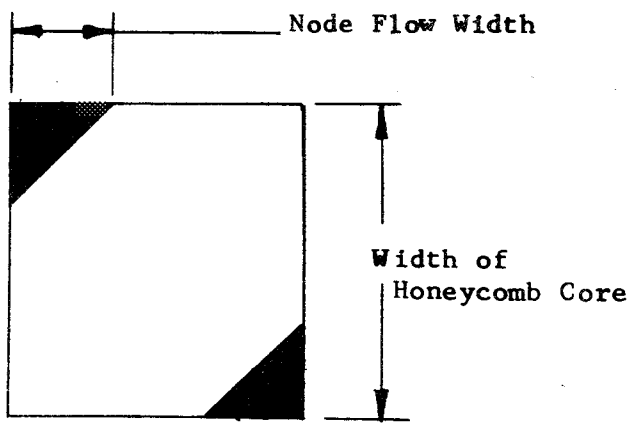

* O_{NF} = Zero Node Flow

A_{NF} = Area, Node Flow

SECTION II

STRESS ANALYSIS FOR S-1C HEAT SHIELD PANELS 30M12571 AND 60B20210

For small deflections within the elastic range, the sandwich heat shield panels behave as homogeneous plates when the proper modulus of rigidity is used. An approximate formula for D which has been used for all calculated data is:

$$D = \frac{E_1 E_2 h_f (h_c + h_f)}{(E_1 + E_2)(1 - \nu^2)}$$

This expression assumes both facings to be of the same material and thickness, and thin compared to the height of the core.

Three panels were considered: the zee panel 30M12571, h_c=1.0"; the two cup panels 60B20210, with h_c=0.6" and 1.0". Each panel was calculated for every reasonable combination of conditions. The results are shown in Tables 4 through 7.

Table 3 lists all the pertinent stress functions as they apply to the heat shield panels. Formulas taken from Timoshenko have had the various series in his expressions evaluated for the maximum value for a square for either the edge or center as required.

Table 4 shows the calculations for the simple support condition on the cup panels, 60B20210. The most severe loading occurs at the center for the maximum ΔT and is 79,524 psi and 63,416 psi for the two thicknesses, respectively. Since the allowable for the maximum ΔT is 140,000 psi*, there is an adequate margin of safety.

Table 5 shows the fully clamped condition for the same panels. Here, the maximum stress occurs at the edge and is 97,885 psi and 81,099 psi for the two panels, respectively, at the maximum ΔT. Again, an adequate margin of safety is indicated.

It is easily recognized that in actual practice neither of the above two edge mounting conditions represent the physical picture. The panel loading imposes a stress condition on the flange and insulation both of which are elastic materials. Table 6 considers the flexibility of the panel, flange and the JM-146 insulation as a system. The per cent of edge fixity was calculated and tabulated for the various conditions for the two panels, and presented in Table 6.

*f_{ty} =170,000 psi at room temperature, Ref. MIL-HDBK-5

Table 7 utilizes the edge fixities determined in Table 6 and tabulates the stress functions for both the edge and center conditions. The results show an appreciable reduction in maximum stresses in the center and a substantial reduction in edge stresses. It is believed that this table represents a realistic resume' of stresses to be expected in the 60B20210 panel. The 1.0" thick panel meets the maximum deflection criteria of 0.5" for all conditions under 280° ΔT. The maximum deflection of .8417 inch at a ΔT of 450° indicates that the M-31 would be cracking and probably breaking off from vibration. Since there is now relatively good indications of appreciable cooling on the back face of the heat shield, the maximum ΔT's are more probable for the terminal flight condition*.

If the M-31 deflection values obtained for the radius of curvature at cracking for the M-31 insulation material is extrapolated, it is found that the probable cracking deflection on these panels is about 0.8". Thus, it appears that the cracking would not start until the latter stages of the flight and probably would be of no actual significance.

Table 8 shows the panel calculations for the mounted 30M12571 unit 1.0" thick. The zee mounting approximates a simple support condition and all panel calculations for this table are based on the assumption of simple support for the panel edges. The maximum deflection is seen to be less than that for the comparable cup panel (h_c=1.0") by about a tenth of an inch. W_{tot} = .7551" for 450° ΔT. Thus, the danger of cracking and flaking off of the M-31 is lessened. Further, the maximum stresses are only nominally greater than the cup panel (elastic support) at maximum ΔT and less at zero ΔT's. The zee mounting is better able to withstand shock than the cup panel mounting as it is essentially a cantilever spring. The damping effect of the zee mounting on vibration is self-evident whereas vibration loads add directly to the possibility of exceeding the core crushing load at the cup area on the 60B20210 panel.

Table 9 shows the calculations for the edge member for the zee type mounting of the 30M12571 panel. The h_z shown is the thickness of the edge member and extended facing to which it is brazed during manufacture. Although the 30M12571 design called for a combined h_z=.060"(.050 + .010), it is seen that the maximum stresses do not exceed the allowable (140,000 @ ΔT = 450°) except for h_z=.030 and .020". Thus, an appreciable weight saving could be effected by using an h_z=.040". This thinner edge member would also increase the vibration damping effect over the present design.

All calculations in the tables are based on the following data and procedures.

The 165 db noise level** was converted to an equivalent pressure of 0.72 psi. This noise loading was used (for both ignition and flight) as an equivalent moment of 102.8 inch pounds per inch. It was assumed to be uniformly distributed over the panel surface for the fully clamped condition; a maximum at the center and zero at the edge for the simply supported condition.

* Ref: NASA memorandum M-P&VE-PH 217-63, Aug. 16, 1963, Figure 5.
**Ref: S-1C Base Heat Shield Design Criteria

No additional load above the equivalent 165 db noise level was used for structural vibration.

For the flight condition, 0.09 psi was added to the 1.0 psi air load as an equivalent pressure based on an acceleration of 140 ft/sec/sec.

The panel dimensions used were 52.778" for the 60B20210 panel and 48.45" for the 30M12571 panel. The dimensions of the 60B20210 panel mounting are shown in Figure 24. The effect of temperature on the elastic properties of PH 15-7Mo is shown in Figure 25.

*Ref: NASA correspondence M-P&VE-SB 3/15/63.

NOMENCLATURE SYMBOLS AND UNITS

A	Area, square inches
a	Panel width, inches
b	Panel length, inches
C	Center
c	subscript, core
D	Modulus of rigidity, inch pounds
E	Young's Modulus, psi
E_m	Average of two values of Young's Modulus
E.F.	Edge Fixity
F	Flange, subscript
f	Stress, psi; subscript, facing
f_{tu}	Tensile ultimate strength, psi
f_{ty}	Tensile yield strength, psi
h	Thickness, inches; core height, inches
I	Moment of inertia; insulation; subscript, insulation
K	Spring constant, in-pounds/in/Radian
ℓ	Length, inches
M	Moment, in-pounds/in.
$M_{\Delta\theta}$	Differential moment due to $\Delta\theta$
p	Subscript, panel
q	Unit pressure loading, psi; subscript, unit pressure loading, psi
Q	Shear, lbs/in
R	Corner reaction force, pounds; radius, inches

NOMENCLATURE SYMBOLS AND UNITS (Cont'd)

RT	Room Temperature
T	Temperature - °F
ΔT	Temperature difference, °F; subscript, temperature difference, °F
V	Edge reaction force, pounds per inch
W	Deflection, inches
x	Axis
y	Axis
z	Subscript, zee edge member
α	Temperature coefficient of expansion, in/in/°F
ϵ	Strain, microinches per inch
θ	Rotation of panel edge, Radians
$\Delta\theta$	Differential rotation of zee edge member, $\Delta\theta=\theta_p-\theta_z$
υ	Poisson's Ratio
σ	Stress, psi

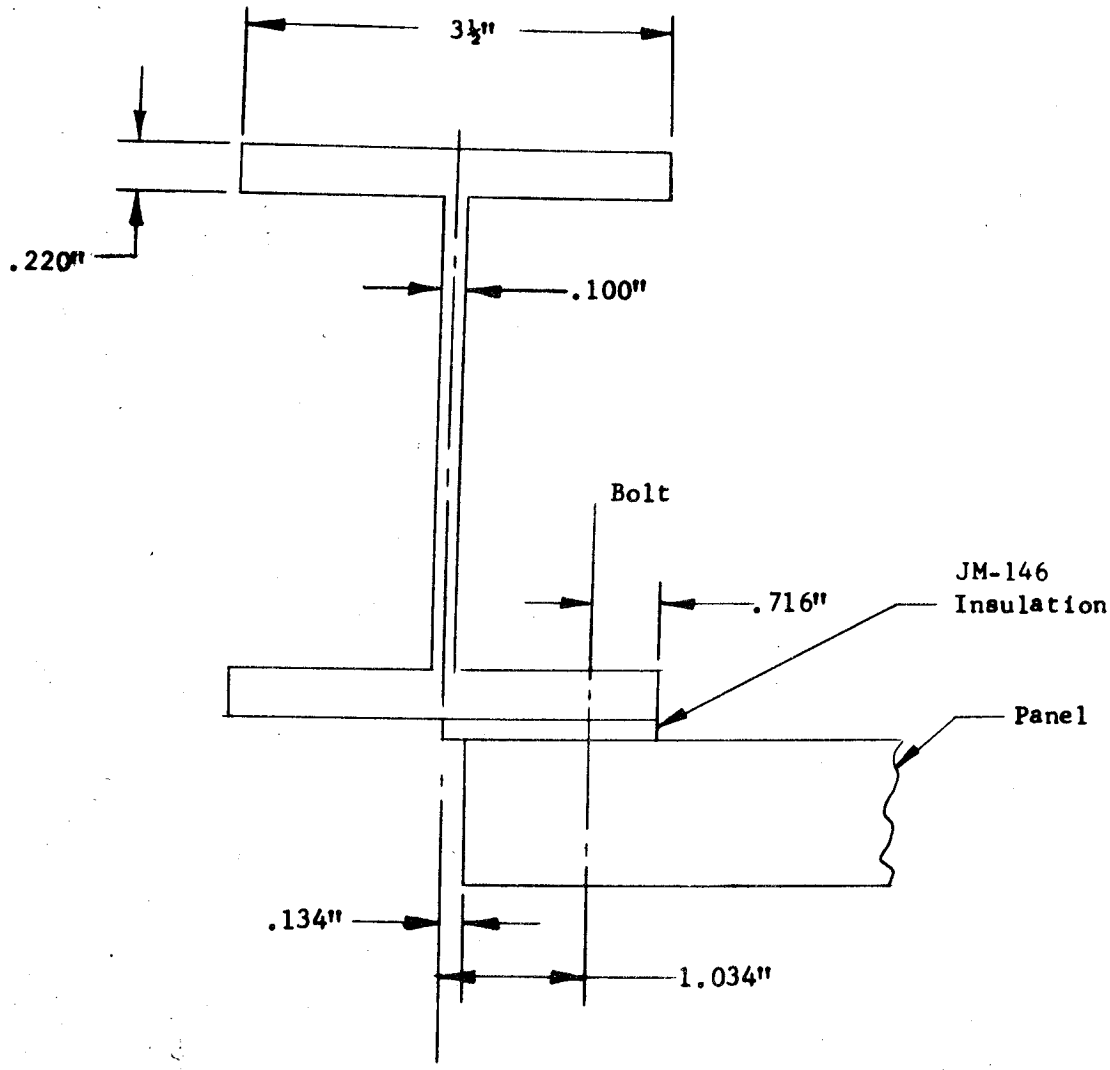

Figure 24 Mounting System for 60B20210 Panel
Showing Calculation Dimensions Only

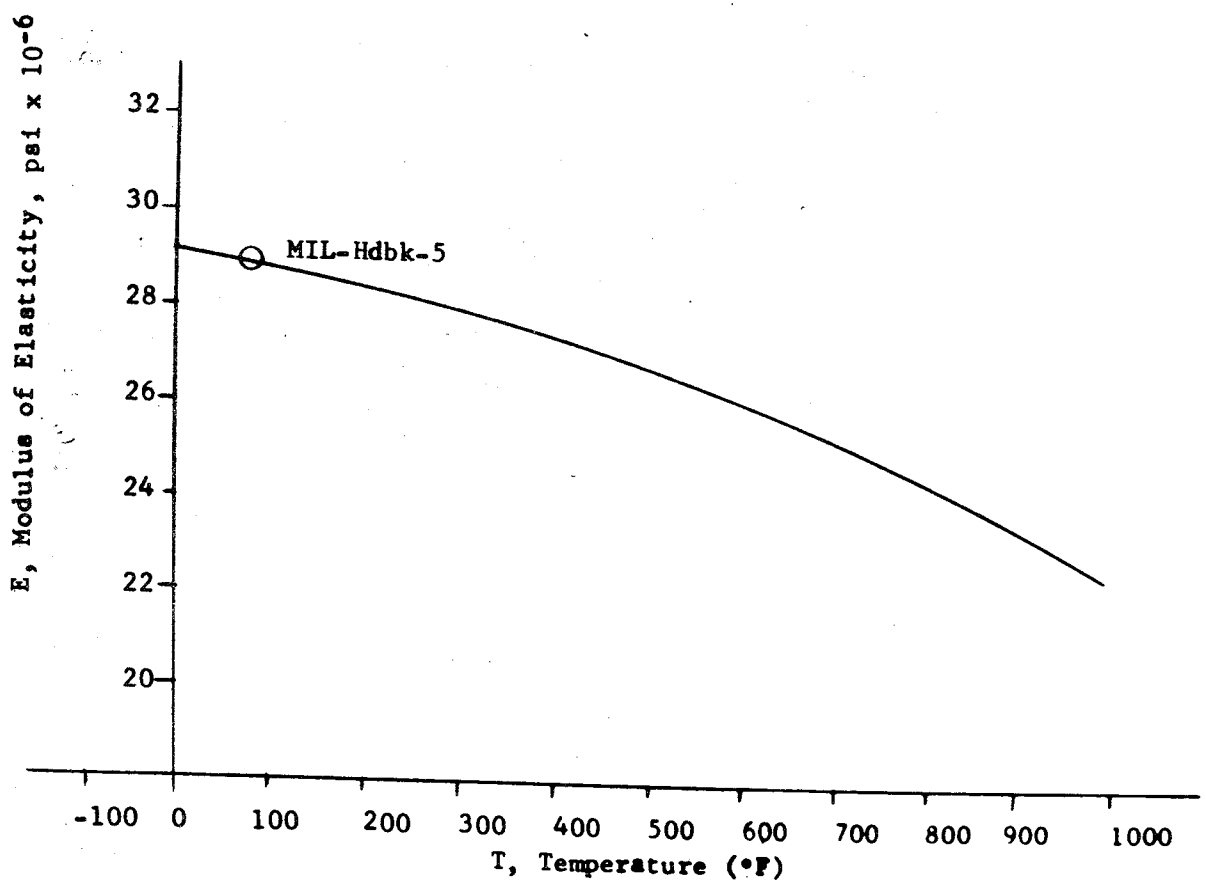

Figure 25 Variation of Modulus of Elasticity with Temperature (Elastic Properties of PH15-7MO (TH 1050) Based on 1958 Armco Data in ARDC TR 59-66)

TABLE 3

EQUATIONS USED IN CALCULATIONS

	Simple Support		Elastic Support		Fully Clamped	
	Center	Edge	Center	Edge	Center	Edge
W_q	$.00406qa^4/D$	Zero	$(.00406-.0028E.F.)qa^4/D$	Zero	$.00126qa^4/D$	Zero
$W_{\Delta T}$	$\frac{0.0958\alpha\Delta Ta^2}{(h_c+2h_f)}$	Zero	$\frac{0.0958\alpha\Delta Ta^2}{(h_c+2h_f)}$ (1-E.F.)	Zero	Zero	Zero
θ_q	Zero	$.01348qa^3/D$	Zero	$.01348qa^3/D(1-E.F.)$	Zero	Zero
$\theta_{\Delta T}$	Zero	$\frac{.31724\alpha\Delta Ta}{(h_c+2h_f)}$	Zero	$\frac{.31724\alpha\Delta Ta}{(h_c+2h_f)}(1-E.F.)$	Zero	Zero
M_q	$.0479qa^2$	Zero	$(.0479-.0248E.F.)qa^2$	$.0513qa^2(E.F.)$	$.0231qa^2$	$.0513qa^2$
$M_{\Delta T}$	$\frac{(1-\nu^2)\alpha\Delta TD}{2(h_c+h_f)}$	$\frac{(1-\nu^2)\alpha\Delta TD}{(h_c+h_f)}$	$\frac{(.455+.845E.F.)\alpha\Delta TD}{(h_c+h_f)}$	$\frac{(.91+.39E.F.)\alpha\Delta TD}{(h_c+h_f)}$	$\frac{(1+\nu)\alpha\Delta TD}{(h_c+h_f)}$	$\frac{(1+\nu)\alpha\Delta TD}{(h_c+h_f)}$
σQ_q	--	.338qa	---	.338qa	----	.338qa
$\sigma Q_{\Delta T}$*	--	$\frac{.825\alpha\Delta Th_ch_fE_m}{a(h_c+h_f)}$	$\frac{.825\alpha\Delta Th_ch_fE_m(E.F.)}{a(h_c+h_f)}$	$\frac{.825\alpha\Delta Th_ch_fE_m}{a(h_c+h_f)}$	$\frac{.825\alpha\Delta Th_ch_fE_m}{a(h_c+h_f)}$	$\frac{.825\alpha\Delta Th_ch_fE_m}{a(h_c+h_f)}$
σM_q	$M_q/h_f(h_c+h_f)$	Zero	$M_q/h_f(h_c+h_f)$	$M_q/h_f(h_c+h_f)$	$M_q/h_f(h_c+h_f)$	$M_q/h_f(h_c+h_f)$
$\sigma M_{\Delta T}$	$M_{\Delta T}/h_f(h_c+h_f)$	$M_{\Delta T}/h_f(h_c+h_f)$	$M_{\Delta T}/h_f(h_c+h_f)$	$M_{\Delta T}/h_f(h_c+h_f)$	$M_{\Delta T}/h_f(h_c+h_f)$	$M_{\Delta T}/h_f(h_c+h_f)$
V		.420qa		.420qa		.420qa
R		$-.065qa^2$		$-.065qa^2$		$-.065qa^2$
K_F	$(\frac{8EI}{3\ell})_{Ign}$	$(\frac{3EI}{\ell})_{Flt}$	E.F. $= 1/(1+\frac{k_F}{k_F}+\frac{k_F}{k_I})$		$K_I = \frac{1}{2}(q_1\ell_1^3 + q_2\ell_2^3)$	

*NAA Structural Design Manual
All other formulas from S. Timoshenko, Plates & Shells, 2nd Ed.

$\ell_1 = .716"$ $\ell_2 = .900"$
Ign $q_1 = 2097$ $q_2 = 3086$
Flt $q_1 = 3086$ $q_2 = 2097$

TABLE 4

MAXIMUM VALUES FOR 60B20210 PANEL
SIMPLY SUPPORTED EDGE CONDITION

		Ignition		Flight							
		Center q=+2.7 ΔT=0°	Edge q=+2.7 ΔT=0°	Center q=1.09 ΔT=0°	Edge q=1.09 ΔT=0°	ΔT=80°	ΔT=180°	ΔT=280°	ΔT=320°	ΔT=450°	*
Cup Panel h_c=0.6"	W_q	+1.433	--	-.5783	---	-.5783	-.5783	-.5783	-.5783	-.5783	C
	$W_{\Delta T}$	--	--	--	---	-.210	-.472	-.735	-.840	-1.181	C
	θ_q	--	-.0901	--	+.03639	+.03639	+.03639	+.03639	+.03639	+.03639	E
	$\theta_{\Delta T}$	--	--	--	---	+.0132	+.0290	+.0461	+.0527	+.0741	E
	M_q	360.2	Zero	145.4	Zero	145.4	145.4	145.4	145.4	145.4	C
	$M_{\Delta T}$	--		--	---	39.4	88.9	140.5	163.3	236.9	C
	M_{noise}	102.8	Zero	102.8	Zero	102.8	102.8	102.8	102.8	102.8	C
	M_{tot}	463.0	Zero	248.2	Zero	287.6	337.1	388.7	411.5	485.1	C
	W_{tot}	+1.433	--	-.5783	Zero	-.7883	-1.0503	-1.3133	-1.4183	-1.7593	C
	θ_{tot}	--	-.0901	--	+.03639	+.04959	+.06599	+.08249	+.08909	+.11049	E
	σ_Q	-97.5	--	+53.0	---	+55.0	+57.5	+60.2	+61.3	+65.1	C
	σ_{tot}	75,901	--	40,688	---	47,147	55,262	63,721	67,459	79,524	C
Cup Panel h_c=1.0"	W_q	+.5224	--	-.2109	---	-.2109	-.2109	-.2109	-.2109	-.2109	C
	$W_{\Delta T}$	--	--	--	---	-.1277	-.2873	-.4469	-.5107	-.7182	C
	θ_q	--	-.0329	--	+.0133	+.0133	+.0133	+.0133	+.0133	+.0133	E
	$\theta_{\Delta T}$	--	--	--	---	+.0080	+.0180	+.0280	+.0320	+.0450	E
	M_q	360.2	Zero	145.4	Zero	145.4	145.4	145.4	145.4	145.4	C
	$M_{\Delta T}$	--	--	--	---	65.3	147.1	235.4	270.3	392.3	C
	M_{noise}	102.8	Zero	102.8	Zero	102.8	102.8	102.8	102.8	102.8	C
	M_{tot}	463.0	--	248.2	---	313.5	395.3	483.6	518.5	640.5	C
	W_{tot}	+.5224	--	-.2109		-.3386	-.4982	-.6578	-.7216	-.9291	C
	θ_{tot}	--	-.0329	--	+.0133	+.0213	+.0313	+.0413	+.0453	+.0583	E
	σ_Q	-58.9	--	+32.0	---	+34.0	+36.5	+39.1	+40.3	+44.0	C
	σ_{tot}	45,842	--	24,574	--	31,040	39,139	47,881	51,337	63,416	C

* - C, Center of Panel E, Edge of Panel

TABLE 5

MAXIMUM VALUES FOR 60B20210 PANEL WITH CLAMPED EDGES											
		Ignition		Flight							
		Center $q=+2.7$ $\Delta T = 0$	Edge $q=+2.7$ $\Delta T = 0$	Center $q=+1.09$ $\Delta T = 0$	Edge $q=+1.09$ $\Delta T = 0$	$\Delta T = 80°$	$\Delta T=180°$	$\Delta T=280°$	$\Delta T=320°$	$\Delta T=450°$	*
Cup Panel $h_c=0.6"$	W_q	+.4444	---	-.1799	---	-.1799	-.1799	-.1799	-.1799	-.1799	C
	θ_{tot}	---	---	---	---	---	---	---	---	---	
	M_q	-173.7	-385.8	+ 70.1	+155.8	155.8	155.8	155.8	155.8	155.8	E
	$M_{\Delta T}$	---	---	---	---	56.3	126.9	200.7	233.2	338.5	E
	M_{noise}	-102.8	-102.8	+102.8	+102.8	102.8	102.8	102.8	102.8	102.8	E
	M_{tot}	-276.5	-488.6	-172.9	+258.6	314.9	385.5	459.3	491.8	597.1	E
	σ_Q	-139.5	-139.5	+75.8	+75.8	+78.7	+82.3	+86.0	+87.9	+93.0	E
	σ_{tot}	-45,328	-80,098	+28.344	+42,393	+51,623	+63,196	+75,295	+80,623	+97,885	
Cup Panel $h_c=1.0"$	W_q	+.1623	---	-.0655	---	-.0655	-.0655	-.0655	-.0655	-.0655	C
	Q_{tot}	---	---	---	---	---	---	---	----	---	
	M_q	-173.7	-385.8	+70.1	+155.8	+155.8	+155.8	+155.8	+155.8	+155.8	E
	$M_{\Delta T}$	---	---	---	---	+93.3	+210.2	+332.3	+386.2	+560.5	E
	M_{noise}	-102.8	-102.8	+102.8	+102.8	+102.8	+102.8	+102.8	+102.8	+102.8	E
	M_{tot}	-276.5	-488.6	+172.9	+258.6	+351.9	+468.8	+590.9	+644.8	+819.1	E
	σ_Q	-84.2	-84.2	+45.8	+45.8	+48.7	+52.2	+56.0	+57.8	+63.0	E
	σ_{tot}	-27,376	-48,376	+17,119	+25,604	+34,842	+46,416	+58,505	+63,842	+81,099	E

* E, Edge of Panel
  C, Center of Panel

TABLE 6

EDGE FIXITY FOR 60B20210 PANEL*
ELASTIC SUPPORT CONDITION

		Ignition		Flight						
		Center q=+2.7 ΔT=0	Edge q=+2.7 ΔT=0	Center q=-1.09 ΔT=0	Edge q=-1.09 ΔT=0	ΔT=80°	ΔT=180°	ΔT=280°	ΔT=320°	ΔT=450°
Cup Panel h_c=0.6"	$\Sigma M_{clamped}$		-385.8		+155.8	+212.1	+282.7	+356.5	+389.0	+494.3
	$\Sigma\theta_{simple\ support}$		-.0901		+.03639	+.04959	+.06599	+.08249	+.08909	+.11049
	K_p		4273		4273	4277	4284	4322	4366	4474
	K_p/K_F		.29193		.2595	.2597	.2601	.2625	.2651	.2717
	K_p/K_I		3.21109		2.83055	2.83320	2.83784	2.86301	2.89216	2.96370
	% E.F.		22.21		25.45	24.43	24.40	24.24	24.05	23.61
Cup Panel h_c=1.0"	$\Sigma M_{clamped}$	---	-385.8	---	+155.8	+249.1	+366.0	+488.1	+542.0	+716.3
	$\Sigma\theta_{simple\ support}$	---	-.0329	---	+.0133	+.0213	+.0313	+.0413	+.0453	+.0583
	K_p		11,714		11,714	11,695	11,693	11,818	11,965	12,286
	K_p/K_F		.8003		.7113	.7102	.7101	.7177	.7266	.7461
	K_p/K_I		8.80288		7.75967	7.74708	7.74576	7.82856	7.92594	8.13858
	% E.F.		9.43		10.56	10.57	10.57	10.48	10.36	10.12

*Panel, support beam flange and JM-146 insulation rotate. The spring constants are:

K_F = 14,637 Ignition, 16,467 Flight

K_I = 1330.7 Ignition, 1509.7 Flight

TABLE 7

MAXIMUM VALUES FOR 60B20210 PANEL
ELASTIC SUPPORT EDGE CONDITION

		Ignition		Flight						
		Center q=+2.7 ΔT=0	Edge q=+2.7 ΔT=0	Center q=-1.09 ΔT=0	Edge q=-1.09 ΔT=0	ΔT=80°	ΔT=180°	ΔT=280°	ΔT=320°	ΔT=450°
h_c=0.6"	W_q	+1.2134	---	-.4769	---	-.4810	-.4858	-.4818	-.4825	-.4842
	$W_{\Delta T}$	---	---	---	---	-.1587	-.3521	-.5568	-.6380	-.9022
	W_{tot}	+1.2134	---	-.4769	---	-.6397	-.8379	-1.0386	-1.1205	-1.3864
	θ_{tot}	---	-.0701	---	+.0271	+.0375	+.0499	+.0625	+.0677	+.0844
h_c=1.0"	W_q	+.4884	---	-.1955	---	-.1955	-.1956	-.1956	-.1945	-.1962
	$W_{\Delta T}$	---	---	---		-.1142	-.2569	-.4001	-.4578	-.6455
	W_{tot}	+.4884	---	-.1955	---	-.3097	-.4525	-.5957	-.6523	-.8417
	θ_{tot}		-.0298		+.0119	+.0190	+.0280	+.0370	+.0406	+.0524
		Panel Edge:								
h_c=0.6"	M_q	---	-85.7	---	+39.6	+38.1	+38.0	+37.8	+37.5	+36.8
	$M_{\Delta T}$		---		---	13.7	31.0	48.6	56.1	79.9
	M_{noise}		-22.8		26.2	25.1	25.1	24.9	24.7	24.3
	M_{tot}		-108.5		+65.8	+76.9	+94.1	+111.3	+118.3	+141.0
	σ_{tot}		-17,787		+10,787	12,606	15,426	18,246	19,393	23,115
h_c=1.0"	M_q		-36.4		16.4	16.5	16.5	16.3	16.1	15.8
	$M_{\Delta T}$		---	---	---	5.9	13.4	21.0	24.2	34.3
	M_{noise}		-9.7		10.8	10.8	10.8	10.8	10.6	10.4
	M_{tot}		-46.1		+27.2	+33.2	+40.7	+48.1	+50.9	+60.5
	σ_{tot}		-4,564		+2,693	3,287	4,030	4,762	5,040	5,990
		Panel Center:								
h_c=0.6"	M_q	-318.8	---	+126.2	---	+127.0	+127.0	+127.1	+127.3	+127.6
	$M_{\Delta T}$	---		---		29.8	67.2	106.4	124.0	181.0
	M_{noise}	-102.8		102.8		102.8	102.8	102.8	102.8	102.8
	M_{tot}	-421.6		+229.0		+259.6	+297.0	+336.3	+354.1	+411.4
	σ_{tot}	-69,115		+37,541		42,557	48,688	55,131	+58,049	67,442
h_c=1.0"	M_q	-342.6		+137.4		+137.4	+137.4	+137.5	+137.6	+137.8
	$M_{\Delta T}$	---		---		35.2	79.5	125.8	146.4	212.9
	M_{noise}	-102.8		102.8		102.8	102.8	102.8	102.8	102.8
	M_{tot}	-445.4		+240.2		+275.4	+319.7	+366.1	+386.8	+453.5
	σ_{tot}	44,099		23,782		27,267	31,653	36,247	38,297	44,901

TABLE 8

MAXIMUM VALUES FOR 30M12571 ZEE EDGE PANEL
1.0" CORE THICKNESS

		Ignition		Flight						
		Center q=+2.7 ΔT=0	Edge q=+2.7 ΔT=0	Center q=-1.09 ΔT=0	Edge q=-1.09 ΔT=0	ΔT=80°	ΔT=180°	ΔT=280°	ΔT=320°	ΔT=450°
h_c = 1.0"	W_q	+.3712		-.1499		-.1499	-.1499	-.1499	-.1499	-.1499
	$W_{\Delta T}$	---		---		-.1076	-.2421	-.3766	-.4304	-.6052
	θ_q		-.0254		+.0103	-.0103	-.0103	-.0103	-.0103	-.0103
	$\theta_{\Delta T}$		--		--	+.0073	..0165	.0257	.0294	+.0413
	M_q	-303.5		+122.5		122.5	122.5	122.5	122.5	122.5
	$M_{\Delta T}$	---		---		65.3	147.1	235.4	270.3	392.3
	M_{noise}	102.8		102.8		102.8	102.8	102.8	102.8	102.8
	M_{tot}	-406.3		+225.3		290.6	372.4	460.7	495.6	617.6
	W_{tot}	+.3712		-.1499		-.2575	-.3920	-.5265	-.5803	-.7551
	θ_{tot}		-.0254		+.0103	+.0176	+.0268	+.0360	+.0397	+.0516
	$\sigma\theta$	-53.9		+29.3		+31.5	+34.2	+37.1	+38.3	+42.4
	σ_{tot}	-40,228		+22,307		28,772	36,871	45,614	49,069	61,148

TABLE 9

MAXIMUM BENDING STRESSES IN EDGE MEMBER
FOR 30M12571 PANEL, ZEE EDGE MEMBER 1.0" CORE THICKNESS

	θ_p	h_z=.060	h_z=.050	h_z=.045	h_z=.040	h_z=.030	h_z=.020
	Ignition Condition						
I_z		18^{-6}	10.42^{-6}	7.59^{-6}	5.34^{-6}	2.25^{-6}	0.666^{-6}
θ_p	.0254						
θ_z		.0503	.0870	.1192	.1694	.4022	1.3580
$\Delta\theta$		-.0249	-.0616	-.0938	-.1440	-.3768	-1.3326
M_q		52.58	52.58	52.58	52.58	52.58	52.58
$M_{\Delta\theta}$		13.58	19.45	21.57	23.30	25.70	26.90
M_{total}		39.0	33.13	31.01	29.28	26.88	25.68
σ_z		65,000	79,486	91,927	109,663	179,200	385,200
	Flight Condition						
θ_z		.0203	.0363	.0510	.0708	.1680	.5670
M_q		21.23	21.23	21.23	21.23	21.23	21.23
$\Delta\theta$-0° ΔT	.0103	-.0100	-.0260	-.0407	-.0605	-.1577	-.5567
180°	.0268	+.0065	-.0095	-.0242	-.0440	-.1412	-.5402
280°	.0360	+.0157	-.0003	-.0150	-.0348	-.1320	-.5310
320°	.0397	+.0194	+.0034	-.0113	-.0311	-.1283	-.5273
450°	.0516	+.0313	+.0153	+.0006	-.0192	-.1164	-.5154
$M_{\Delta\theta}$-0° ΔT		-5.45	-8.21	-9.36	-9.79	-10.75	-11.25
180°		+3.54	-3.00	-5.59	-7.12	-9.63	-10.91
280°		8.56	-0.09	-3.45	-5.63	-9.00	-10.93
320°		10.58	+1.07	-2.60	-5.03	-8.75	-10.65
450°		17.07	4.83	+0.14	-3.11	-7.94	-10.41
M_{total}-0° ΔT		15.78	13.02	11.87	11.44	10.48	9.98
180°		24.77	18.23	15.66	14.11	11.60	10.32
280°		29.79	21.14	17.78	15.60	12.23	10.50
320°		31.81	22.30	18.63	16.20	12.48	10.58
450°		38.30	26.06	21.37	18.12	13.29	10.82
σ_z-0° ΔT		26,289	31,235	35,183	42,843	69,860	149,700
180°		41,267	43,734	46,416	52,842	77,326	154,800
280°		49,630	50,715	52,700	58,422	81,525	159.500
320°		52,995	53,498	55,219	60,669	83,192	158,700
450°		63,808	62,518	63,341	67,859	88,591	162,300

NOTE: The value of the moment arm ℓ used for the zee calculations was 0.957", the distance from center line of mounting hole to the vertical leg of the zee.

SECTION III

DESIGN PARAMETERS FOR BRAZED HONEYCOMB HEAT SHIELD PANELS WITH SIMPLY SUPPORTED EDGES

Air Load Deflection

Figure 26 shows the deflection at the center of panel versus core thickness for an air load q of 2.7 psi, for the ignition condition. This graph can be used for determining the face sheet thickness and core thickness for a given deflection.

Thermal Deflection

Figure 27 shows thermal deflection at center of panel versus height of panel for various temperature differences. This graph shows the thermal deflection pattern for constant temperature differences. The lower panel height gives the greater influence on deflection.

Combined Deflection

Figures 28 and 29 show the combined thermal and air deflections versus height of panel for constant temperature difference, air load, and face sheet thickness and also give deflection for constant air load without temperature differences.

Figure 30 shows the same information as Figures 28 and 29, but is plotted in a different form to show the pattern of the temperature difference.

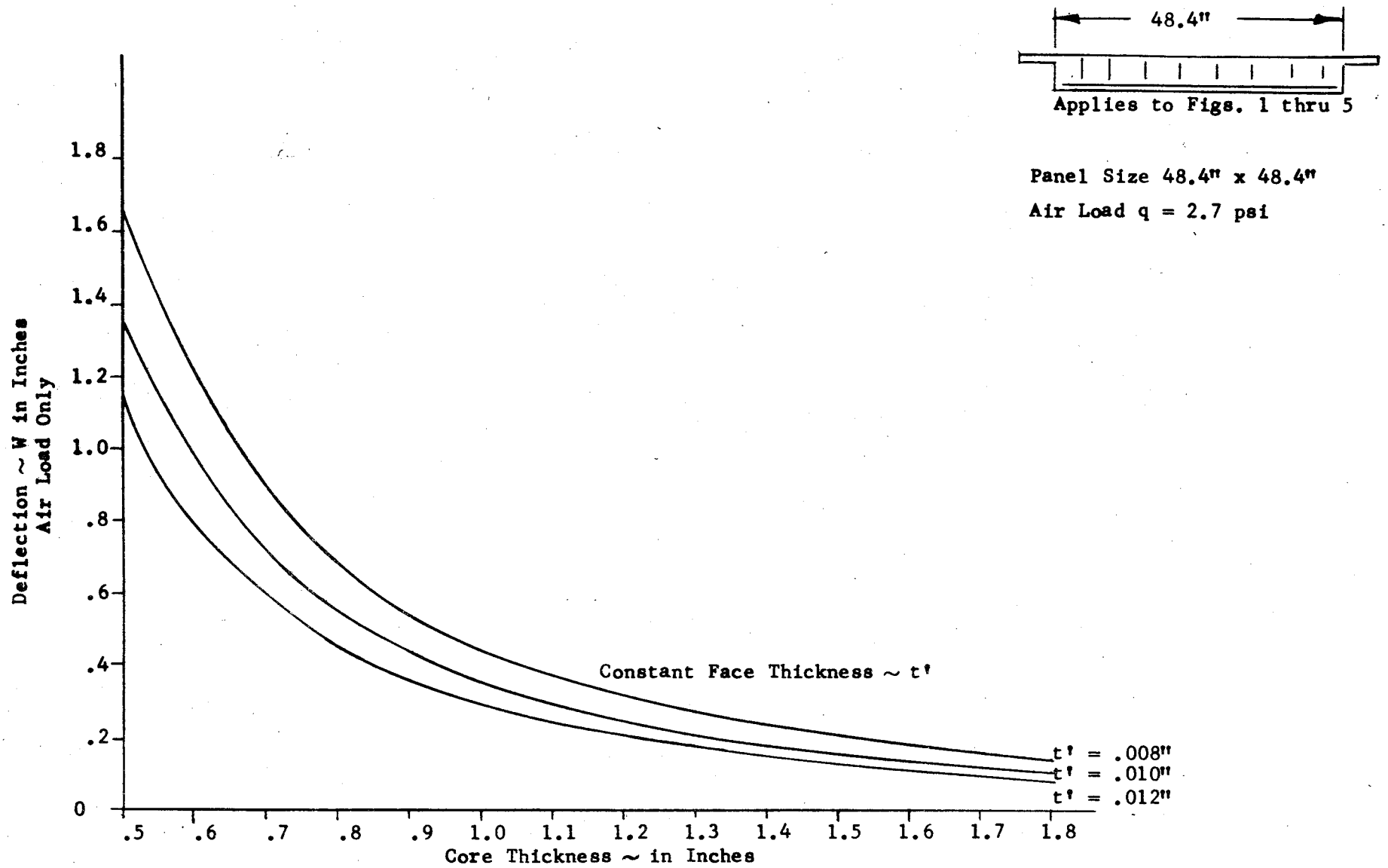

Figure 26 Deflection at Center of Panel Vs. Core Thickness

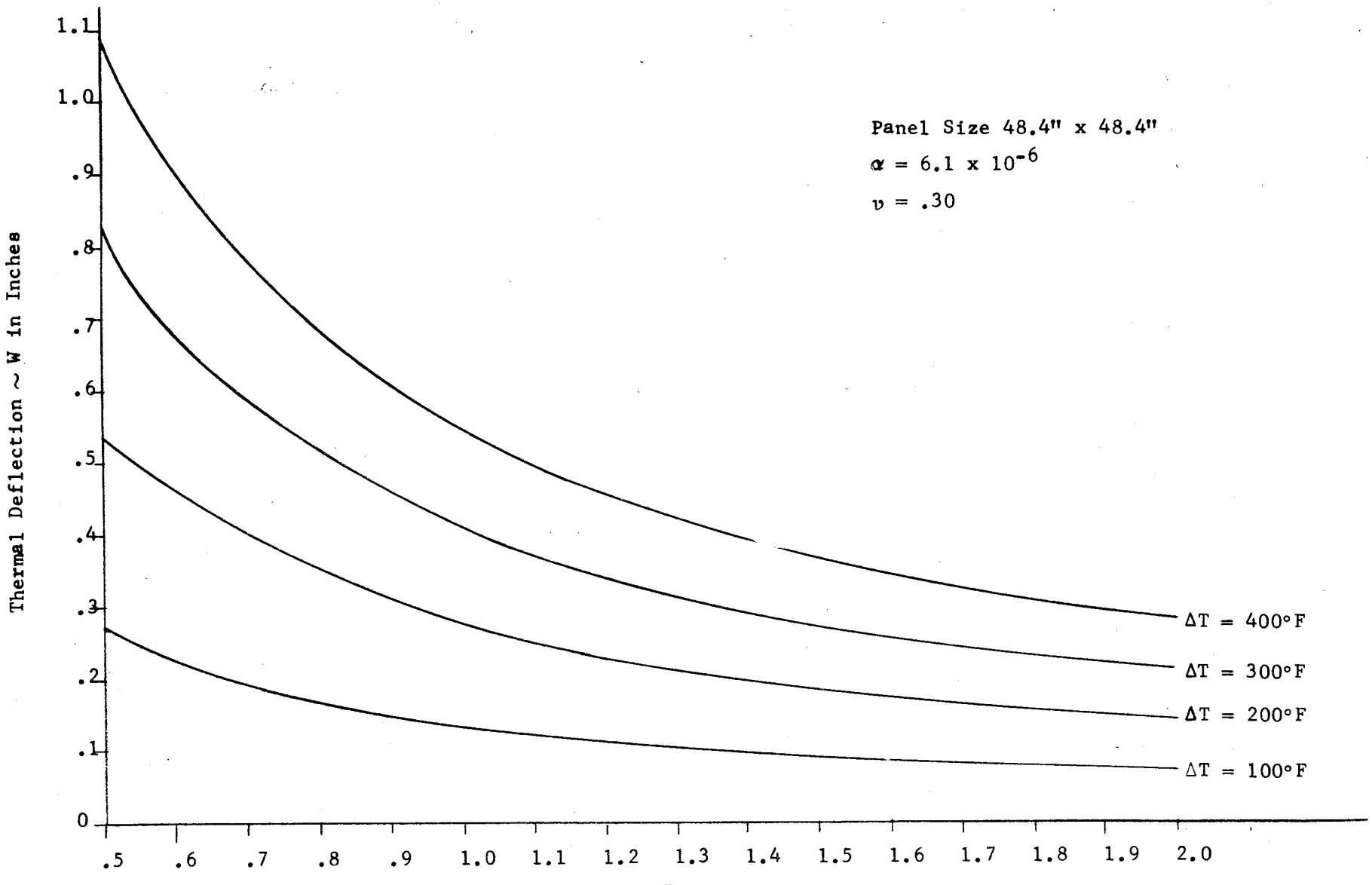

Figure 27 Thermal Deflection at Center of Panel Vs. Height of Panel for Constant Temperature Differences

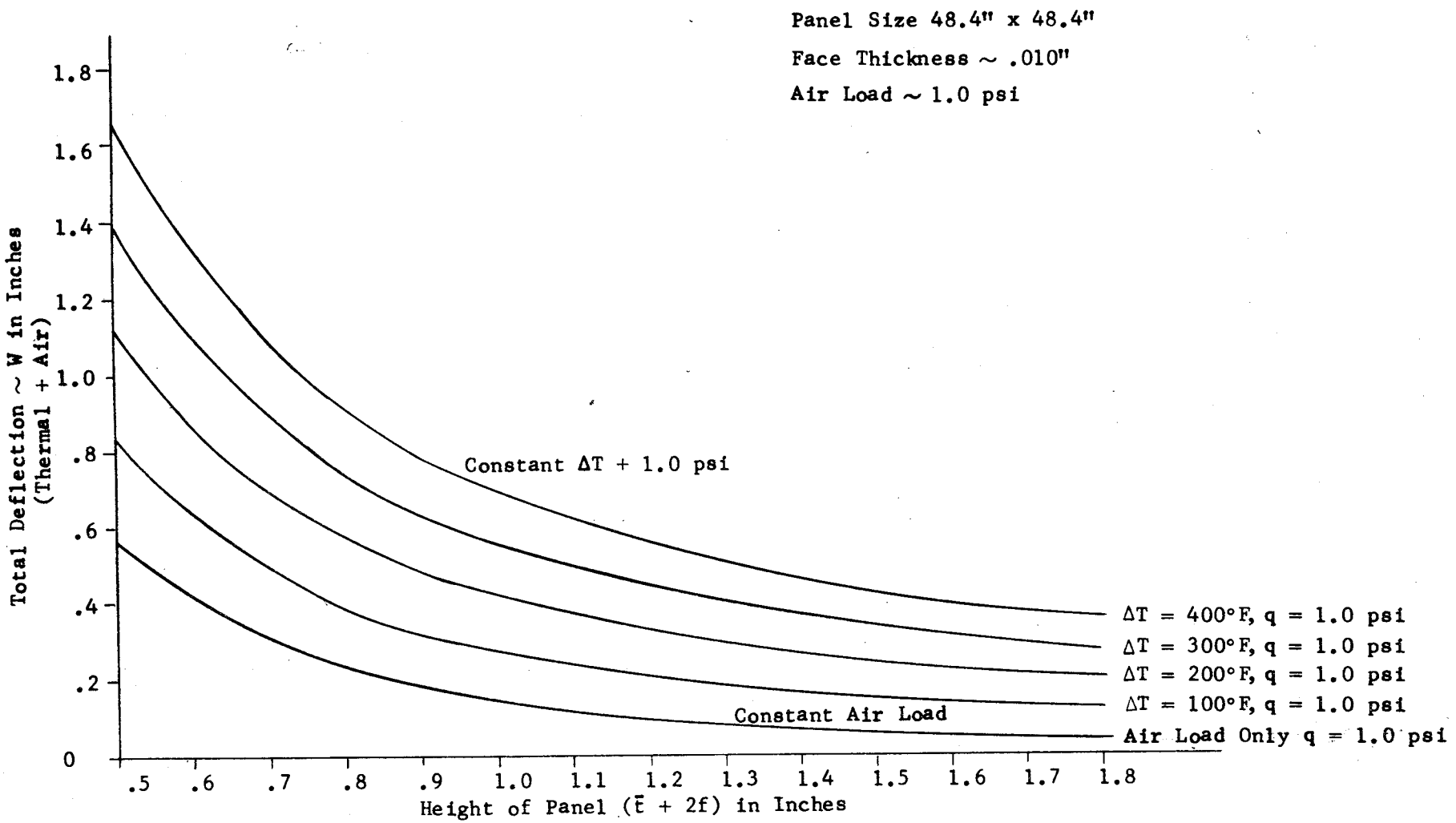

Figure 28 Thermal + Air Load Deflection at Center of Panel Vs. Height of Panel For Constant Temperature Differences and 1 psi

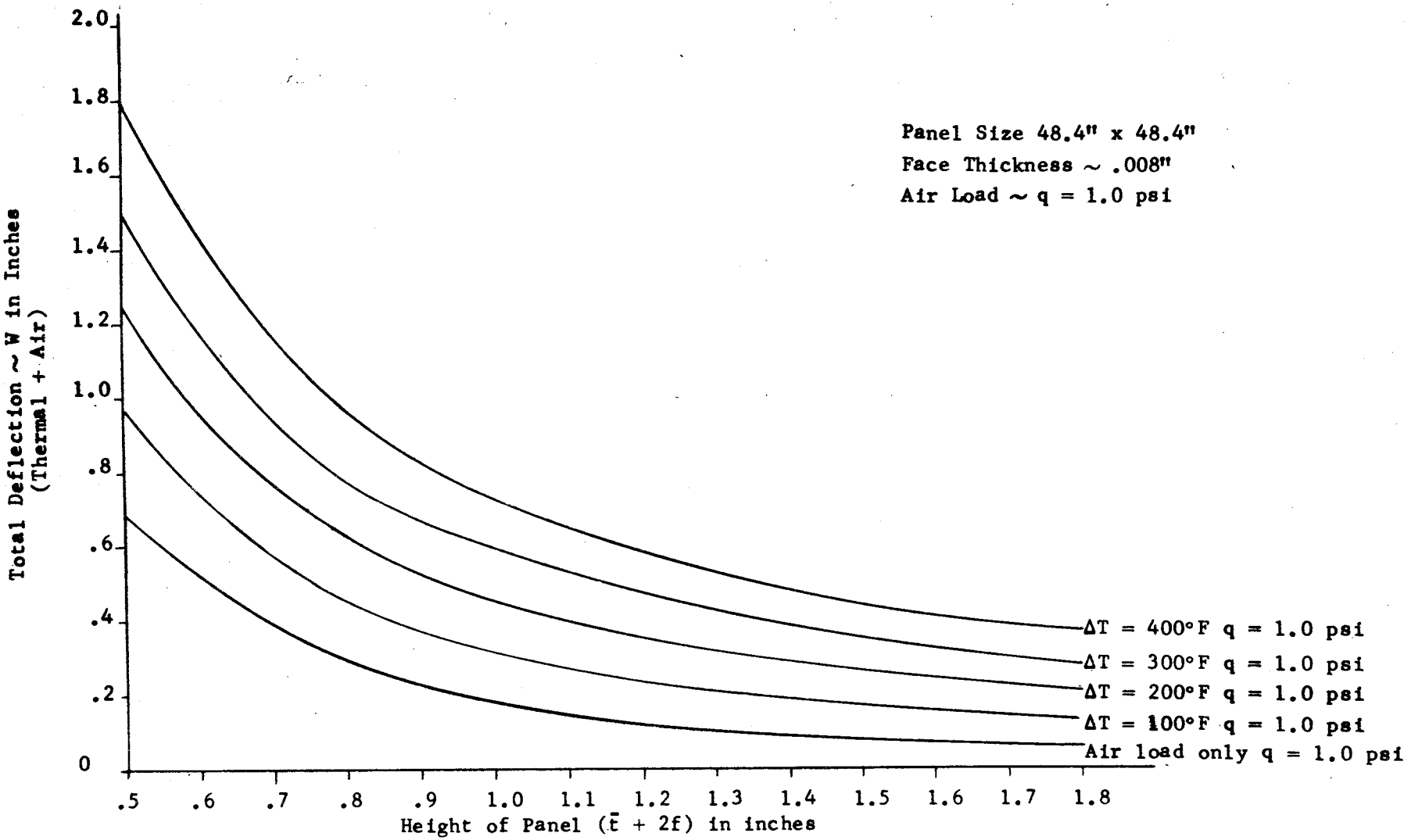

Figure 29 Thermal + Air Load Deflection at Center of Panel Vs. Height of Panel - For Constant Temperature Differences and 1 psi

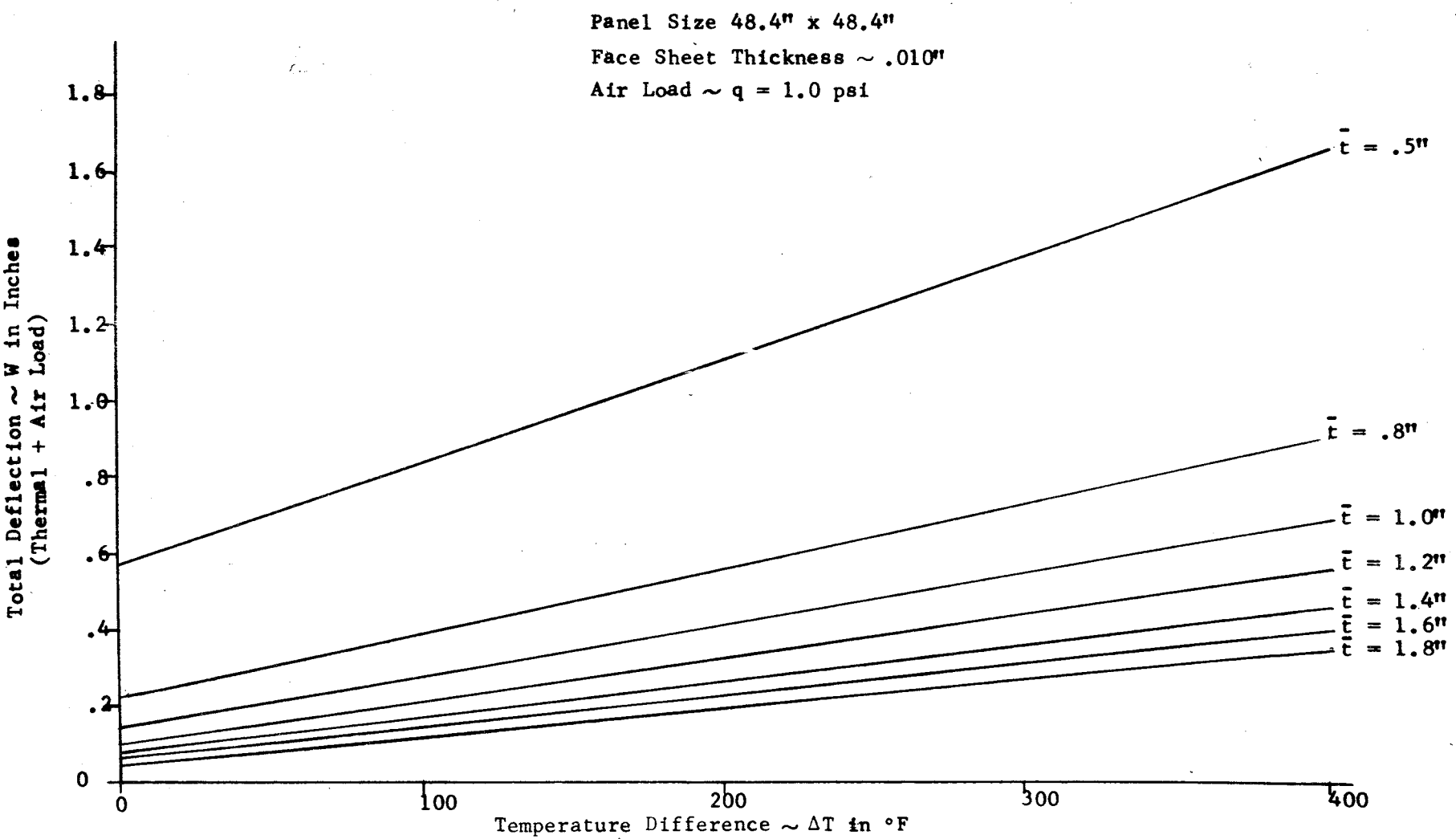

Figure 30 Thermal + Air Load Deflection at Center of Panel Vs. Temperature Difference For Constant Core Thickness ($\bar{t}$)

SECTION IV

APPLICATION OF BERYLLIUM TO HEAT SHIELD PANELS

Preliminary Analysis of Zee Section Edge Member Heat Shield Panel with Beryllium Facings and Edge Members

The use of cross rolled beryllium sheet components for facings and edge members were evaluated for potential heat shield panel application using the 30M12571 panel design as a basis.

Panel stresses, deflections and margins for the ignition and flight conditions are given in Table 10.. The critical item from a stress view point is the relatively high stress in the zee section edge member which would require a minimum thickness of .08".

The allowables for silver brazed beryllium sheet employed were:

f_{t_u} = 50,000 psi

f_{t_y} = 35,000 psi

% Elongation = 1-2½%

and reflect our experience in beryllium brazing and fabrication*. These values for .04" gage material are substantially less than the allowables for unbrazed beryllium sheet, which presently are:

f_{t_u} = 70,000 psi

f_{t_y} = 50,000 psi

% Elongation = 5%.

The reduction in strength and loss of ductility results principally from the the reaction between the beryllium and the silver brazing alloy (99.5Ag-.5Li) and cannot be eliminated or further minimized with presently available brazing methods or brazing alloys within the current state of art. Current studies being conducted at Aeronca are aimed at the development of low melting braze alloys for beryllium. A reduction of braze temperatures below recrystallization and diffusion temperatures would overcome many of the problems which cause embrittlement and loss of strength. The braze alloy compositions which show the greatest promise in this regard would either be zinc base or aluminum base with zinc additions.

*Contract AF 33(657)-7151,
Sheet Beryllium Composite Structures

TABLE 10

DEFLECTION AND STRESS CHARACTERISTICS OF THE 30M12571 PANEL DESIGN

WITH BERYLLIUM FACINGS AND EDGE MEMBERS

Load Condition	Panel Configuration	Deflection at Center	Facing Stress	Edge Member Thickness	Edge Member Stress	Edge Member ℓ_1*	Edge Member M.S.*
FLIGHT	1.0" Core	0.232"	20,370 psi E (edge)	.02	47,260	.813	-.33
1.0 psi + 180°F ΔT	.03" Be Faces		13,816 psi C (center)	.03	43,130	1.069	-.26
	& Edge Members			.04	39,930	1.347	-.20
	Cell Size 4-15			.05	37,350	1.646	-.15
				.06	35,210	1.964	-.10
				.07	33,260	2.310	-.04
				.08	31,850	2.654	+.00
						$\frac{\ell_1}{1.043}$	
	1.0" Core	0.216"	20,187 psi E	.02	42,100		-.24
	.04" Be Faces		12,791 psi C	.03	38,950	1.315	-.18
	& Edge Members			.04	36,450	1.606	-.13
	Cell Size 4-15			.05	34,350	1.917	-.07
				.06	32,590	2.245	-.02
				.07	31,080	2.590	+.02

*ℓ_1 - Distance from bolt center to vertical leg of zee.

*M.S. - Margin of Safety based on a load factor of 1.1 and yield strength

Material: Beryllium, Room Temperature, After Brazing

f_{tu} 50,000 psi

f_{ty} 35,000 psi

TABLE 11

DEFLECTION AND STRESS CHARACTERISTICS OF THE 30M12571 PANEL DESIGN WITH BERYLLIUM FACINGS AND EDGE MEMBERS

Load Condition	Panel Configuration	Deflection At Center	Facing Stress	Thickness	Stress	ℓ_2*	M.S.*
IGNITION 2.7 psi, Zero ΔT	1.0" Core .03" Be Faces & Edge Members	0.096"	9,806 psi C (center)	.02	44,860	0.286	-.29
				.03	40,950	0.376	-.223
				.04	37,910	0.474	-.16
				.05	35,460	0.579	-0.10
				.06	33,430	0.691	-.05
				.07	31,720	0.809	+.002
	1.0" Core .04" Be Faces & Edge Members	0.071"	7,284 psi C			ℓ_2	
				.02	35,110	.322	-.09
				.03	32,540	.406	-.02
				.04	30,380	.497	+.05
				.05	28,690	.592	+.11
				.06	27,200	.694	+.17
				.07	25,920	.801	+.23

*ℓ_2 - Distance from vertical leg of zee to edge of support beam flange.

*M.S. - Margin of Safety based on a load factor of 1.1 and yield strength.

Material: Beryllium, Room Temperature, After Brazing
(Facing)

f_{tu} 50,000 psi

f_{ty} 35,000 psi

Core: PH15-7Mo Material

Other characteristics of beryllium which make it undesirable for brazed heat shield panels are:

1. The high modulus, 43,000,000 psi, while desirable for stiffness is undesirable for thermal loads which produce a high thermal moment. This high moment along with the relatively low strength of beryllium soon produces stresses comparable to the yield or ultimate of the material.

2. The highly directional tensile properties of beryllium sheet, with low ductility in the short transverse direction, results in a sharply limited and unpredictable capacity to accept multi-axial loads without catastrophic failure. Consequently, an extensive test program would be required to support a production design.

3. The maximum width sheet at present is 36" which would require a load carrying splice. The poor welding characteristics of beryllium and erratic joint properties preclude the use of fusion welding; consequently, the facing sheet splices would have to be accomplished during the panel brazing and would consist of a butt joined sheet with a brazed on doubler reinforcement. For the open faced core side of the panel, the reinforcing doubler would probably have to be located in a rabbet machined in the load bearing honeycomb core (at increased cost).

4. The susceptibility of beryllium sheet in the large sizes required and in gages less than .04" to breakage during shop handling imposes additional fabrication problems.

5. An experimental program to determine the material allowables for brazed beryllium sheet for a range of thicknesses would be required as well as an optimum brazing cycle for beryllium panels of this size (53"x53").

As a consequence of the foregoing considerations, the use of beryllium sheet is not recommended for brazed honeycomb sandwich heat shield panels within the present state of art.

Preliminary Analysis of Heat Shield Panel with Beryllium Facings and Cup Type Edge Attachments per drawing 60B20210

The use of cross rolled beryllium sheet facings was evaluated for potential use in the cup type edge heat shield panel design shown in NASA drawing No. 60B20210 based on the following assumptions:

1. A facing gage of .030" beryllium sheet, load bearing core Type 4-15 PH 15-7 Mo 1.0" thick

2. Allowables for brazed beryllium sheet using a brazing alloy of fine silver with 0.5% lithium.

f_{t_u} = 50,000 psi

f_{t_y} = 35,000 psi

% Elongation in 2" = 1-2½%

E = 43×10^6 psi at R.T.

E = 37×10^6 psi at 600°F

υ = 0.1

Panel stresses, deflections and margins were calculated for the flight conditions at four levels of edge fixity and are given in Tables 12 and 13. The compressive stresses in the honeycomb core area under the cup flange were also calculated for the same loading conditions and three levels of edge fixity (Tables 14 and 15).

Based on any degree of edge fixity and 180° ΔT representative of the 100% node flow condition this panel design shows positive margins for .03" beryllium sheet facings. As the thermal gradient increases, the margins decrease rapidly as shown in Table 13 for a 320°F ΔT representative of the zero node flow condition; however, small positive margins exist for most of the edge fixity conditions. Consequently, the use of beryllium facings of cross rolled beryllium sheet .03" thick appear feasible from a stress viewpoint for this panel design. However, the use of beryllium sheet facings in this application is subject to the same qualifications (items 1 thru 5) previously noted and is not considered to be a suitable material for brazed honeycomb sandwich heat shield panels.

Compression load on insulation (JM-146)

$$\frac{P}{A} = \frac{M}{C \cdot \ell \cdot W} = \frac{16}{.6 \times .9 \times 1} = 30 \text{ psi}$$

Simply Support Edge Condition

$$W_A = \frac{.00406 \times 1.0 \times \overline{50.978}^4}{624,018} = .044"$$

$$W_T = \frac{\alpha \Delta T (1+\upsilon) 4a^2 .5708}{\pi^3 h} = \frac{6.0 \times 10^{-6} \times 180 \times 1.1 \times 4 \times \overline{50,978}^2 \times .5708}{32.86654}$$

W_T = .214"

W_{TOTAL} = .258"

TABLE 12

DEFLECTION AND STRESS CHARACTERISTICS
OF THE 60B20210 PANEL DESIGN WITH BERYLLIUM FACINGS

Load Condition - Flight 10 psi + 180° ΔT

Edge Fixity	Deflection W (inches at center)	Moment M ($\frac{\text{in-lb}}{\text{in}}$)	Bearing Stress f_b (psi)	Margin of Safety M. S.
100%	.012	832E	26,926E	+0.18
94.91	0.172	286C	9,256	+2.44
		290E	9,385	+2.39
		409E	13,236	+1.40
*1.927	0.253C	431C	13,948	+1.28
		16E	518	+ very large
		617E	19,968	+0.59
0%	0.258C	439C	14,207	+1.24
		629E	20,356	+0.56

* Beam flanges, flange insulation and panel rotate.

M.S. based on a load factor of 1.1 and yield strength.

Moment is normal to panel surface.

Material: Beryllium, Room Temperature, After Brazing (Facing)

f_{tu} 50,000 psi

f_{ty} 35,000 psi

Core: PH15-7Mo Material

TABLE 13

DEFLECTION AND STRESS CHARACTERISTICS
OF THE 60B20210 PANEL DESIGN WITH BERYLLIUM FACINGS

Load Condition - Flight 10 psi air load + 1.15 psi dynamic (2.15 psi) plus 320° ΔT

Edge Fixity	Deflection W (inches at center)	Bending Moment M ($\frac{\text{in-lb}}{\text{in}}$)	Bearing Stress f_b (psi)	Margin of Safety M. S.
100%	0.027	1530E	49,515E	-0.36
34.91%	0.319	539C	17,443C	+0.82
	0.319	534E	17,282E	+0.84
*2.514%	0.464	807C	26,117C	+0.22
	0.464	38E	1,230E	+ very large
		1091E	35,307E	-0.10
0%	0.475	828C	26,796C	+0.19

* Beam flange, flange insulation and panel rotate.

M.S. based on a load factor of 1.1 and yield strength.

Moment is normal to panel surface.

Material: Beryllium, Room Temperature, After Brazing
(Facing)

f_{tu} 50,000 psi

f_{ty} 35,000 psi

Core: PH15-7Mo Material

TABLE 14

COMPRESSIVE STRESS IN HONEYCOMB CORE
FOR 60B20210 PANEL DESIGN WITH BERYLLIUM FACINGS

Loading Condition	Edge Fixity	Compressive Stress in core area under cup flange (psi) (PH15-7Mo Material)	Core Compression Allowable Stress
1. Flight 1.0 psi + 180° ΔT (100% node flow)	100%, beam flange, panel and flange insulation rigid	7,371 psi	(PH15-7Mo Material) RT-760 psi 340° - 722 psi 600° - 675 psi for Type 4-15 core. Ref: NAA Structural Design Manual
	34.91% beam flange and panel rotate flange insulation rigid	2,570 psi	
	1.927% beam flange panel and insulation rotate	142 psi	

Material: (Facing) Beryllium, Room Temperature, After Brazing

f_{tu} 50,000 psi

f_{ty} 35,000 psi

TABLE 15

COMPRESSIVE STRESS IN HONEYCOMB CORE
FOR 60B20210 PANEL DESIGN WITH BERYLLIUM FACINGS

Loading Condition	Edge Fixity	Compressive Stress in core area under cup flange (psi) (PH15-7Mo Material)	Core Compression Allowable
Flight **1.0 psi air load plus 1.15 psi dynamic load (2.15 psi) plus 320°ΔT (zero node flow)**	**100% beam flange, panel and flange insulation rigid**	13,547	(PH15-7Mo Material) RT - 760 psi 340° - 722 psi 600° - 675 psi for Type 4-15 core. Ref: NAA Structural Design Manual.
	34.91% beam flange and panel rotate flange insulation rigid	4,731	
	2.514% beam flange, panel insulation rotate	340	

Material: Beryllium, Room Temperature, After Brazing
(Facing)

f_{tu} 50,000 psi

f_{ty} 35,000 psi

$$M_A = .0479\ q\ a^2 = .0479 \times 1.0 \times \overline{50.978}^2 = 124.48 \text{ in-lbs/in at center of panel}$$

$$M_T = \frac{\alpha\ \Delta T(1-\nu^2)D}{h} = \frac{180 \times 6.0 \times 10^{-6} \times .99 \times 624{,}018}{1.06} = 629.43 \text{ in-lbs/in at edge of panel}$$

Clamped Edge Condition

$$W_T = 0$$

$$W_A = \frac{.0137 \times q \times a^4}{12 \times D(1-\nu^2)} = \frac{.0137 \times 1.0 \times \overline{50.978}^4}{12 \times 624{,}018 \times .99} = .012"$$

$$M_A = .0513\ q\ a^2 = .0513 \times 1.0 \times \overline{50.978}^2 = 133 \text{ in-lbs/in at edge of panel}$$

$$M_T = \frac{\alpha\ \Delta T\ D\ (1+\nu)}{h} = \frac{6.0 \times 10^{-6} \times 180 \times 624{,}018 \times 1.1}{1.06} = 699 \text{ in-lbs/in at edge of panel}$$

$$M_{total} = 832 \text{ in-lbs/in at edge}$$

Then the edge moment of panel with 34.91% fixity is:

$$M = 832 \times .3491 = 290 \text{ in-lbs/in.}$$

Load reacted by cup:

$$p = \frac{290 \times 7.463}{.9} = 2405 \text{ lbs/cup}$$

Compression load on panel core:

$$\frac{2405}{.93593} = \underline{\underline{2570 \text{ psi}}}$$

Assume rotation of panel, flange and insulation

Use K = 3,086 lb/in-in^2 (25-50 psi)

$$C = .60" \qquad \ell = .90"$$

$$K_1 = \frac{CK\ell^2}{2} = \frac{.6 \times 3086 \times \overline{.9}^2}{2} = 750 \text{ in-lbs/in/Rad.}$$

K_p = 36,753 in-lbs/in/Radian

K_F = 19,711 in-lbs/in/Radian

K_l = 750 in-lbs/in/Radian

$$\text{Edge Fixity} = \frac{1}{\frac{36,753}{750} + \frac{36,753}{19,711}} = \frac{1}{51.86859} = 1.927\%$$

M = 832 x .01927 = 16 in-lbs/in

Load reacted by cup:

$$p = \frac{16 \times 7.463}{.9} = 133 \text{ lbs/cup}$$

Compression load on panel core:

$$\frac{133}{.93593} = 142 \text{ psi}$$

Detail Calculations

.030" Beryllium facing and Flight Condition $\Delta T = 180°$, q = 1.0 psi panel 50.928" $\mathcal{L}$ of fasteners.

f_{t_y} = 35,000 psi

f_{t_u} = 50,000 psi

α = 6.0×10^{-6} (RT-500)

E = 43×10^6 RT psi

E = 37×10^6 600°F psi

ν = .1

M = .94736 in-lbs/in

$$D = \left[\frac{\overline{1.03}^2}{1.94736}\right]\left[\frac{37.8 \times 10^6 \times .030}{1 - t^2}\right]$$

D = 624,018 in/lb.

Assume no rotation:

$$M_T = \frac{6.0 \times 10^{-6} \times 180 \times 624,018\ (1.1)}{1.06} = 699 \text{ in-lbs/in}$$

$$M_A = .0513 \times 1.0 \times \overline{50.978}^2 = 133 \text{ in-lbs/in}$$

$$M_{total} = 832 \text{ in-lbs/in}$$

Load reacted at cup:

$$p = \frac{832 \times 7.463}{.9} = 6,899 \text{ lbs/cup}$$

Compression load on panel core:

$$\frac{6899}{.93593} = 7,371 \text{ lb/in}^2$$

Assume the insulation to be incompressible and allow the flange and panel rotate.

Assume the spring rate of the panel is the average of the pressure and thermal condition.

Thermal

$$K_p = \frac{M_{clamp}}{\theta_{Free}} = \frac{\alpha\ \Delta T\ D(1+\nu)\ 2h}{h\ a\ \alpha\ \Delta T} = \frac{2D(1+\nu)}{a}$$

$$K_p = \frac{2x624,018x1.1}{50.978} = 26,930 \text{ in-lbs/in/Radian}$$

Pressure

$$K_p = \frac{M_{clamp}}{\theta_{S.S.}} = \frac{.0513 \times \pi^4 \times D}{1.31330\ a} = \frac{.0513 \times \pi^4 \times 624,018}{1.31330 \times 50.978}$$

$$K_p = 46,576 \text{ in-lb/in/Radian}$$

Use average spring rate:

$$K_p = \frac{46,576 + 26,930}{2} = 36,753 \text{ in-lb/in/Radian}$$

Flange spring rate:

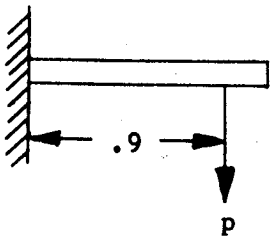

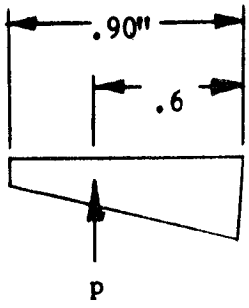

ℓ = .90"

C = .60"

$$K_F = \frac{M}{\theta_F} = \frac{M\ 2EI}{M\ell} = \frac{2 \times 10 \times 10^6 \times 887 \times 10^{-6}}{.9} = 19,711 \text{ in-lb/in. Rad.}$$

$$E.F. = \frac{\theta_P}{\theta_{total}} = \frac{\theta}{\theta_P \left(\frac{K_P}{K_F} + 1 \right)} = \frac{1}{\frac{K_P}{K_F} + 1}$$

$$E.F. = \frac{1}{\frac{36,753}{19,711} + 1} = \frac{1}{2.86459} = 34.91\%$$

Flight Condition:

q = 2.15 $\qquad$ $\Delta T = 320°F$

.030 Beryllium Facing

Panel size 50.978 $\mathbb{Q}$ of bolts

D = 624,018

Assume no rotation:

$$M_T = \frac{6.0 \times 10^{-6} \times 320 \times 624,018 \times 1.1}{1.06} = 1243 \text{ in-lbs/in}$$

$$M_A = .0513 \times 2.15 \times \overline{50.978}^2 = 286 \text{ in-lbs/in.}$$

$$M_{total} = 1529 \text{ in-lbs/in}$$

Load reacted at cup:

$$p = \frac{1529 \times 7.463}{.9} = 12,679 \text{ lbs/cup}$$

Compression load on panel core:

$$\frac{12,679}{.93593} = 13,547 \text{ lb/in}^2$$

Assume the insulation to be incompressible and allow the flange and panel to rotate.

Assume the spring rate of the panel is the average of the pressure and thermal condition.

Thermal

$$K_p = \frac{M}{\theta} = \frac{2D(1+\mu)}{a}$$

$$K_p = \frac{2 \times 624,018 \times 1.1}{50,978} = 26,930 \text{ in-lb/in/Radian}$$

Pressure

$$K_p = \frac{.0513 \times \pi^4 \times 624,018}{1.31330 \times 50.978} = 46,576 \text{ in-lb/in/Radian.}$$

Average: $K_p = \frac{46,576 + 26,930}{2} = 36,753$ in-lb/in/Radian

Flange spring rate:

$K_F = 19,711$ in-lb/in/Radian.

E.F. = 34.91% same as above (page 65)

Then the edge moment of panel with 34.91% fixity is:

$M = 1529 \times 34.91\% = 534$ in-lb/in.

Load reacted by cup:

$$p = \frac{534 \times 7.463}{.9} = 4,428 \text{ lbs/cup}$$

Compression load on panel core:

$$\frac{4428}{.93593} = \underline{4,731 \text{ psi}}$$

Assume rotation of panel, flange, and insulation.

Use K = 4098 (50-75 psi) Ref.

$C = .6"$ $\ell = .90"$

$$K_i = \frac{CK\ell^2}{2} = \frac{.6 \times 4098 \times \overline{.9^2}}{2} = 996 \text{ in-lb/in Radians}$$

$K_p = 36,753$ in-lb/in. Radians

$K_F = 19,711$ in-lb/in. Radians

$K_i = 996$ in-lb/in. Radians

$$E.F. = \frac{1}{\frac{36,753}{996} + \frac{36,753}{19,711} + 1} = \frac{1}{39.76519} = 2.514\%$$

$M = 1529 \times .02514 = 38.4$ in-lb/in.

Load reacted by cup:

$$p = \frac{38.4 \times 7.463}{.9} = 318 \text{ lbs/cup}$$

Compression load on panel core:

$$\frac{318}{.93593} = 340 \text{ psi}$$

Compression load on insulation (JM-146)

$$\frac{P}{A} = \frac{M}{C \cdot \ell \cdot W} = \frac{38.4}{.6 \times .9 \times 1} = 71 \text{ psi}$$

which is within the limits (50-75 psi) assumed above.

Simply Supported Edge Condition:

$q = 2.15$ psi $\Delta T = 320°F$

$$W_A = \frac{.00406 \times 2.15 \times \overline{50.978^4}}{624,018} = .094"$$

$$W_T = \frac{\alpha \Delta T(1+\nu)\, 4a^2 \cdot .5708}{\pi^3 h} = \frac{6.0 \times 10^{-6} \times 320 \times 1.1 \times 4 \times \overline{50.978^2} \times .5708}{32.86654}$$

$W_T = .381"$

$W_{total} = .475"$

$$M_A = .0479\ q\ a^2 = .0479 \times 2.15 \times \overline{50.978}^2 = 268 \text{ in-lb/in center of panel}$$

$$M_T = \frac{\alpha\ \Delta T\ (1-\nu^2)D}{h} = \frac{6.0 \times 10^{-6} \times .99 \times 320 \times 624{,}018}{1.06} = 1119 \text{ in-lb/in at edge of panel.}$$

Clamped Edge Condition:

$q = 2.15$ psi $\qquad \Delta T = 320°F$

$W_T = 0$

$$W_A = \frac{.0137 \times 2.15 \times \overline{50.978}^4}{12 \times 624{,}018 \times .99} = .027"$$

$$M_A = .0513 \times 2.15 \times \overline{50.978}^2 = 287 \text{ in-lb. edge}$$

$$M_T = \frac{6.0 \times 10^{-6} \times 320 \times 624{,}018 \times 1.1}{1.06} = 1243 \text{ in-lb. edge}$$

$M_{total} = 1530$ in-lb/in.

Preliminary Design Considerations for Beryllium Faced Honeycomb Sandwich Heat Shield Panels

Based on the previously indicated feasibility stresswise of using beryllium facings for the cup type edge design heat shield panel, and assuming that none of the previously described undesirable characteristics of beryllium sheet is applicable, the following design considerations are recommended.

Using the cup type edge design, per drawing 60B20210, with the changes noted below:

1. 0.03" beryllium facings
2. Cups 0.063" Ti-13V-11Cr-3Al

the weight reduction would be 5.69 lbs., or 9.2%, compared with the all-stainless steel configuration having a calculated weight per drawing of 61.75 lbs.

Weights

(2) Beryllium Facings
.03"x52.76x52.76x.066 = 11.02 lbs.

(2) .03"x52.76"x1.5" doublers - 0.31 lbs.

(28) cups (Ti-13V-11Cr-3Al) 4.2 x 62% = 2.6 lbs.

Total Weight 13.93 lbs.

(2) PH15-7Mo Stainless Steel facings
.01x52.76x52.76x0.277 = 15.42 lbs.

(28) cups at 0.15 lb/each = 4.2 lbs.

Total Weight 19.62 lbs.

Note that the use of the high strength titanium alloy Ti-13V-11Cr-3Al proposed for the cups and having comparable mechanical properties to PH 15-7Mo (TH 1050 condition) is considered suitable for either the beryllium faced design proposed or the 60B20210 stainless steel configuration. As previously indicated for the Zee section edge member panel design, the use of beryllium facings for the cup type edge design will require a brazed doubler type facing sheet splice accomplished during the panel brazing, the reason being the present 36" maximum width availability of beryllium sheet and inability to make a sound structural weld in beryllium sheet.

Since the main consideration in the use of beryllium sheet for heat shield panels was for weight reduction purposes, other material configurations might be considered. The most attractive at present would be a silver brazed titanium alloy such as Ti-6Al-4V or Ti-13V-11Cr-3Al. A modest development program (by comparison with beryllium) would be required to support such a design and would include such items as:

1. Optimum brazing alloy and base metal alloy studies.
2. Determination of process parameters for brazed titanium sandwich configurations.
3. Determination of material allowables for brazed titanium sandwich configurations.

Cost Considerations for Beryllium Faced Heat Shield Panels

The principal item of additional cost in a brazed honeycomb sandwich heat shield panel with beryllium facings for the 60B20210 design compared with the all-stainless steel design is the material cost for the beryllium sheet since the fabricating and/or brazing operations are essentially unchanged. The experience factor of considerable importance in handling and fabricating beryllium is also significant but is not really determinable from a cost viewpoint and will not be evaluated.

The material cost of the 0.03" thick cross rolled beryllium sheet for one (1) heat shield panel per 60B20210 design is $5877 (Table 16). This compares with a cost of $240 for two (2) 0.01" x 52" x 54" PH 15-7 Mo facings having one fusion weld splice, roll planished and radiographically inspected.

TABLE 16

Material Cost for Beryllium Faced Heat Shield Panel

(60B20210 Design)

	Size	Quantity	Cost
1. Facings - .03" cross rolled beryllium sheet	53" x 36"	2	$3816
2. Doubler strips - .03" cross rolled beryllium sheet	53" x 17"	2	1802
	53" x 15"	2	159
			$5877
			for one (1) panel

Note: The doubler strips are required for the brazed facing sheet splice accomplished during the panel brazing.

SECTION V

DEFLECTION CHARACTERISTICS OF M-31 INSULATION WITH STAINLESS STEEL HONEYCOMB REINFORCEMENT

An important consideration in the use of ceramic materials for heat shield panel applications is the deflection allowable; i.e., the amount of bending the composite panel can withstand before failure of the ceramic occurs from the resultant tensile stress. The deflection characteristics of M-31 were recently determined by Aeronca as part of the S-1B heat shield panel program (Contract NAS8-4016) and are included as pertinent design information.

The test arrangement employed, shown in Figures 31 and 32, utilized a 3"x15" specimen with two point loading. Specimen configuration was a 1.02" thick load bearing panel with 0.250" thick 8-15 open faced core deformed to about 0.2" in height; M-31 thickness was 0.3". The test data is given in Table 17.

The radius of curvature for the deflection at which failure occurred may be calculated by

$$R = \frac{(C/2)^2}{2H}$$ where C = chord length, H = deflection

$$R = \frac{(7/2)^2}{.029} = 418 \text{ inches}$$

For the 30M12571 panel using the ½" deflection allowable, the corresponding radius of curvature is:

$$R = \frac{(48.3/2)^2}{1} = 583 \text{ inches}$$

Therefore, the safety factor with regard to the deflection produced cracking of the M-31 is approximately 583/418 or 1.38.

The requirement for deformed honeycomb core to insure adherence of the M-31 insulation was established by the NASA S-1C Heat Shield Panel Test Program. These tests showed conclusively that deformation of the open faced honeycomb core was necessary to prevent separation of the M-31 under a simulated S-1C acoustic and thermal environment.

TABLE 17

FLEXURE TEST OF HEAT SHIELD TEST SAMPLE*

Dial Gage In.	Dial Gage In.	Load Lbs.	Deflectometer In.	Midpoint Deflection With Respect To Load Points - Inches	
.0105	.012	100	.0104		
.0185	.02	200	.0195		
.026	.027	300	.0274		
.033	.034	400	.0357		
.0405	.0405	500	.0440		
.047	.047	600	.0524		
.054	.054	700	.06		
.061	.061	800	.0688		
.0685	.0685	900	.0784		
.076	.075	1000	.0875		
.093	.096	.250	.09		
.1085	.1065	1310	.122	.0145 (.122 - .1075) for 7" span	Failure of M-31 occurred at thi point. Failure consisted of a slight crack extending the full panel width and through the ent depth of the M-31. Separation the M-31 from the panel facing not occur.

*Ref: Aeronca Test Report TR-50-63

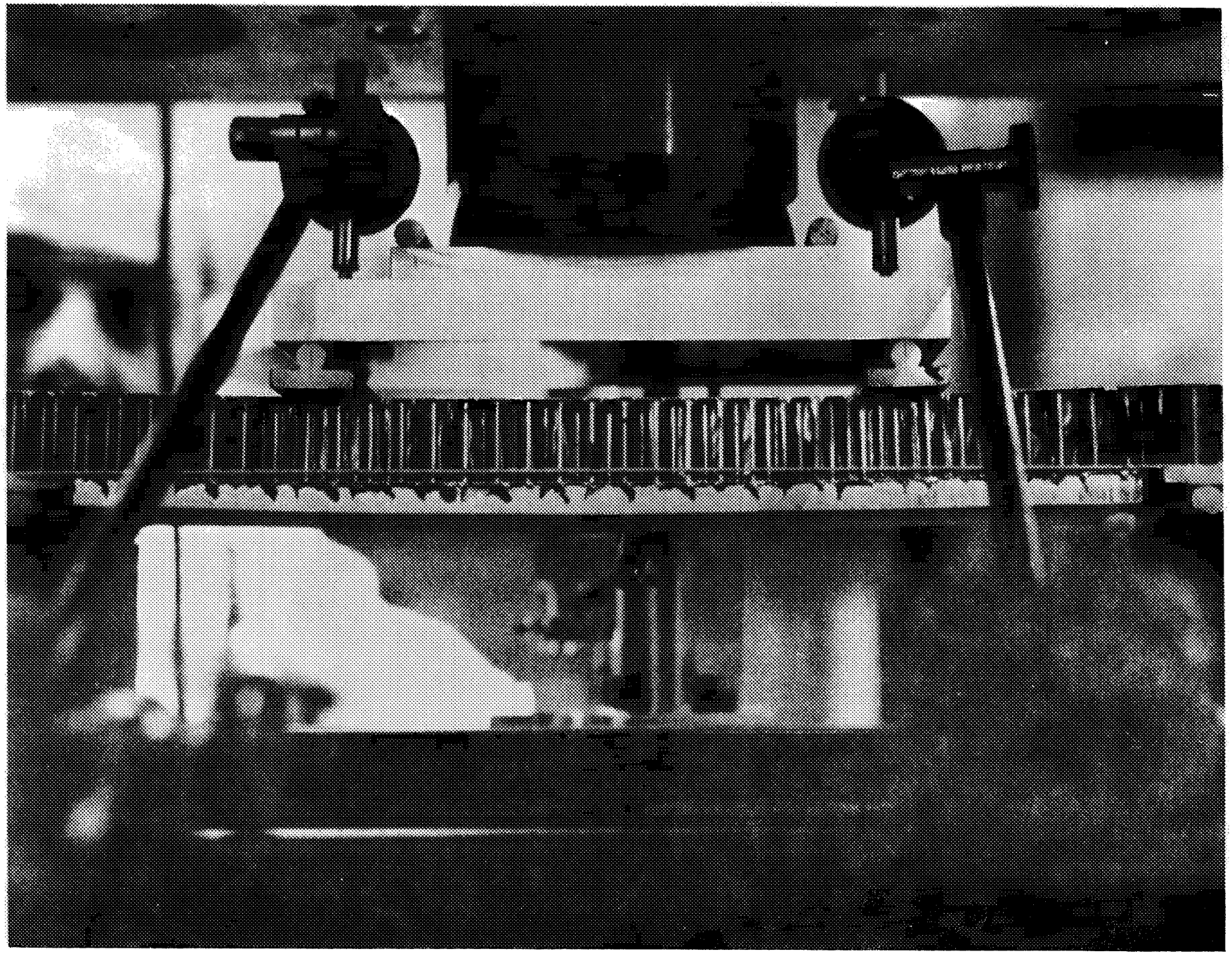

Figure 31 Flexure Test of Sandwich Section with M-31 Insulation

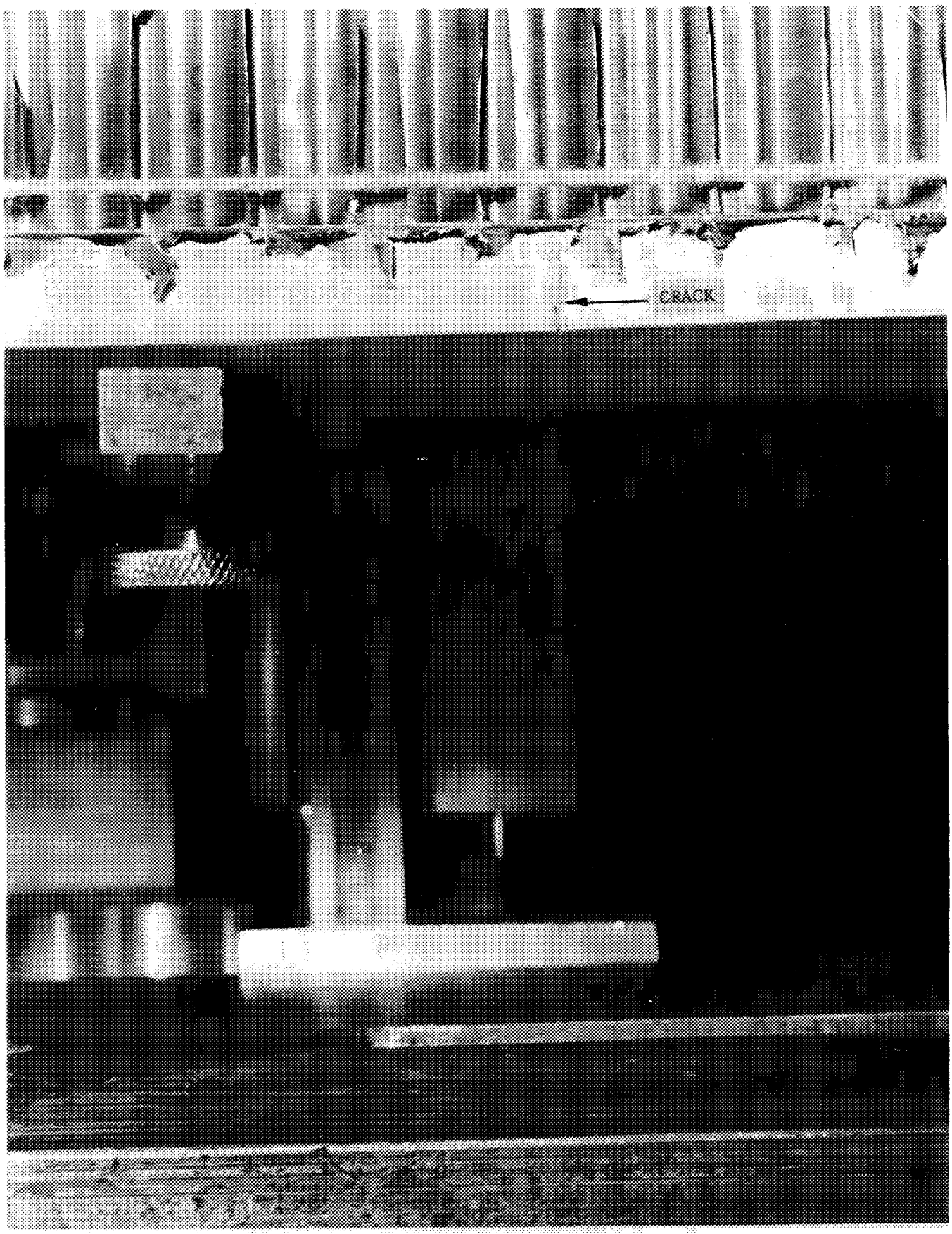

Figure 32 Flexure Test of Sandwich Section with M-31 Insulation at Failure

SECTION VI

ANALYSIS OF BRAZE DEFECTS QUALITY STANDARDS AND REPAIR METHODS

Heat Shield Panel Braze Quality

The types and sizes of typical braze discrepancies that are acceptable for heat shield panels of the 30M12571 design produced by Aeronca for NASA on Contract NAS8-6976 are shown in Figures 33 through 38. The discrepancies include:

1. Core to facing braze light fillets (LF).
2. Core to facing braze cell wall voids (CWV).
3. Core to facing braze gross voids (GV).
4. Metal to metal or faying surface braze voids (FSV).
5. Core to metal or shear tie braze voids.

Examination of these radiographic inspection reports shows the discrepancies to be principally confined to the metal to metal braze area in the edge members. The core to facing braze imperfections were confined to light fillet areas and small isolated cell wall void areas.

An unacceptable level of braze quality is shown in Figure 37. Note the large area exhibiting cell wall voids and light fillets which also contains a large gross void on both panel faces. These conditions resulted from retort leakage during brazing caused by failure of welded joints in the retort which results in contamination (oxidation) of the protective atmosphere. The net result of oxidized surfaces on the panel components during brazing is inability of the brazing alloy to properly wet the panel surfaces resulting in either very poor fillet formation or none at all.

It should be noted that the core to facing braze quality exhibited in Figures 33through 36 radiographic reports is typical of acceptable braze quality by airframe brazed panel standards. The metal to metal and core to metal braze is likewise acceptable.

The following sections contain a detailed analysis of the effect of these five types of braze discrepancies on heat shield panels typical of the 30M12571 design and repair methods where applicable for these conditions.

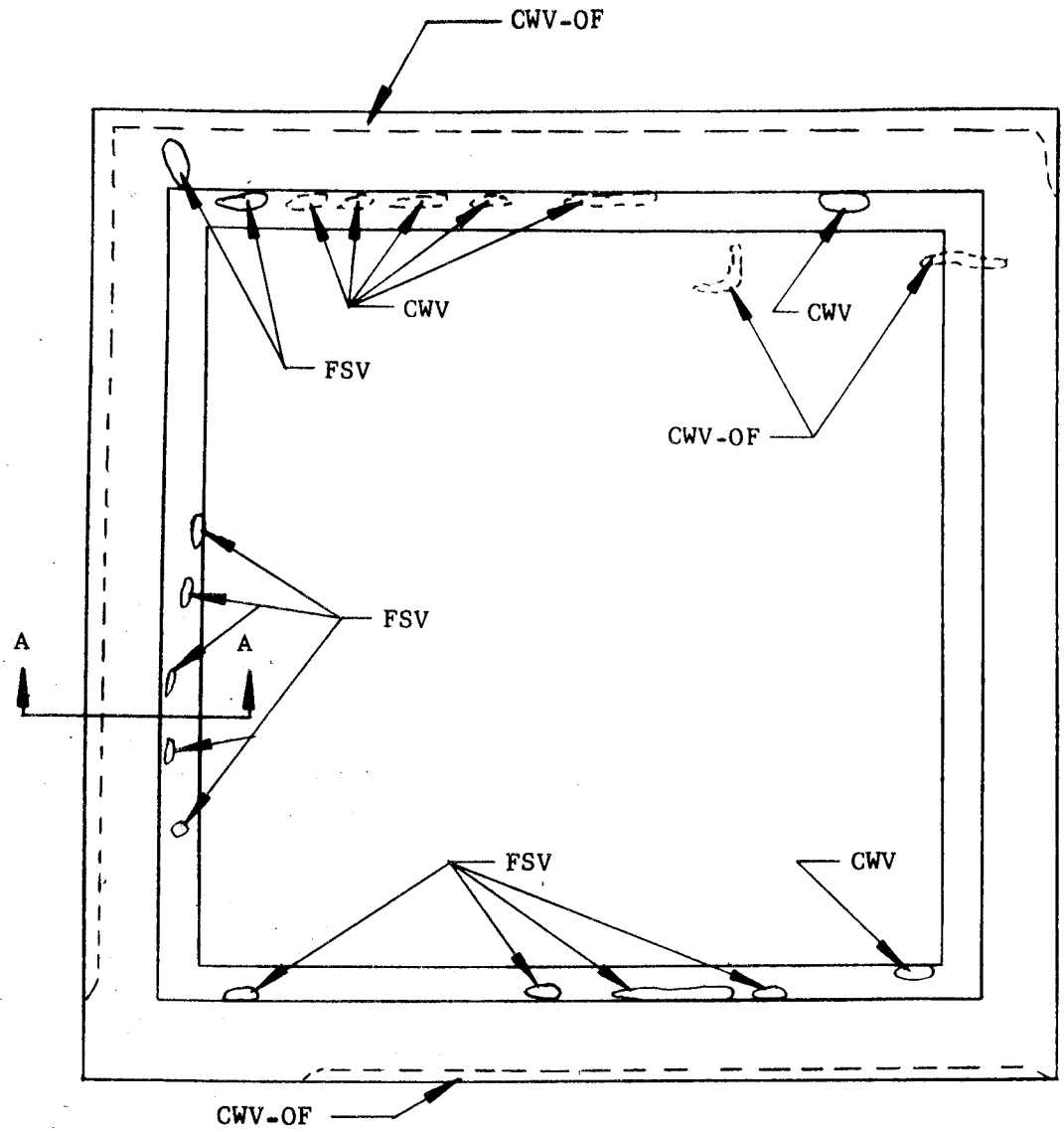

Internal Core Avg. Fillet Size .020
External Core Avg. Fillet Size .025
Node Flow Condition 100%

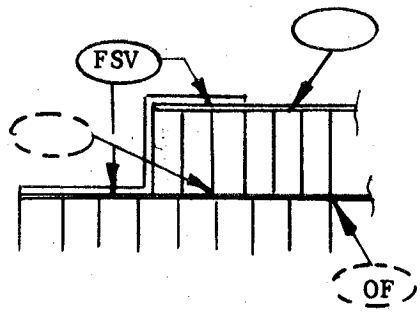

SECTION A-A

Code: CWV--Cell Wall Void
FSV--Faying Surface Void
OF--Outer Face

Figure 33 Quality Modifying Conditions Revealed by Radiographic Examination

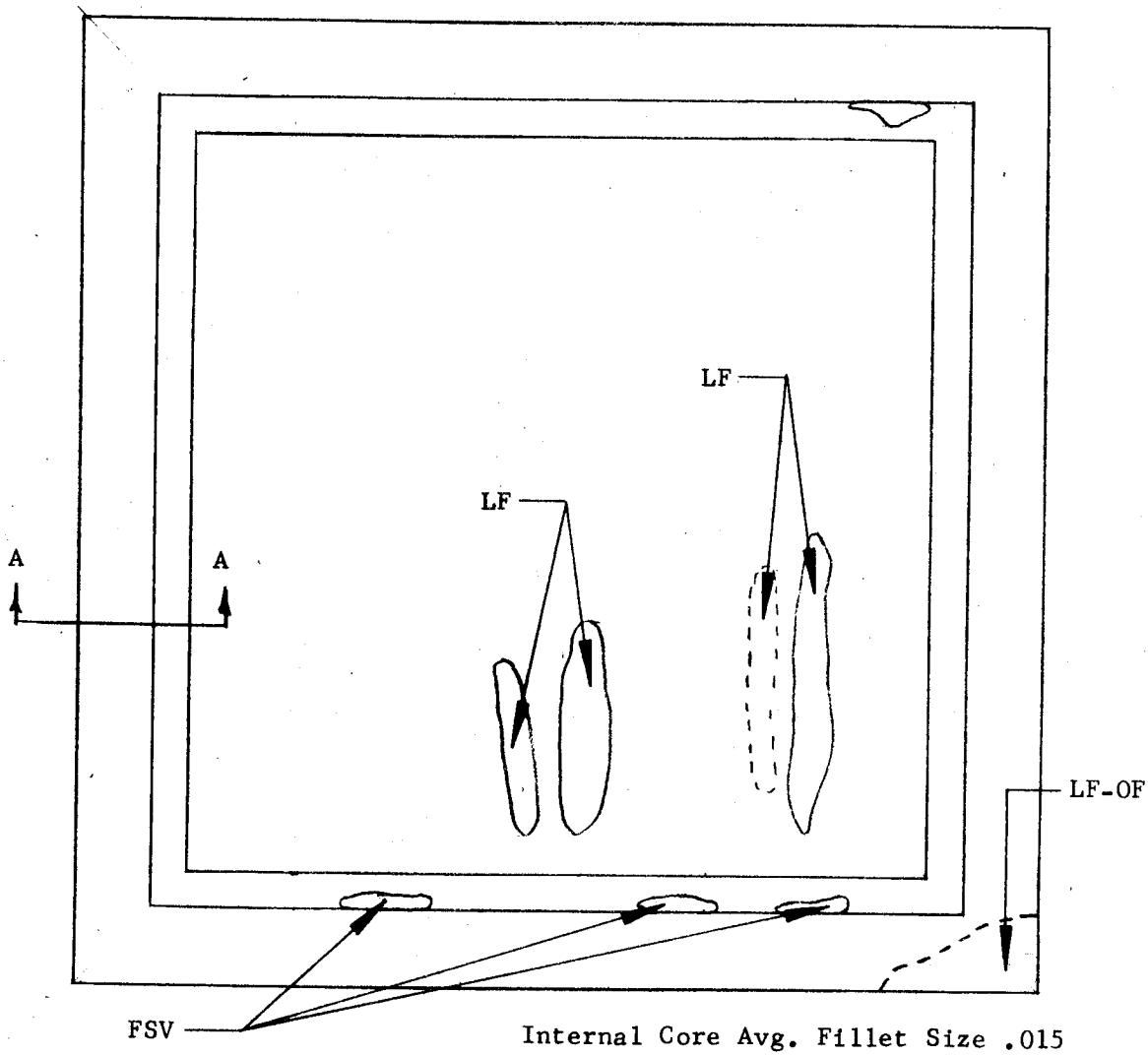

Internal Core Avg. Fillet Size .015
External Core Avg. Fillet Size .025
Node Flow Condition 100%

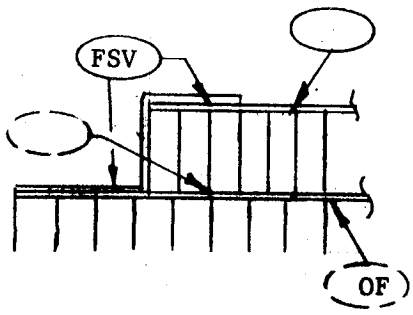

SECTION A-A

Code: LF--Light Fillets
FSV--Faying Surface Void
OF--Outer Face

Figure 34 Quality Modifying Conditions Revealed By Radiographic Examination

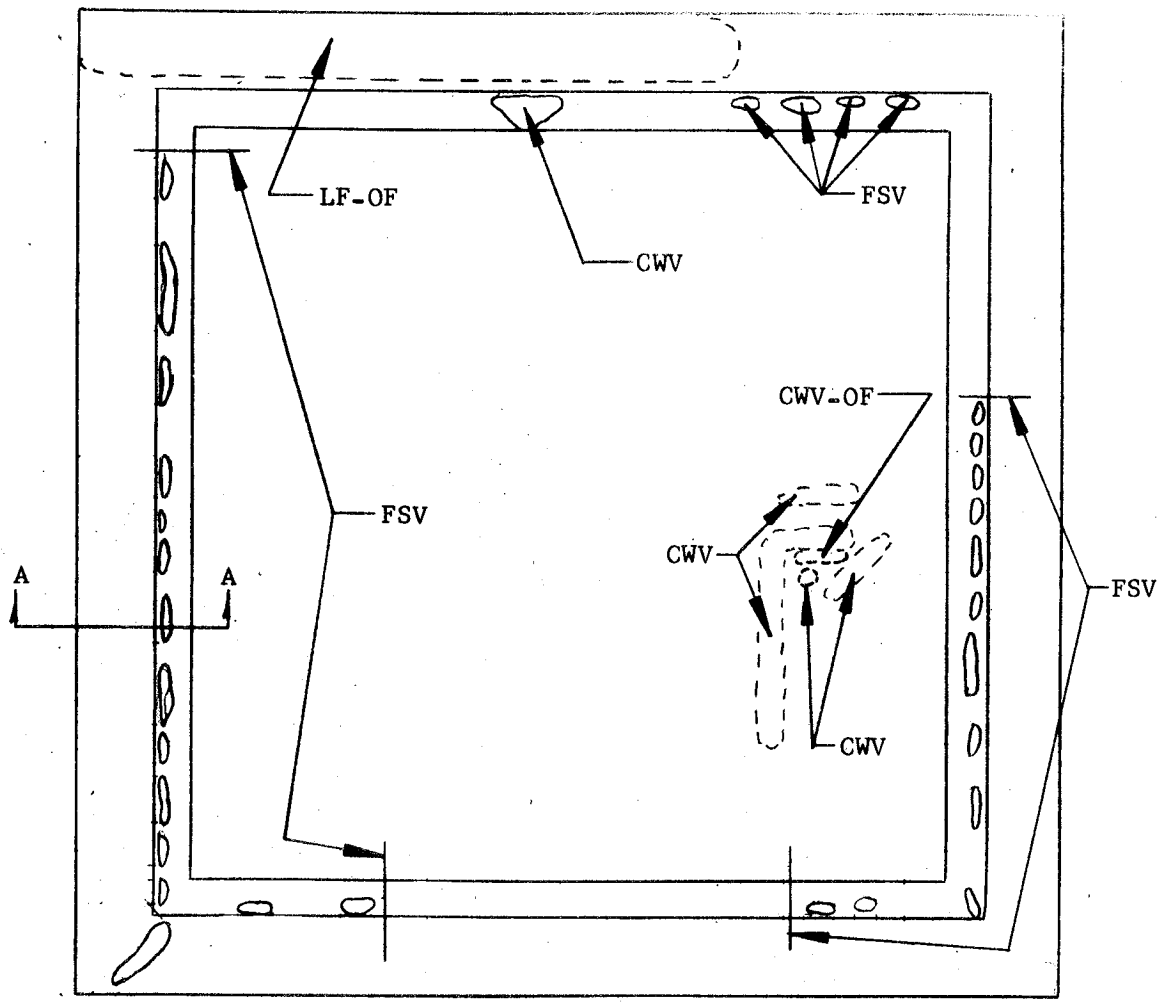

Internal Core Avg. Fillet Size .020
External Core Avg. Fillet Size .025
Node Flow Condition 100%

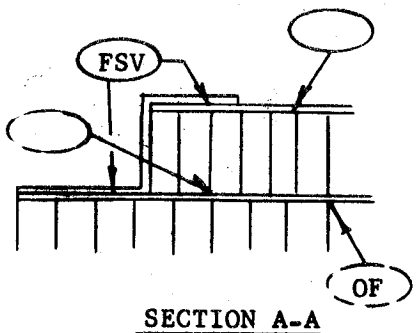

SECTION A-A

Code: LF--Light Fillets
CWV--Cell Wall Void
FSV--Faying Surface Void
OF--Outer Face

Figure 35 Quality Modifying Conditions Revealed by Radiographic Examination

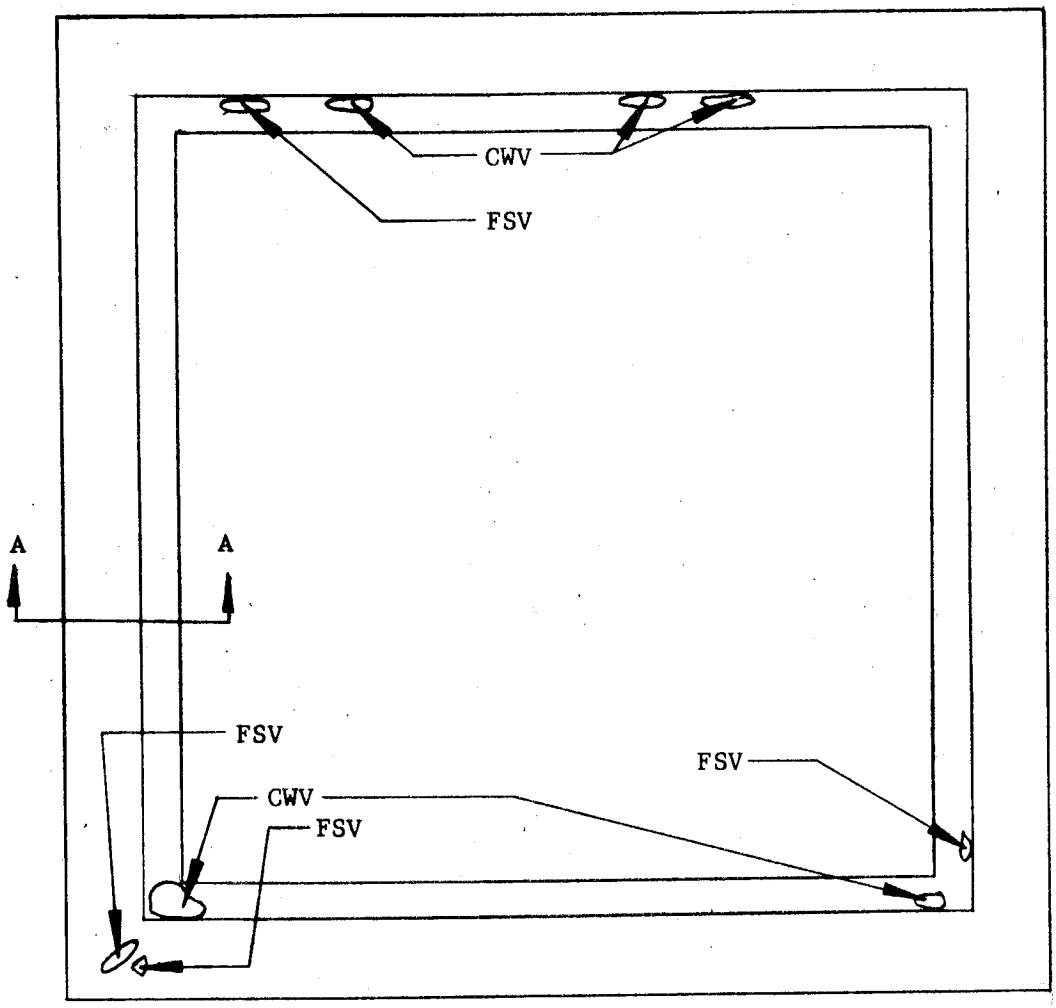

Internal Core Avg. Fillet Size .015
External Core Avg. Fillet Size .030
Node Flow Condition 100%

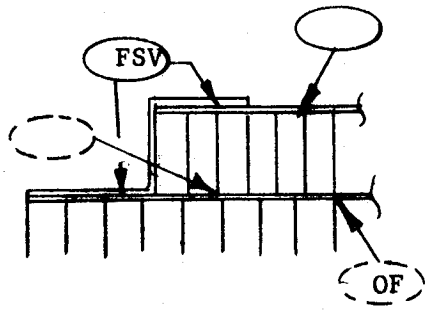

SECTION A-A

Code: CWV--Cell Wall Void
FSV--Faying Surface Void
OF--Outer Face

Figure 36 Quality Modifying Conditions Revealed By Radiographic Examination

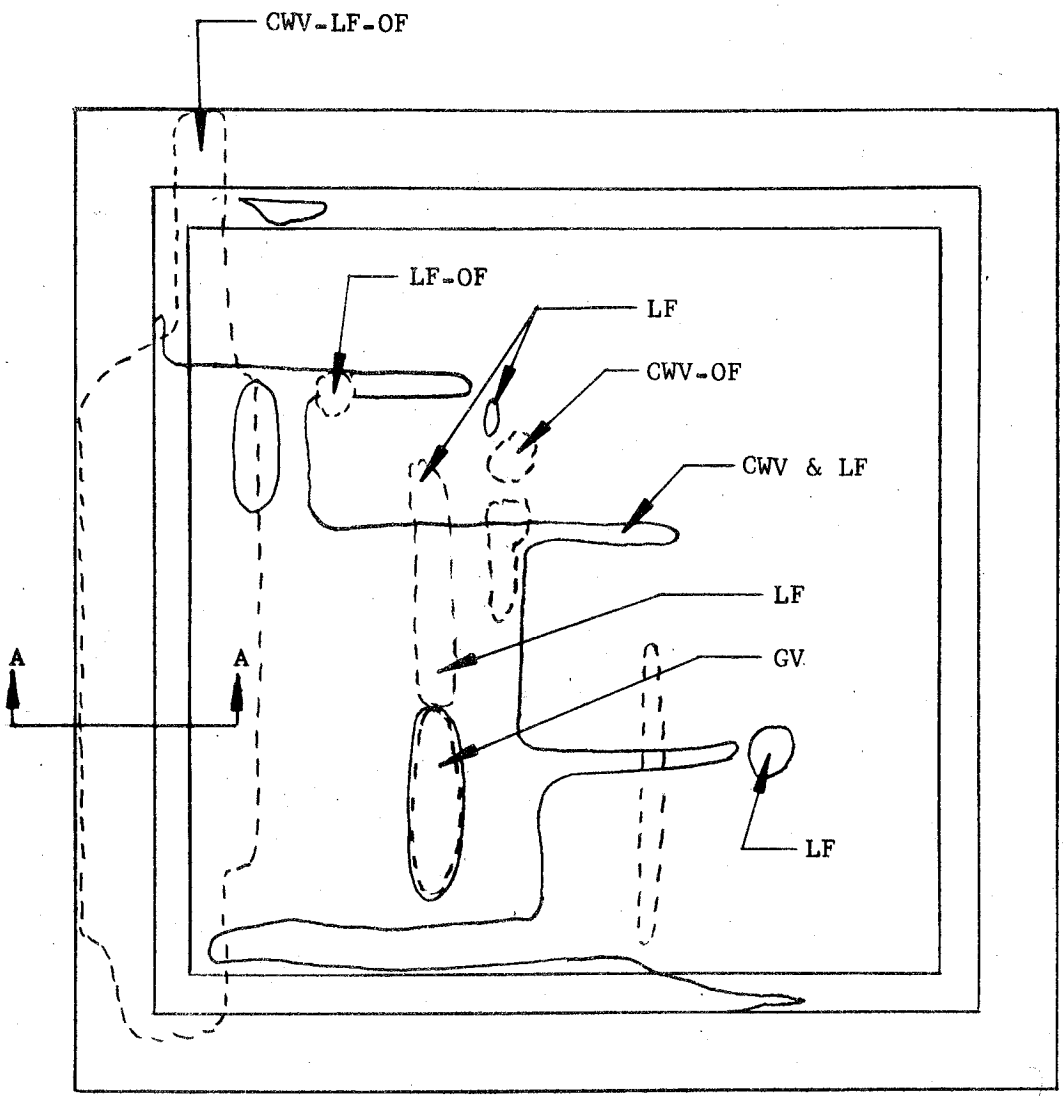

Internal Core Avg. Fillet Size .015
External Core Avg. Fillet Size .025
Node Flow Condition 100%

Code: LF--Light Fillets
CWV--Cell Wall Void
FSV--Faying Surface Void
GV--Gross Void
OF--Outer Face

(Note: Panel Scrapped)

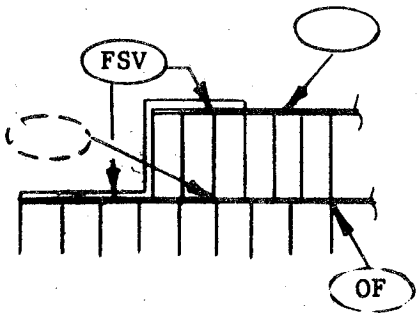

SECTION A-A

Figure 37 Quality Modifying Conditions Revealed by Radiographic Examination

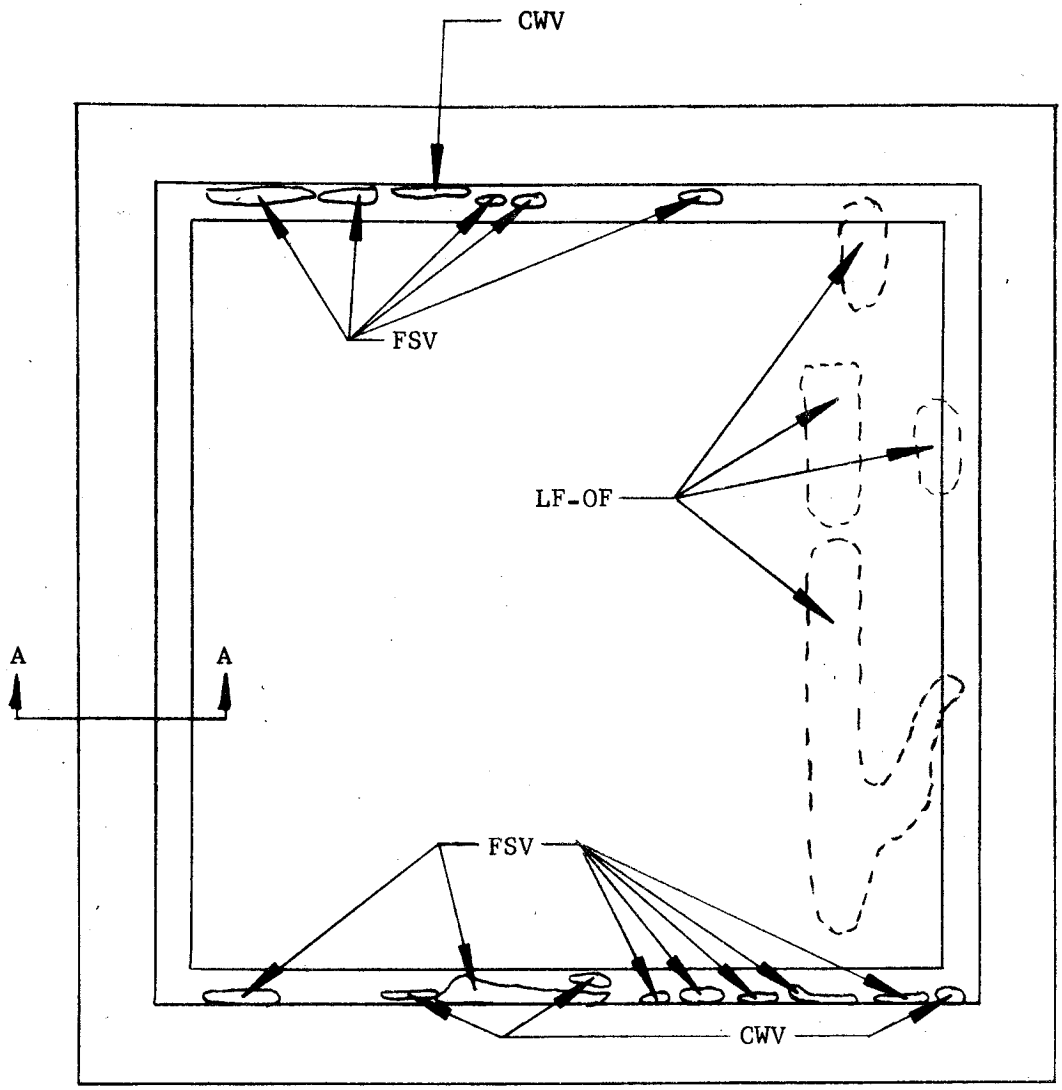

Internal Core Avg. Fillet Size .015
External Core Avg. Fillet Size .030
Node Flow Condition 100%

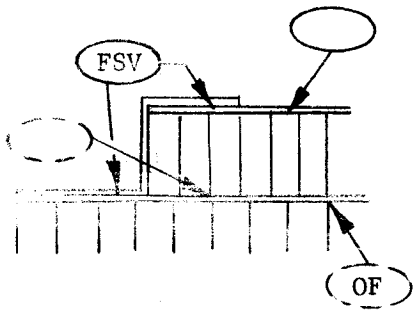

SECTION A-A

Code: LF--Light Fillets
CWV--Cell Wall Voids
FSV--Faying Surface Voids
OF--Outer Face

Figure 38 Quality Modifying Conditions Revealed by Radiographic Examination

Core to Facing Voids

A core to facing void is an area showing partial or total lack of braze attachment between the honeycomb core and facing sheet. This type of discrepancy is commonly encountered in brazed honeycomb sandwich panels and in numerous variations of size and shape. The effect of such unbrazed or unattached areas is a function of size and the type of loading; i.e., tension or compression. Since any sandwich panel subjected to a bending load has one facing in compression while the opposite facing is in tension, the stability of the facing(s) under a compression load in voided or unbrazed areas is of critical importance. Consequently, the analysis of core to facing voids is based on the local buckling strength of the unattached facing sheet under a compression load.

Two types of core to facing voids are commonly encountered. These are:

a. Cell Wall Void (CWV)--The condition where the cell walls are unattached to the face sheet but where attachment is present at the cell nodes. This condition may be continuous or intermittent.

b. Gross Void (GV)--A gross void is a condition where at least one node is unattached to the facing sheet.

Circular Gross Voids

For the condition shown in Figure 39A, the critical buckling strength of the unattached area is given by

$$\frac{F_{cr}}{\eta} = .9E \left[\frac{t_f}{d}\right]^{1.5} \qquad (1)$$

where η = plasticity correction factor $= \frac{2E_T}{E+E_T}$

E = Modulus of Elasticity of facing material.

E_T = Tangent modulus of facing material from compression stress-strain curve.

Rectangular Gross Voids (line or Rectangular)

For the condition shown in Figure 39B where dimension b is the loaded edge. the facing behaves as a uniaxially loaded wide plate column. Tests indicate that when the void is surrounded by good braze attachment, the end restraint condition approaches 100% fixity. The local allowable buckling stress for this condition is given by:

$$\frac{F_{cr}}{\eta_1} = \frac{2.62E}{1-\nu^2} \left[\frac{t_f}{h}\right]^2 \qquad (2)$$

ν = Poisson's Ratio

where $\eta_1 = \frac{E_T}{E}$ the plasticity correction factor for b the loaded edge.

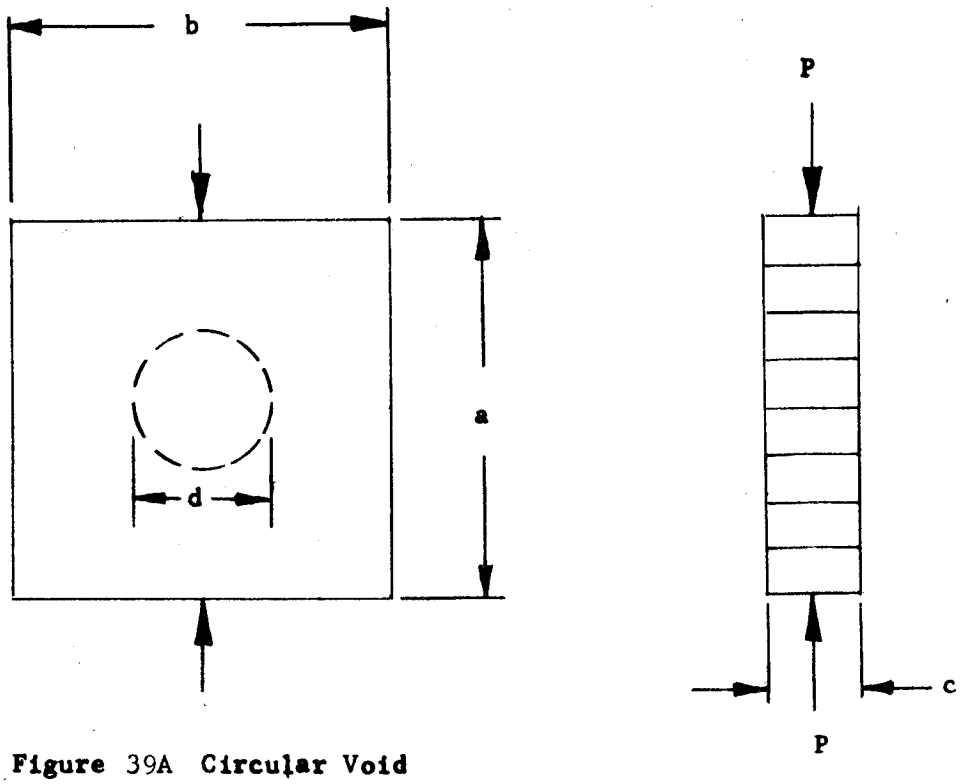

Figure 39A **Circular Void**

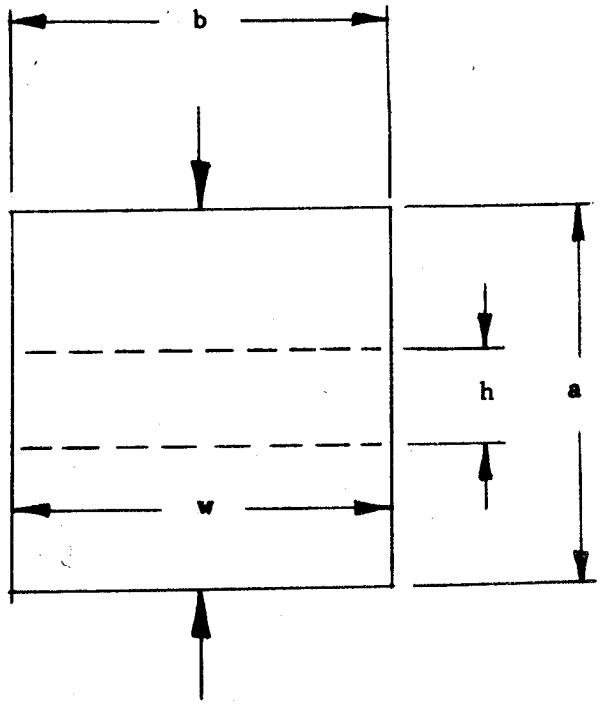

Figure 39B **Line Void**

Panel Dimensions a, b

Fig. 39A - Circular Void
Diameter, d

Fig. 39B - Line Void
Dimensions h, a

Figure 39 **Basic Void and Buckling Configurations**

Where dimension a is the loaded edge, the rectangular void is considered a long plate elastically restrained on the unloaded edges with intermediate fixity. The buckling stress for this condition is:

$$\frac{f_{cr}}{\eta_2} = \frac{4.5E}{(1-\nu^2)} \left[\frac{t_f}{h}\right]^2 \qquad (3)$$

$\eta_2 E = \left[E_S \quad 0.352 + 0.648 \sqrt{.25 + \frac{3E_T}{4E_S}}\right]$ where η_2 is the plasticity correction factor for a the loaded edge.

Curves for the preceding equations (1), (2), (3) are shown in Figure 40 and allow ready assessment of the buckling stress for these three core to facing void conditions. Since the maximum stress condition for the 30M12571 panel is 35,644 psi*, all voids must be stable to this minimum buckling allowable. Voids exhibiting f_{cr} values below 35,644 psi would be unacceptable "as is" and would require suitable repair. From Figure 40 the maximum **circular** void size acceptable "as is" without repair would be:

$$\frac{.01}{d} = .012$$

$$d = 0.83" \text{ diameter}$$

For the line void conditions in Figure 39B the comparable values for h are (Fig. 40) 0.5" (curve 2) and 0.66" (curve 3).

Cell Wall Voids

Two conditions of this type of void may be present, a (connected) row of cell walls void or an area with intermittent cell wall voids. The former case may be treated by the use of formulas (2) or (3) for gross line voids. For the latter case (area with intermittent cell wall voids), the following empirical equation for the local buckling stress is used:

$$f_{cr} = \frac{2.958 + \log_{10}\left[\frac{t_f}{d}\right]}{1.34} \; f_{allowable}$$

$f_{allowable}$ = compression wrinkling stress in facing (177,000 psi for 4-15 core)

$$\frac{t_f}{d} \leq .025$$

*Third Monthly Report, Page 37

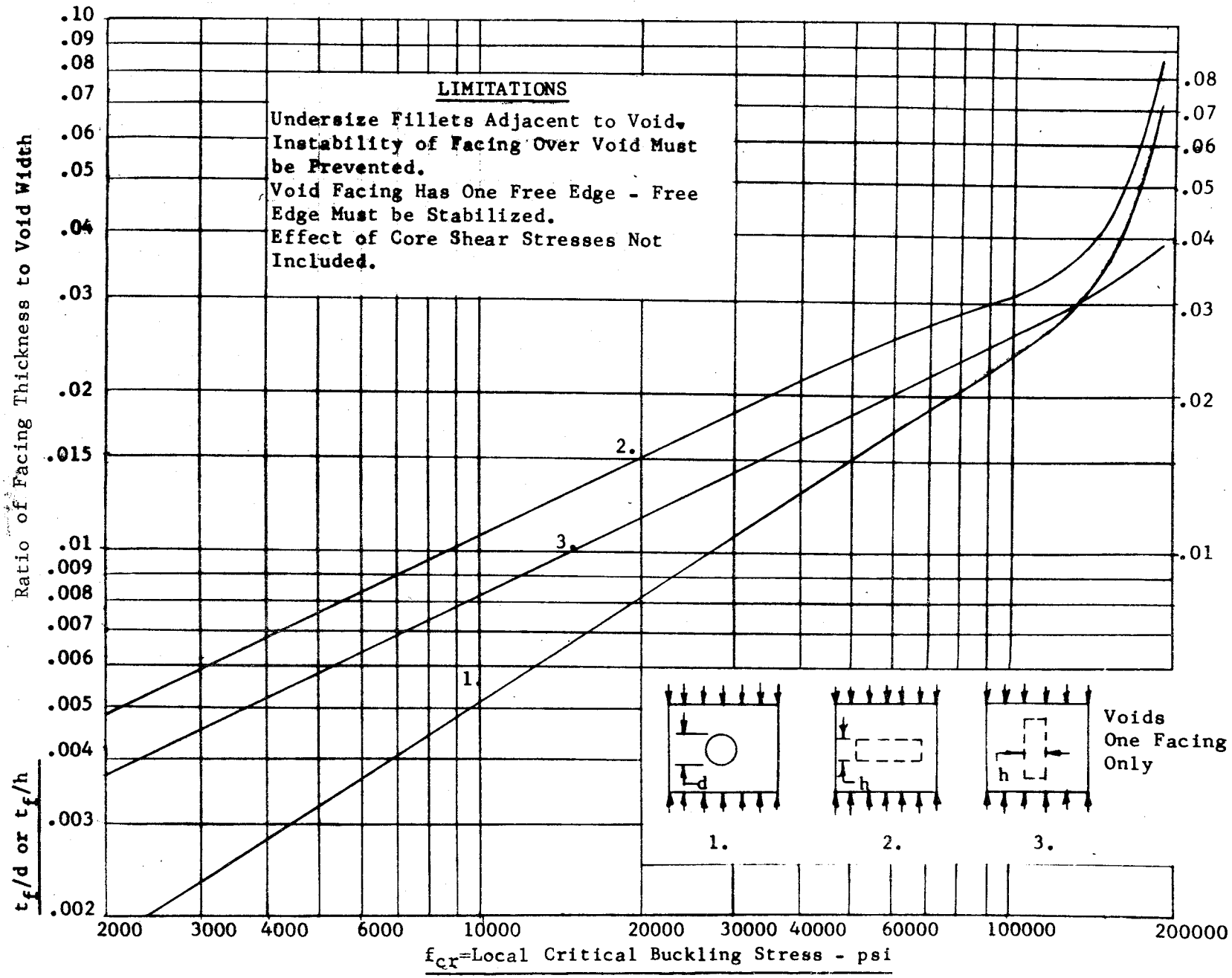

Figure 40 Effect of Gross Voids - Local Uniaxial Compression Allowable PH15-7Mo (RH1050)

The curve for this equation is shown in Figure 41. For a buckling stress f_{cr} of 35,644 psi, the maximum cell wall void acceptable "as is" would be:

$$\frac{35,644}{177,000} = .2 \text{ and } \frac{t_f}{d} = .002$$

for t = .01" d = 5" diameter and h = 5".

(Ref. NAA Structural Repair Manual /buckling equations and curves/).

Fillet Size

For in plane loads a certain minimum fillet size is required to permit development of the face sheet allowable in compression loading which in turn subjects the braze fillet to a tensile load. This critical tension stress may be calculated by the following empirical equation:

$$f = \frac{1.75W}{S} f_S$$

W = actual braze fillet width at base, inches

S = honeycomb core cell size

f_S = braze lap shear allowable, p.s.i.

For type 4-15 core and the sterling lithium braze alloy f_S = 15,000 psi*. f is 840 psi for the minimum fillet size requirement (0.008") recommended for this application. Typical fillet size for the 30M12571 panels was 0.015". The effect of undersize fillets on face sheet stability is shown in Figure 42.

Node Flow Requirements

For the S-1C heat shield panel applications in question, brazing alloy node flow in the load bearing core is desirable from the standpoint of minimizing the thermal gradient (ΔT), resulting panel deflection and facing stresses rather than providing increased core shear properties.

*Ref. Convair Spec. FZS-4-162A

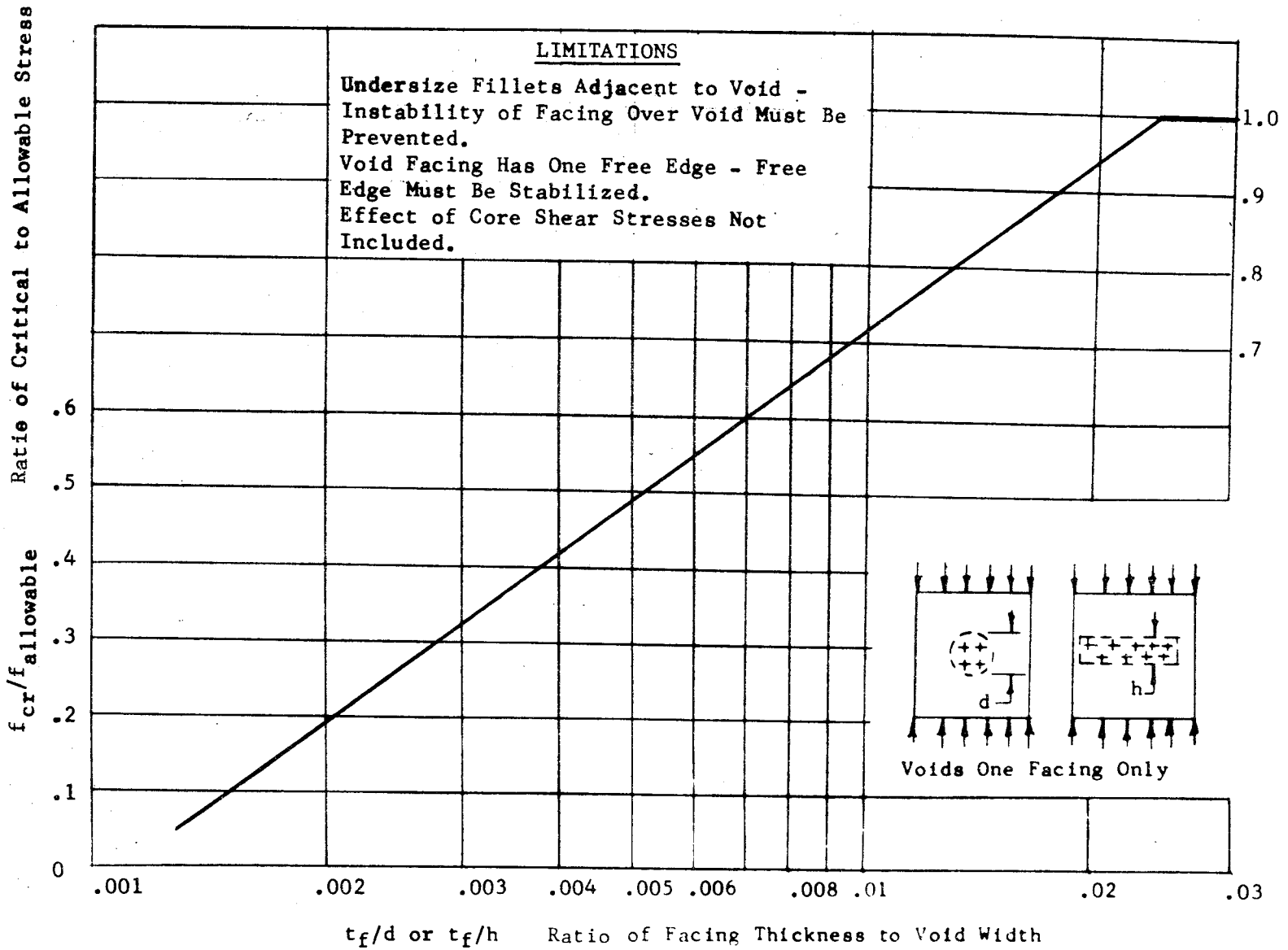

Figure 41 Effect of Cell Wall Voids - Local Uniaxial Compression Allowable PH15-7Mo (RH1050)

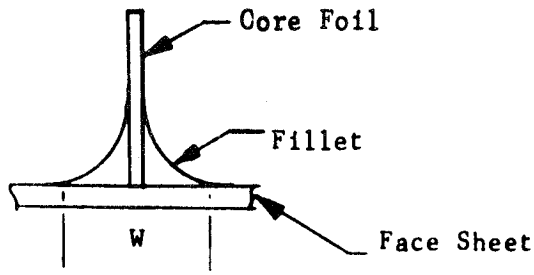

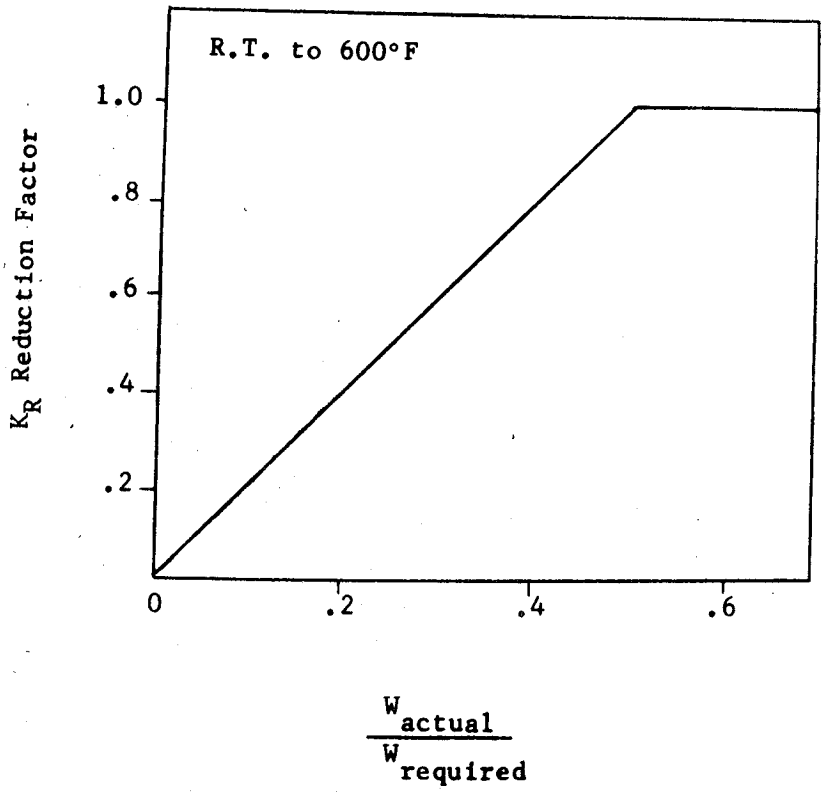

Typical Minimum Fillet Size Requirement for 1.0" Thick Core

Core Type		$W_{req'd}$
3-15	-	.009"
4-15	-	.008
6-20	-	.010

Ref: NAA Structural Repair Manual

Figure 42 Effect of Undersize Fillet on Face Sheet Stability

However, since the combined facing stresses for the flight condition are quite low (26,238 psi*) for the zero node flow (maximum ΔT) condition with a M.S. of +4.1 node flow is not considered a mandatory requirement for heat shield panel acceptance.

Size and Spacing Requirements for Core to Facing Voids

The maximum sizes of core to facing voids recommended for acceptance "as is" (unrepaired) are given in Tables 18 and 19 which also include the minimum recommended spacing requirements. The spacing requirements, essentially, represent the minimum distance necessary to prevent catastrophic propagation of adjacent voids and are based on empirical standards used for brazed honeycomb sandwich air frame panels. Because of the large + M.S. associated with the maximum panel stress (35,644 psi), the maximum permissible acceptable gross void has been defined as 1.0" rather than 0.83".

Repair Procedures

Repair procedures suitable for core to facing voids in excess of the sizes listed in Tables 18 and 19 consist basically of stabilizing the unbrazed area by means of a doubler which is structurally attached to the facing in the sound panel area surrounding the void as well as the unbrazed facing area. The basic methods of doubler attachment applicable to heat shield panels include:

a. Adhesive bonding using a high temperature epoxy type adhesive such as HT-424.

b. Spot brazing--A method which employs a lower melting point braze alloy than the sterling lithium braze alloy used for the panel brazing. Localized braze attachment in the form of spots 3/16", 1/4", or 5/16" in diameter is accomplished by electrical resistance heating using a single electrode gun applied to one side of the part only. The brazing alloy recommended for this application is the silver-copper eutectic plus 0.2-.5% lithium with a melting and flow point of approximately 1400°F.

c. Area Brazing--A method using a lower melting point brazing alloy as in item b. with heat applied either locally by means of an indirectly heated copper block or by heating the entire panel using the original brazing tooling. The latter method gives very good results but requires specialized manufacturing facilities and is relatively expensive. The local heating method is highly dependent on operator skill, limited to small size or areas, and frequently results in excessive panel warpage.

*Ref: Monthly Report No. 3, Page 37

TABLE 18

SIZE AND SHAPE OF CORE TO FACING GROSS VOID DEFECTS*
WITH MINIMUM SPACING REQUIREMENTS

Circular Defect	Line Defect	Minimum Distance to Next Defect For Acceptable Panel Quality
up to 0.25"	up to 0.25"	2 inches
0.26 to 0.50"	0.26 to 0.75"	6 inches
0.51 to 1.0"	0.76 to 1.25"	10 inches
MINIMUM SPACING REQUIREMENT FOR ABOVE DEFECTS FROM EDGE OF PANEL		
up to 0.25"	up to 0.25"	1 inch
0.26 to 0.50"	0.26 to 0.75"	3 inches
0.51 to 1.0"	0.76 to 1.25"	5 inches

* Continuous Cell Wall Voids are included in this category.

TABLE 19

SIZE AND SHAPE OF CORE TO FACING INTERMITTENT CELL WALL VOIDS

Diameter of Circumscribed Area Containing Defects	Maximum Permissible Number of Cell Wall Voids
up to 1.50"	7
1.51" to 3.0"	25
3.01" to 5"	50

d. Mechanical Fasteners--Limited use may be made of blind mechanical fasteners such as DuPont L-Nickel noiseless explosive rivets of the protruding head type (PN-134A) 0.134" ±.001" in diameter. The rivet holes must be located in the center of the core cells in the sound braze area to avoid undesirable core to facing braze damage.

Of the foregoing methods, the adhesive bonding, spot brazing and blind mechanical fasteners are directly applicable for heat shield panel repairs. In any case, however, doubler repairs are only practical for the forward panel facing (cold side); the hot side facing bearing the open face honeycomb core effectively prevents repairs from being accomplished. Welding as a means of doubler attachment, either directly as along the doubler edge or via fusion spots, burn down welds of pins passing through a doubler and top and bottom facings, is likewise not feasible with conventional TIG welding equipment on panels with 0.010" facings essentially because of inadequate control resulting in burn through.

Analysis of Metal to Metal and Core to Metal Voids in 30M12571 Heat Shield Panel

Core to Metal Voids:

The core to metal joint is assumed to carry the entire load. Since the vertical leg of the Zee is 1", the total shear area for the panel is 4a sq. in.; where a is the length of the core (48.3 in.). The shear load per inch of perimeter then becomes $qa^2/4a$ or $qa/4$ psi of wall area. The core to metal attachment area for Type 4-15 core per square inch of surface would be 4 x .005 = .020 in^2 of shear area*. The shear stress on the braze attachment is:

$$f_s = \frac{qa}{4 \times .02} = \frac{48.3\ q}{.08} = 603q \text{ psi}$$

The shear strength allowable for the silver-copper-lithium braze alloy is 15,000 psi at R.T. and 12,750 at 500°F **.

For q = 2.7 air load plus 0.72 psi dynamic load (noise and vibration)

q = 1.0 air load plus 0.72 psi dynamic load (noise and vibration)

f_s = 2050 and 1025 psi, respectively.

Thus for the worst condition, the maximum void allowable is

$$1 - \frac{2050}{15000} \times 100 = 85\%$$

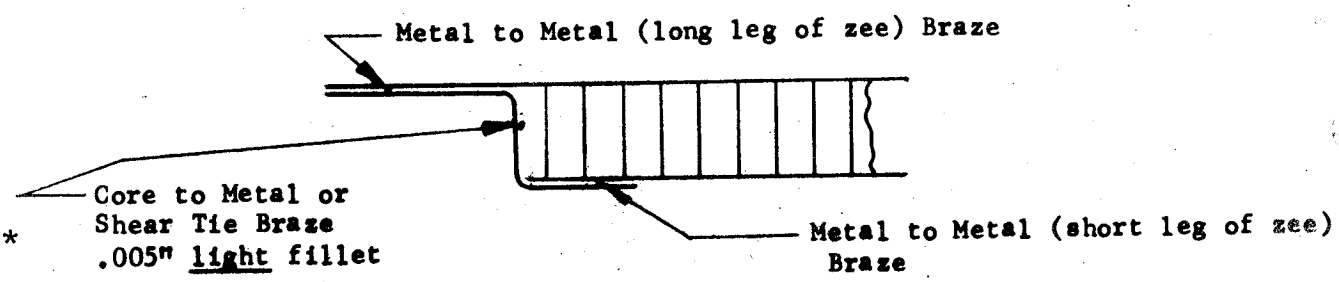

*

** Ref: Convair Spec. FZS-4-162A.

Metal to Metal Voids--Short Leg of Zee Member:

Assume the short leg of the zee must carry the entire panel load as a tensile loading on the facing to short leg zee braze. The width of this braze area is 0.875" and the total braze area is (4a - 3.5); a = 48.3". The panel load is qa^2 with the tensile stress in the braze given by $qa^2/4a-3.5 = 12.3q$ psi. Applying the worst loading condition q = (2.7 + 0.72) = 3.42 psi. The stress in the braze is 42 psi. The braze tensile allowable is approximately 25,000 psi, (15000/.6) consequently a very large margin is present for this loading condition.

Metal to Metal Voids--Long Leg of Zee Member:

When the composite edge member (long leg of zee) and facing is bent by a shear load at point P the edge

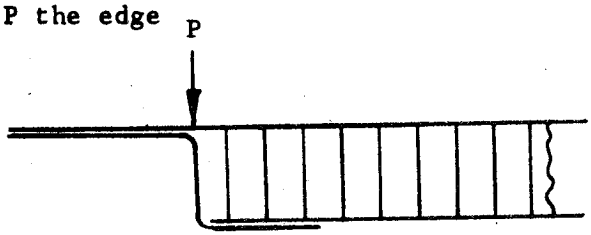

rotation is given by:

$$\theta = \frac{PL^2}{2EI} = \frac{ML}{2EI} = \frac{41.4 \times (.897)^2}{2 \times 29 \times 10^6 \times 1.84 \times 10^{-6}} = .03125 \text{ radians}$$

Where P = ¼ aq lbs/inch

a = 48.3"

q = (2.7 + 0.72) = 3.42 psi

The stress in the braze is:

$$f = \frac{MC}{I} \quad \text{where } M = \frac{2EI\theta}{L}$$

$$f = \frac{2E\theta C}{L} = \frac{2 \times 10.2 \times 10^6 \times .03125 \times .019}{.897} = 13{,}500 \text{ psi}$$

Since the braze must withstand the shearing force resulting from bending, the 13,500 psi value may be compared with the braze shear allowable namely, 15,000 psi. Actual values, however, for the silver-copper-lithium braze alloy are 19,600 psi (R.T.).*

With the panel edge secured by means of bolts to the support beam flanges the principal concern with voids between the facing and zee occurs when the facing experiences a compression loading resulting from bending of the .06"

*Ref: Convair Spec. FMS-0036

thick composite edge member (flight condition loading). As a result, the facing would tend to buckle in unbrazed areas so that voids might propagate into the core to facing areas, particularly, if core to facing voids near the edge members were present. Where no core to facing voids near the panel edge are present, metal to metal void propagation is unlikely since the panel edge rotation is very small. As a consequence, the compressive forces required for extensive buckling in metal to metal voided areas will not be produced.

Repair Methods for Metal to Metal Voids

Repair methods applicable to metal to metal braze voids include:

a. Mechanical Fasteners--Either blind or countersunk rivet fasteners depending on the void location and interference requirements may be used. A recommended fastener is the DuPont Aircraft Blind Expansion Rivet (PN series) of low carbon nickel alloy. This fastener is available with either a modified brazier head or 100% flush head. Expansion of the rivet shank is accomplished by applying a heated tool to the rivet head which activates the sealed internal chemical charge. This type of rivet has been widely used for applicable brazed panel repairs with complete success. Certain NASA test panels produced on Contract NAS8-6976 were repaired using this type rivet, as shown in Figure 43. Repairs to voids in either the short or long leg of zee member can be readily accomplished with this fastening system both in the field as well as by the panel fabricator.

b. Spot Welds--This joining method has been used for metal to metal repairs where the area to be repaired is accessible; i.e., the long leg of the zee and the faying surfaces are sufficiently clean (unoxidized) so a sound nugget can be formed. As a consequence, this method is limited with respect to void location and equipment availability.

c. Fusion Welding--This is applicable to metal to metal voids between long leg of zee and facing that extend the full width (edge to edge). Essentially a burndown weld is performed which joins the facing and edge member. The presence of silver brazing alloy in the fusion zone is not detrimental to the joint; however, it does cause some difficulty because of the tendency to "blow out". Consequently, a complete void condition is preferred for this type of repair.

Repair Methods for Core to Metal (Shear Tie) Voids

Repair for core to metal or shear tie voids consists of injection of a foam type adhesive through holes drilled in the vertical leg of the zee, curing the adhesive and plugging the drilled holes with a sealer or potting compound.

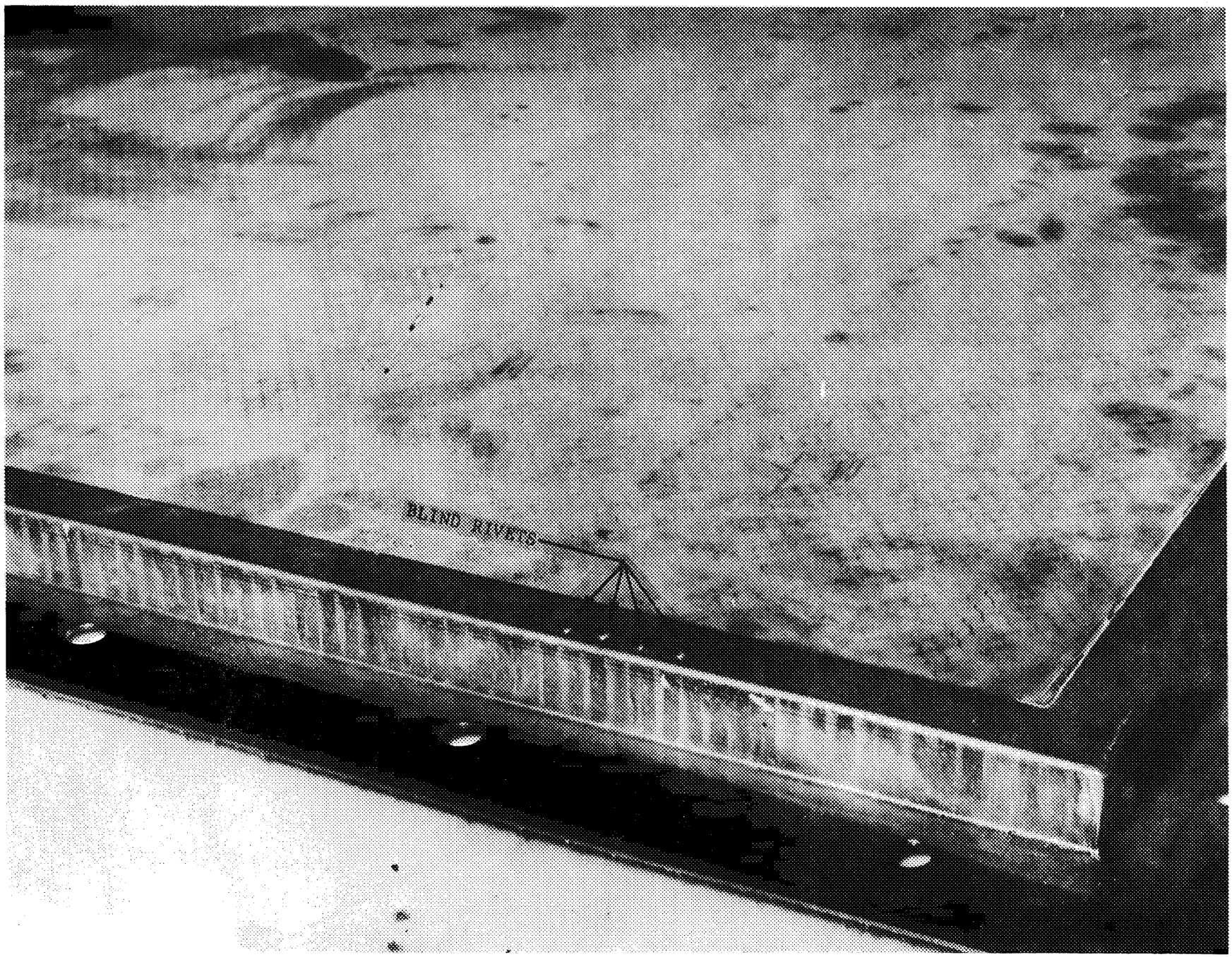

Figure 43 Typical Metal to Metal Braze Void Repair with Mechanical Fasteners (Rivets)

The detail requirements are:

a. Clean surface (MEK) and lay out hole pattern using 1.0" hole spacing and drill holes (No. 50 drill).

b. Inject with a lever type gun Thermo-Foam 607, Type I (Hexcel Products). Cover holes with one layer masking tape, reopen holes and add another layer of tape same area (no holes). This provides an expansion area for adhesive overflow during the curing.

c. Attach thermocouple(s) to the area to be repaired and cure in oven at:

180°-190°F for 25-30 min. followed by

225°-240°F for 50-60 min. followed by

325°-350°F for 25-30 min.

d. Reopen holes used for injection to a depth of approximately 0.1" and seal with Silastic RTV.

Braze Quality Standards for Metal to Metal and Core to Metal Joints

The maximum sizes of metal to metal and core to metal braze voids recommended for aceeptance "as is" are given in Table 20. These size and spacing requirements are based on empirical standards modified for the S-1C heat shield panel requirements.

TABLE 20

METAL TO METAL AND CORE TO METAL BRAZE REQUIREMENTS

Metal to Metal (faying surface void)	The voided area shall not exceed 25% of the joint area for each lineal inch of braze joint. A metal to metal void shall not be continuous from edge to edge.
Core to Metal (shear tie void)	Any vertical shear tie 50% or more brazed is acceptable. The maximum number of unbrazed or completely void shear ties shall be not more than 3 in any 5 consecutive shear ties.

SECTION VII

ANALYSIS OF HOLES IN HEAT SHIELD PANELS

Methods for calculation of stress concentration factors around holes in sandwich panels are outlined in ANC-23, Part II, 1951, sections 3.715, 3.7151, 3.7152, 3.7153. (See Figure 44 for notation and typical hole diagrams.)

The parametric equations describing the boundary of the hole (with no doubler) are:

$$X = A \cos \theta + D \cos 3\theta$$

$$y = B \sin \theta - D \sin 3\theta$$

$$\text{where } \tan \theta = \frac{y}{x}$$

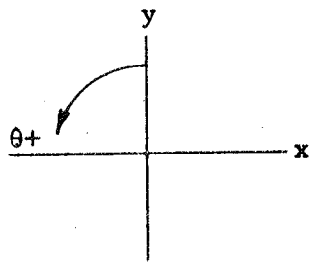

The stress in the facing at the edge of the hole in a tangent direction is given by:

$$\left[(A^2 + 6DB) \sin^2 \theta + (B^2+6DA) \cos^2 \theta - 6D (A+B) \cos^2 2\theta + 9D^2\right] f_t =$$

$$= (f_x+f_y) (A^2 \sin^2 \theta + B^2 \cos^2 \theta - 9D^2) - \left\{ f_{xy} (A+B)^2 \left[\frac{A+B+6D}{A+B+2D} \sin 2\theta \right] + \frac{(A^2-B^2)(f_x+f_y) - (A+B)^2 (f_x-f_y)}{A+B-2D} \left[(A-3D) \sin^2 \theta - (B-3D) \cos^2 \theta \right] \right\}$$

For a round hole where A = B = 1 and D = 0, the above expression becomes:

$$f_t = (f_x+f_y) - 4f_{xy} \sin 2\theta - 2 (f_x-f_y) \cos 2\theta$$

$$f_t = (1-2 \cos \theta) f_x + (1+2 \cos 2\theta) f_y - 4f_{xy} \sin 2\theta$$

For an assumed unistress condition, where $f_y = 0$, we have a maximum value for f_x at $\theta = \pi/2$. Thus $f_t (\pi/2) = 3f_x$.

Thus the maximum stress concentration factor for a round hole in a plate subjected to a uniaxial stress is 3 and is independent of the hole size and the distance of the point of interest from the hole.

The recent analytical work on stress concentration factors in plates by G. H. Savin reported by W. Griffel* also gives a factor of 3 for the above case but also considers the size of the hole and the distance or location of the point of interest with respect to the hole; consequently, Savin's results are considered to be the more useful.

For a square hole theory indicates $\sqrt{2}$ as the stress concentration factor at the center (p) of a side parallel to the applied stress.

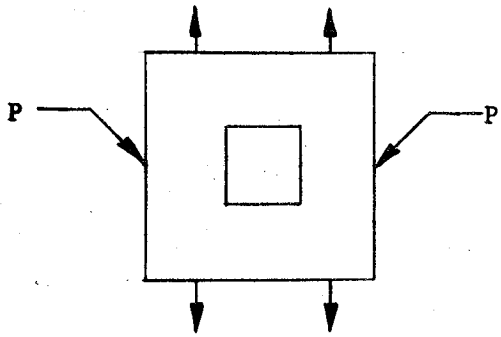

At the corners the stress concentration factor is a function of the corner radius to side length ratio, $\frac{r}{\ell}$

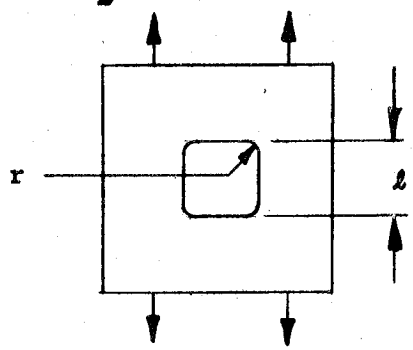

Figure 45 shows a plot of K vs $\frac{r}{\ell}$ for square and diamond holes taken from Savin's data. Table 21 and Figure 44 show the stress concentration factors for different hole shapes and locations.

For the case of a round hole near a boundary edge of the panel for the case where (distance of hole center from edge/hole radius = 2) the stress at the panel edge adjacent to the hole will be zero; at the hole boundary adjacent to the panel edge k + 3.3; at the hole boundary opposite to the panel edge K = 3.1.

*Product Engineering, 9/16/63

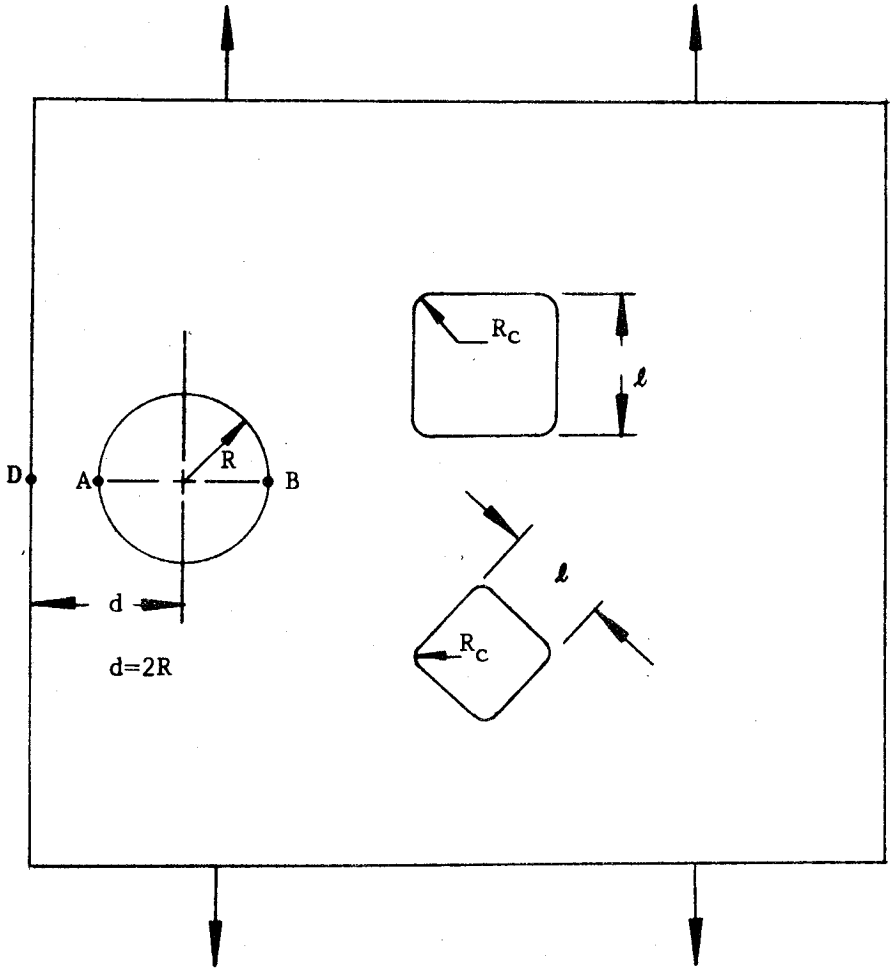

Figure 44 Hole Diagrams, Typical
(See discussion of Stress Concentration Factors, pages 98-104)

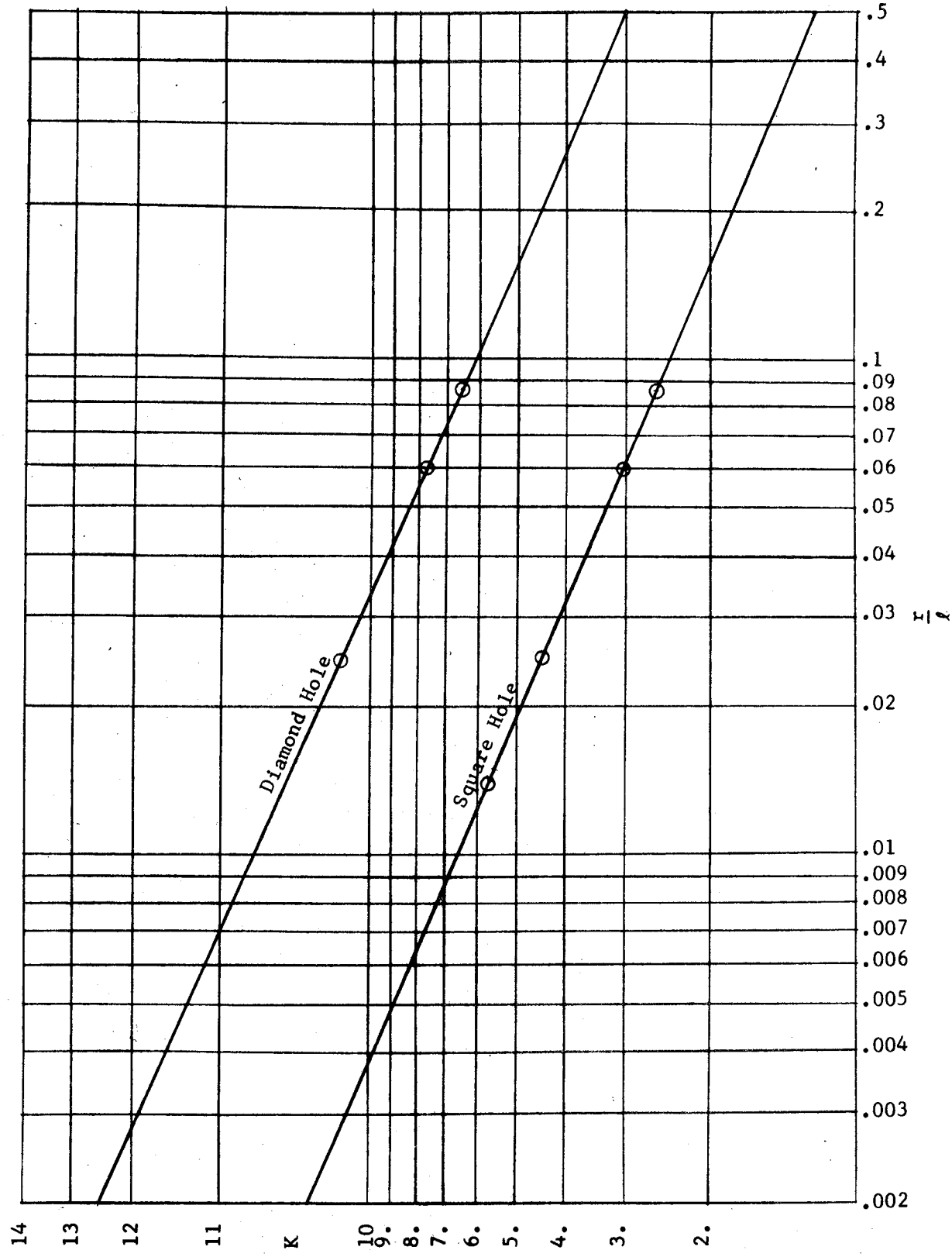

Figure 45 Stress Concentration Factor, K
at $\theta=\pi/4$ for Square and Diamond Holes

TABLE 21

VALUES OF THE STRESS CONCENTRATION FACTOR K FOR VARIOUS SHAPED HOLES WITHOUT DOUBLER UNDER A UNIAXIAL STRESS

	K at $\theta=0$	K at $\theta = \frac{\pi}{2}$	K Max. Value
Round Hole (per ANC-23)	-1	3	3
Round Hole (per G. H. Savin)	-1	3	3
Round Hole (d=2R) Near Edge per G. H. Savin	-1	3.3 at A 0 at D 3.1 at B	3.3
Square Hole R_c = .086L per	-0.828	1.645	3.3
Square Hole per G. H. Savin			
R_c = .086L	-.86	1.4	2.8 at 50°*
R_c = .06L	-.8	1.6	3.9 at 50°*
R_c = .025L	-95	1.8	4.5 at 50°*
R_c = .014L	+1.4	-.9	5.8 at 45°
Diamond Hole per G. H. Savin			
R_c = .086L	+.35	+.35	6.5 at 45°
R_c = .06L	+.4	+.4	7.8 at 45°
R_c = .025L	+.5	+.5	11.6 at 45°

*These values are 2.6; 3.1; and 4.5, respectively, at $\theta = \pi/4$ as shown in Figure 45.

When biaxial stresses are present as will be the case with the heat shield panels and the test samples, the factor for the tangential stress at the boundary of a round hole is a maximum of 4 when $f_x = f_y$, for steady state load conditions.

For dynamic loads (noise and vibration) the stress concentration factor for a round hole is approximately 2.8*.

Accordingly, the maximum stress at the boundary of a round hole with no doubler in a heat shield panel is given by:

$$f_t = 4.79 \times (4 \times 2.7 \text{ psi} + 2.8 \times 0.72 \text{ psi}) \times (48.3)^2 = 142{,}313 \text{ psi}$$

Since this value is well below the yield strength minimum of 170,000 psi and assuming 100% core to facing braze attachment in the panel area surrounding the hole, a positive margin is indicated. If the hole was located in an area of light fillets or voids, the addition of a doubler around the hole would be necessary.

Holes with Doubler Reinforcement

The stress in the facing at the boundary of a round hole with a doubler on one facing where $\frac{H_D}{H} = \frac{3}{2}$ and $\frac{R_1}{R_2} = \frac{1}{2}$ is:

$$f_{t_1} = (f_1 + f_2)\, C - 4\,(f_1 - f_2) \left[B + 3F \frac{R_1^2}{R_2^2} \right] \cos 2\theta \qquad (1)$$

H = extensional stiffness of panel, $2t_f E$

H_D = extensional stiffness of panel in doubler area, $3t_f E$

R_1 = radius of hole, inches

R_2 = outside radius of doubler, inches

f_1, f_2 = thickness of facing and doubler, respectively, inches

The stress in the facing at the junction of the doubler is given by:

$$f_{t_2} = \frac{(f_1 + f_2)}{2} (1\text{-}A) - \frac{(f_1 - f_2)}{2} (6J\text{-}1) \cos 2\theta \qquad (2)$$

The values of the parameters A - J for the the conditions set forth above are:

*Ref: Dynamical Stress Concentrations in An Elastic Plate, J. of Applied Mechanics, June 1962, pg. 304.

$$A = \frac{3\left(1 - \frac{R_1^2}{R_2^2}\right)\frac{H_D}{H} - 5\frac{R_1^2}{R_2^2} - 3}{5\left(1 - \frac{R_1^2}{R_2^2}\right)\frac{H_D}{H} + 5\frac{R_1^2}{R_2^2} + 3} = -0.886$$

$$C = \frac{8}{5\left(1 - \frac{R_1^2}{R_2^2}\right)\frac{H_D}{H} + 5\frac{R_1^2}{R_2^2} + 3} = +0.81$$

$D = +0.228$

$F = -0.5897$

$J = +0.5272$

$B = +0.423$

Thus,

$$f_{t_1} = (f_1+f_2)\ .81 - 4\ (f_1-f_2)\left[.423 - 3 \times \frac{.587}{4}\right] \cos 2\theta$$

or

$f_{t_1} = .88\ f_1$ at $\theta = 0$; $f_{t_1} = .74\ f_1$ at $\theta = \frac{\pi}{2}$; (for $f_2 = 0$)

$f_{t_1} = \underline{1.62}\ f_1$ for all values of θ when $f_1 = f_2$

For the stress in the facing at the edge of the doubler from Equation (2):

$f_{t_2} = -1.023\ f_1$ at $\theta = 0$; $f_{t_2} = -1.137\ f_1$ at $\theta = \frac{\pi}{2}$ (for $f_2 = 0$)

$f_{t_2} = 0.114\ f_1$ at all θ for $f_1 = f_2$; $f_{t_2} = 1.08$ at $\theta = \frac{\pi}{2}$ (for $f_2 = -f_1$)

Consequently, the maximum stress concentration factors tangentially for a hole with a doubler under biaxial stress conditions are:

K_{facing} =1.62 at the edge of the hole P_1 for a biaxial stress condition; and

K_{facing} =1.08 at the edge of the doubler P_2 for a biaxial stress condition.

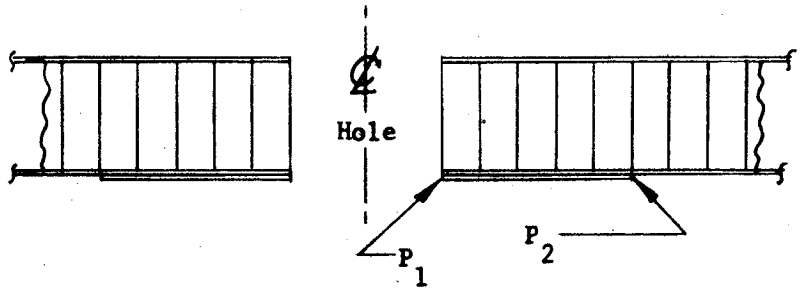

Since the biaxial factor without a doubler was 4, these results indicate the substantial reduction in peak stress values for round holes produced by the addition of a doubler framing the panel opening.

Predicted Values of Stress, Deflection, Moment, Shear Edge Loading, and Corner Reaction for the Test Panels and Heat Shield Panels (30M12571)

Test Panel Configuration:

Size--20"x30"x1.02" thick
Facings--0.010 PH15-7Mo Alloy
Core--Type 4-15 1.0" thick PH15-7Mo Alloy
Braze Alloy--Silver-Copper-Lithium

		For 30M12571 Heat Shield Panel for q = 2.7 + 0.72 psi
1. Deflection at center of test panel for q = 1 and 14 psi	$W = (.00772\ q\ a^4/D) = .0076"; .1063"$	$W = (.00406\ q\ a^4/D) = 0.469"$
2. Stress at center		
	$N_x = (8.12\ q\ a^2) = 3250; 45,500$ psi	$N_x = (4.79\ q\ a^2) = 38,350$ psi
	$N_y = (4.98\ q\ a^2) = 1995; 27,900$ psi	$N_y = (4.79\ q\ a^2) = 38,350$ psi

3. Moment at center

$$M_x = \left[.0812\ q\ a^2\right] = 32.5;\ 455\ \text{in-lb/in} \qquad M_x = \left[.0479\ q\ a^2\right] = 388\ \text{in-lb/in}$$
$$M_y = \left[.0498\ q\ a^2\right] = 19.95;\ 279\ \text{in-lb/in} \qquad M_y = \left[.0479\ q\ a^2\right] = 383\ \text{in-lb/in}$$

4. Shear at center

$$Q_x = \left[0.424\ q\ a\right] = 8.48;\ 118.7\ \text{psi} \qquad Q_x = \left[0.338\ q\ a\right] = 56\ \text{psi}$$
$$Q_y = \left[0.363\ q\ a\right] = 7.26;\ 101.6\ \text{psi} \qquad Q_y = \left[0.338\ q\ a\right] = 56\ \text{psi}$$

5. Edge Loading (on support beam) at center of side

$$V_x = \left[0.486\ q\ a\right] = 9.72;\ 136.2\ \text{psi} \qquad V_x = \left[0.420\ q\ a\right] = 69.5\ \text{psi}$$
$$V_y = \left[0.480\ q\ a\right] = 9.6;\ 134.4\ \text{psi} \qquad V_y = \left[0.420\ q\ a\right] = 69.5\ \text{psi}$$

6. Reaction at corners

$$R = \left[.085\ q\ a^2\right] = -34;\ -476\ \text{lbs.} \qquad R = \left[.065\ q\ a^2\right] = -521\ \text{lbs.}$$

NOTE: The foregoing calculations use the following equations from Timoshenko, Plates and Shells, 2nd Edition) 139, (ℓ pg 117), pg 120, pg 121, pg 122.

For comparison purposes the characteristics of the 30M12571 panel have been included. Inasmuch as the test panels will be subjected to a maximum q of 14 psi in a vacuum box, the resulting stresses, moments, etc., will be comparable to the 53"x53" 30M12571 heat shield panel (maximum conditions).

EXPERIMENTAL MEASUREMENT OF STRESS CONCENTRATIONS AT HOLE BOUNDARIES

Two identical sample panels were fabricated of the same materials, core type, facing gage and panel thickness as the heat shield panels. Size of the panels was 20"x30"x1.02 thick. A vacuum box (see Fig. 46) to simulate simple support conditions was made with the centerline of support 19"x29". It was believed that the use of corner reaction forces would overcome the slight compressibility of the support ridges around the fixture edge and thus offset the tendency of the panel to curl. Had this been successful, the calculations would have been made much simpler as the face edges would lie in a plane and the formulas and expressions for simple support edge condition would apply. However, no amount of corner reaction force would hold the edges to a straight line. This necessitated considering the deflection of the panel with all four edges elastically supported*.

Panel No. 1 was drilled to provide a 2-3/8" hole through the center. Deflection data was recorded and a second 2-3/8" hole placed near a corner with the center distant from the edge, d/R = 2. Stresscoat and deflection data were obtained. This test was repeated again with strain gage data also being taken. The center round hole was then cut out to make a square of the same size. A stresscoat pattern was obtained in the vicinity of the square hole, then deflection and strain gage data were recorded. No edge reinforcement doublers around the holes were employed. The test arrangement is shown in Figures 47 and 48. No failures of any nature in the vicinity of the holes occurred during the panel tests.

Table 22 shows the summary of the dial indicator deflection data. Dial indicator locations appear in Figure 49. The deflections tabulated for each test have been adjusted to a common value of 28.5" of mercury. The two corner indicators (No. 1 and No. 7) were used as a reference plane and the mean deflection of the five tests at the other positions on the panel were listed as the observed deflection of the panel. The value of α was then computed for each of the indicator positions other than the corners 1 and 7 for a panel aspect ratio of 1.5 with elastically supported edges. These are tabulated. The value of $q\,a^4/D$ is 13.768. The tabulated values of $W_{calc.}$ are thus 13.768α. A comparison of the observed and calculated deflections shows in general good agreement in the central panel area of greatest deflection.

The strain patterns for each condition are clearly shown in Figures 50 through 54 and particularly the areas of stress concentrations around the holes, Figures 51, 52 and 53. Stress concentration factors were determined by the comparative strains at the same points and for the same loading for the panel with holes versus the panel with no holes. Consequently, the simple ratios of hole strain

* See Theory of Plates and Shells, 2nd Ed., page 218, by Timoshenko.

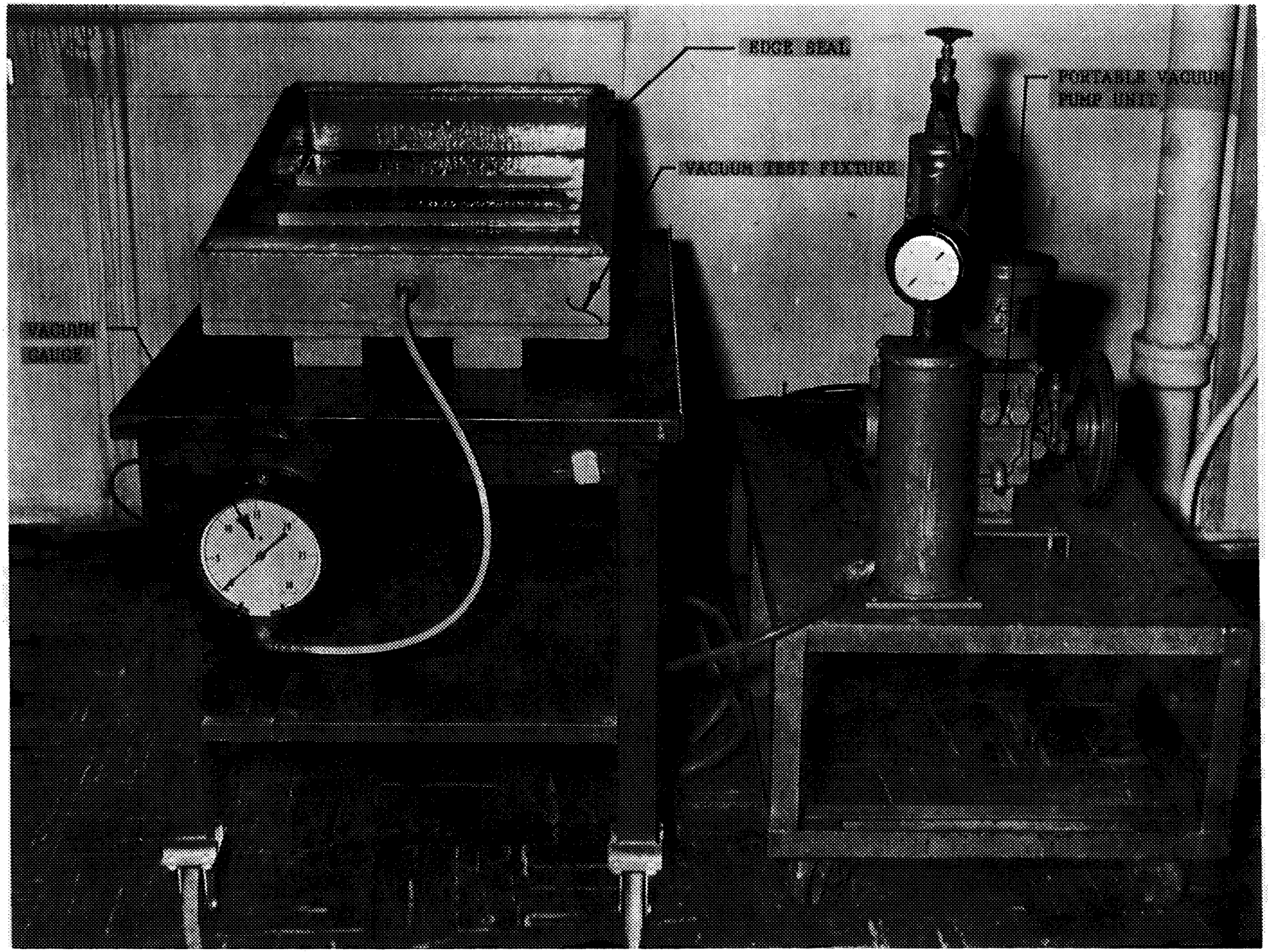

Figure 46 Vacuum Box Text Fixture

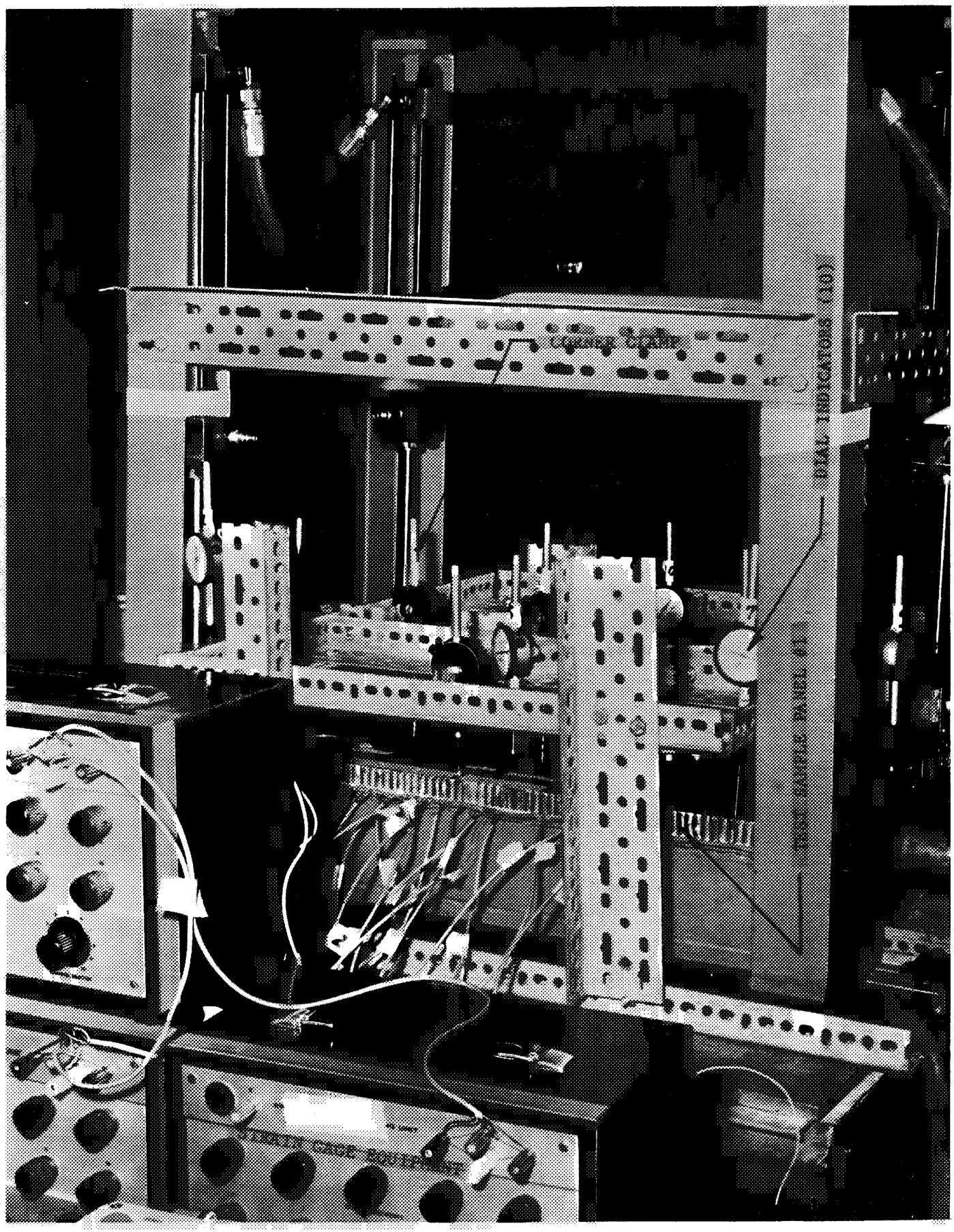

Figure 47 Side View, Test Assembly, Panel No. 1

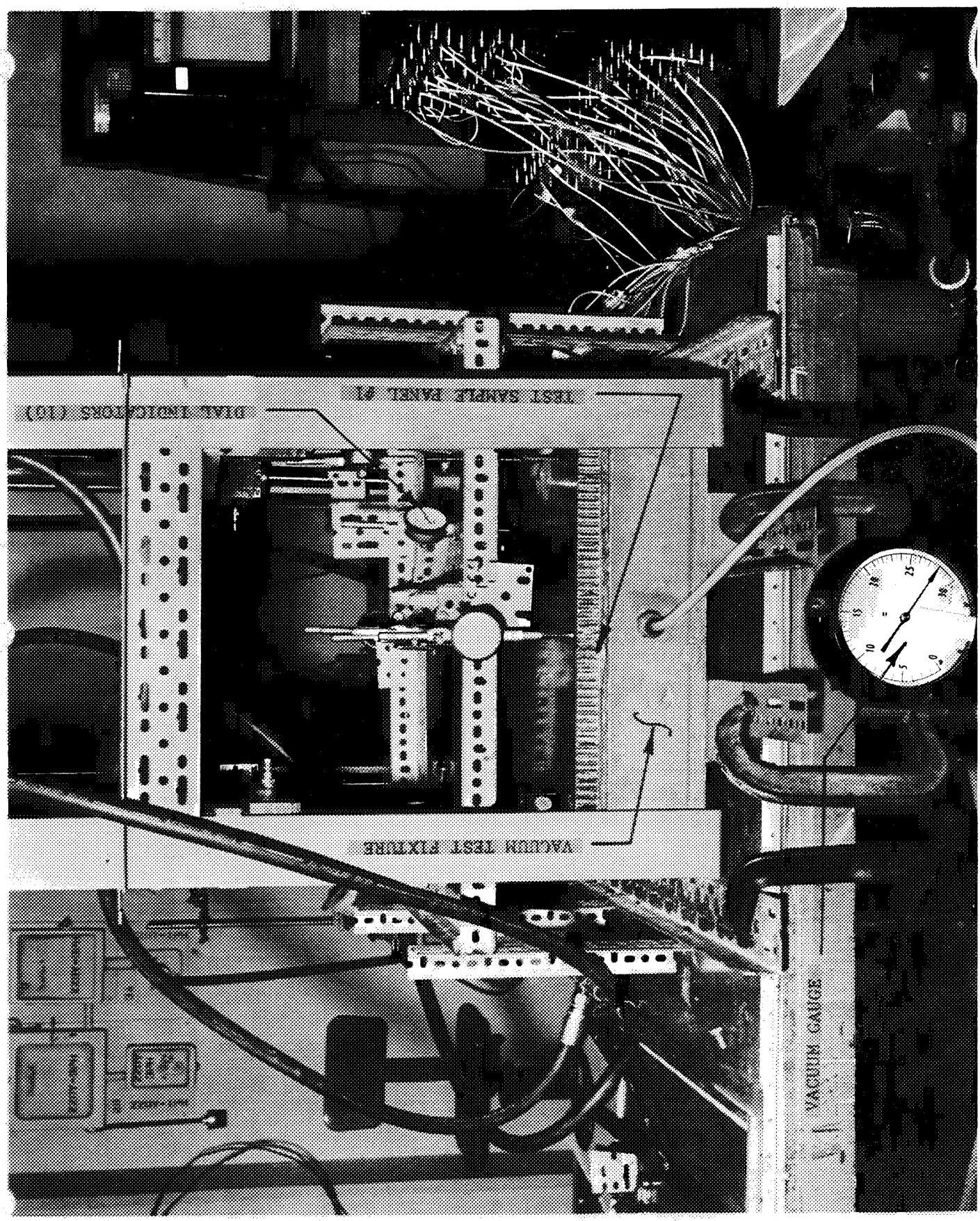

Figure 48 End View, Test Assembly

TABLE 22

TEST PANEL DEFLECTION DATA

Dial Indicator	Panel No. 1 One Hole W_{obs} for 28.5"Hg$^{\Delta}$	Panel No. 2 No Hole W_{obs} for 28.5"Hg$^{\Delta}$	Panel No. 1 Two Round Holes W_{obs} for 28.5"Hg$^{\Delta}$	Panel No. 1 Two Round Holes O_{obs} for 28.5"Hg$^{\Delta}$	Panel No. 1 One Square One Round Hole W_{obs} for 28.5"Hg$^{\Delta}$	Mean Value	$W_{obs.}$*	α calc.	$W_{calc.}$**
1	.150	.190	.211	.197	.194	.188	0	---	--
2	.205	.196	.220	.233	.220	.215	.027	.0028	.039
3	.306	.305	.327	.331	.325	.319	.136	.00996	.137
4	.347	.347	.380	.379	.383	.367	.187	.0136	.187
5	.268	.315	.322	.330	.332	.313	.133	.01026	.141
6	.222	.250	.228	.243	.239	.236	.056	.00884	.122
7	.157	.180	.165	.180	.186	.173	0	---	--
8	.306	.296	.324	.317	.328	.314	.141	.00996	.137
9	.220	.190	.211	.194	.201	.203	.030	.0028	.039
10	.356	.267	.316	.301	.303	.309	.129	.00884	.122

* W observed is net deflection below the plane established by Corners 1 and 7

** W calculated from $\frac{\alpha Q a^4}{D}$ where $\frac{Qa^4}{D} = 13.768$

Δ Inches of mercury vacuum on test fixture. Data was reduced to this value for all tests to provide a common reference value. This is an equivalent ΔP of 13.99 psi.

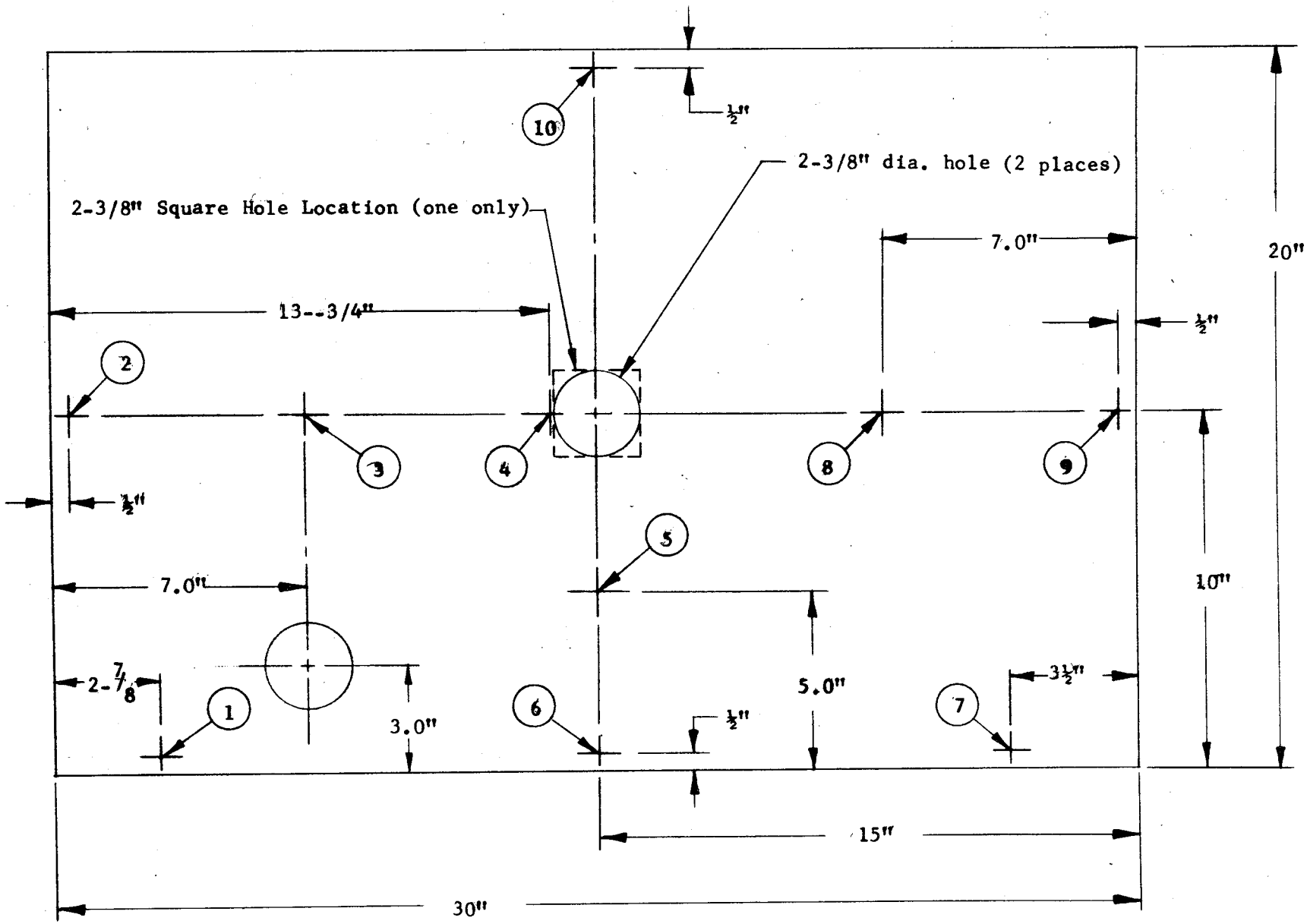

Figure 49 Dial Indicator Positions for Test Panels

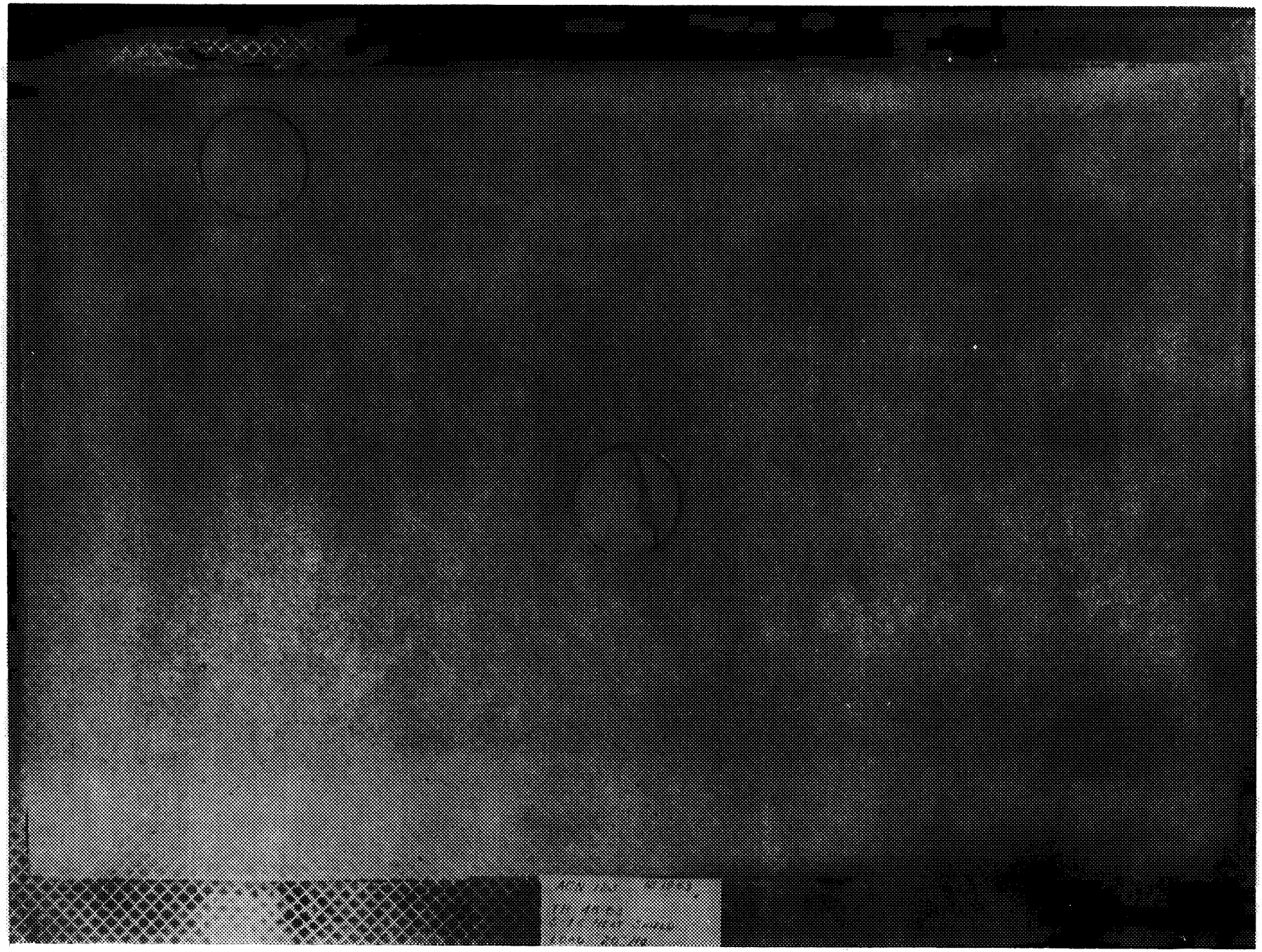

Figure 50 Stress Coat, Panel No. 1, Initial Hole Pattern

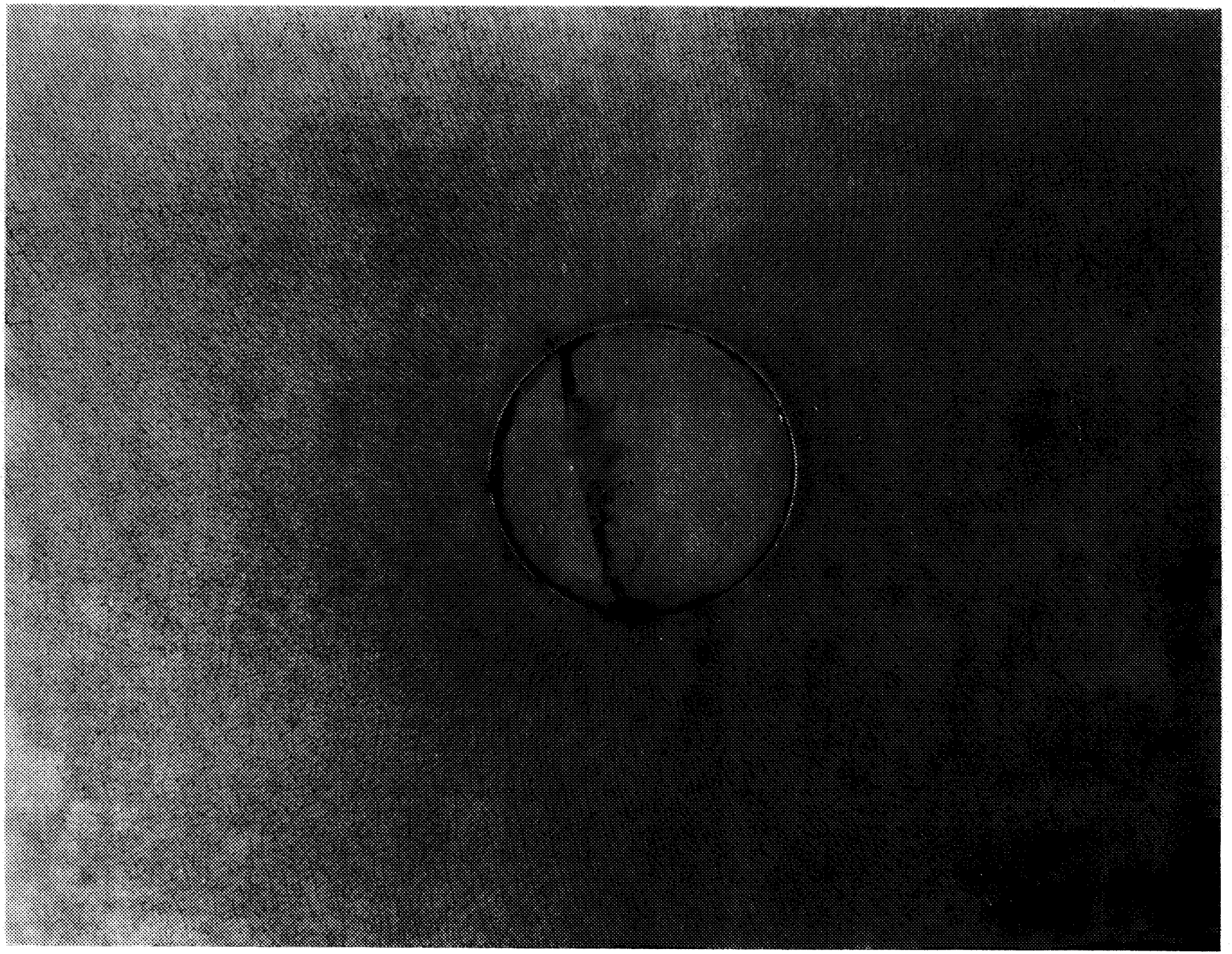

Figure 51 Center Hole Stress Coat Close-up, Panel No. 1, Initial Hole Pattern

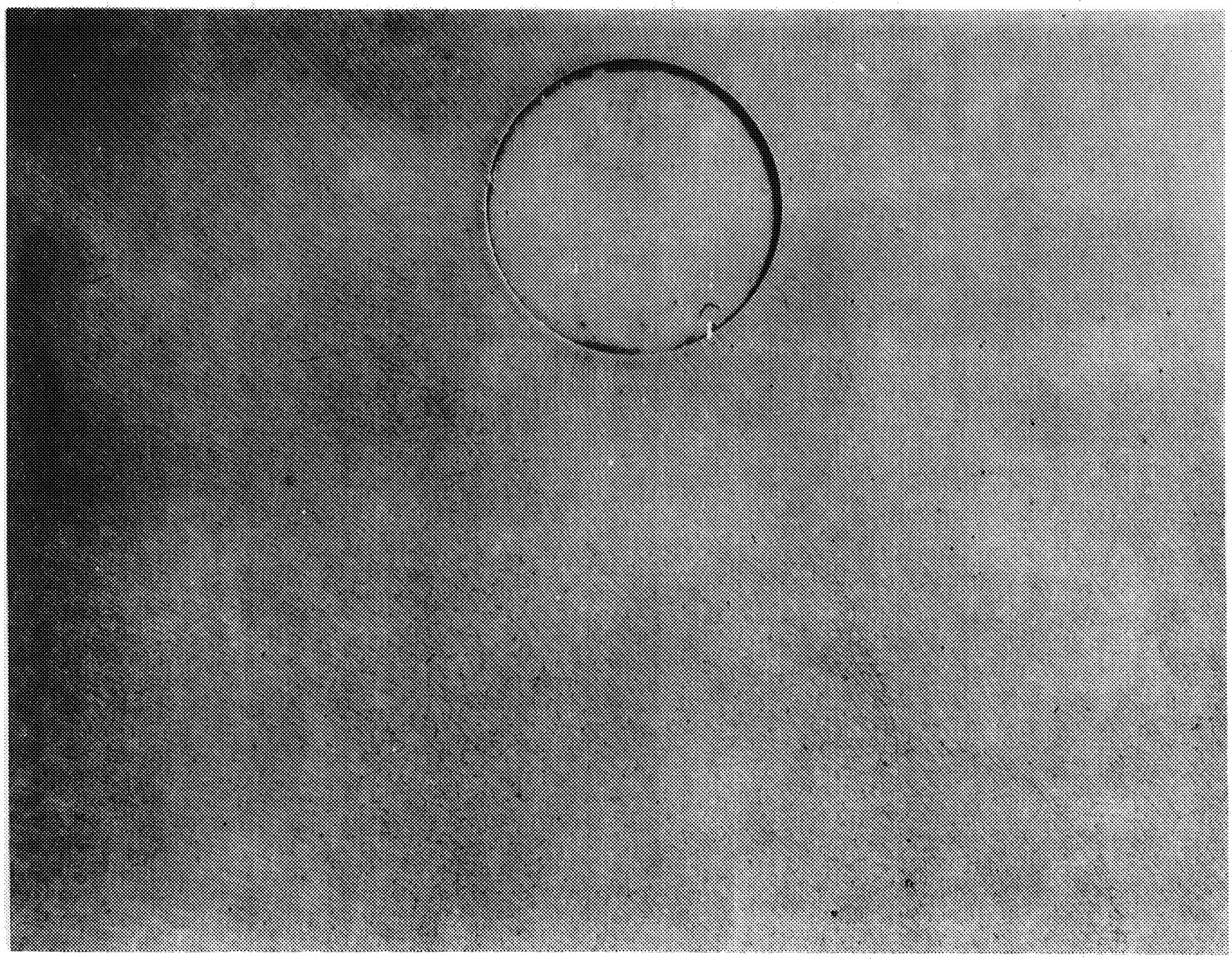

Figure 52 Edge Hole Stress Coat Close-up, Panel No. 1, Initial Hole Pattern

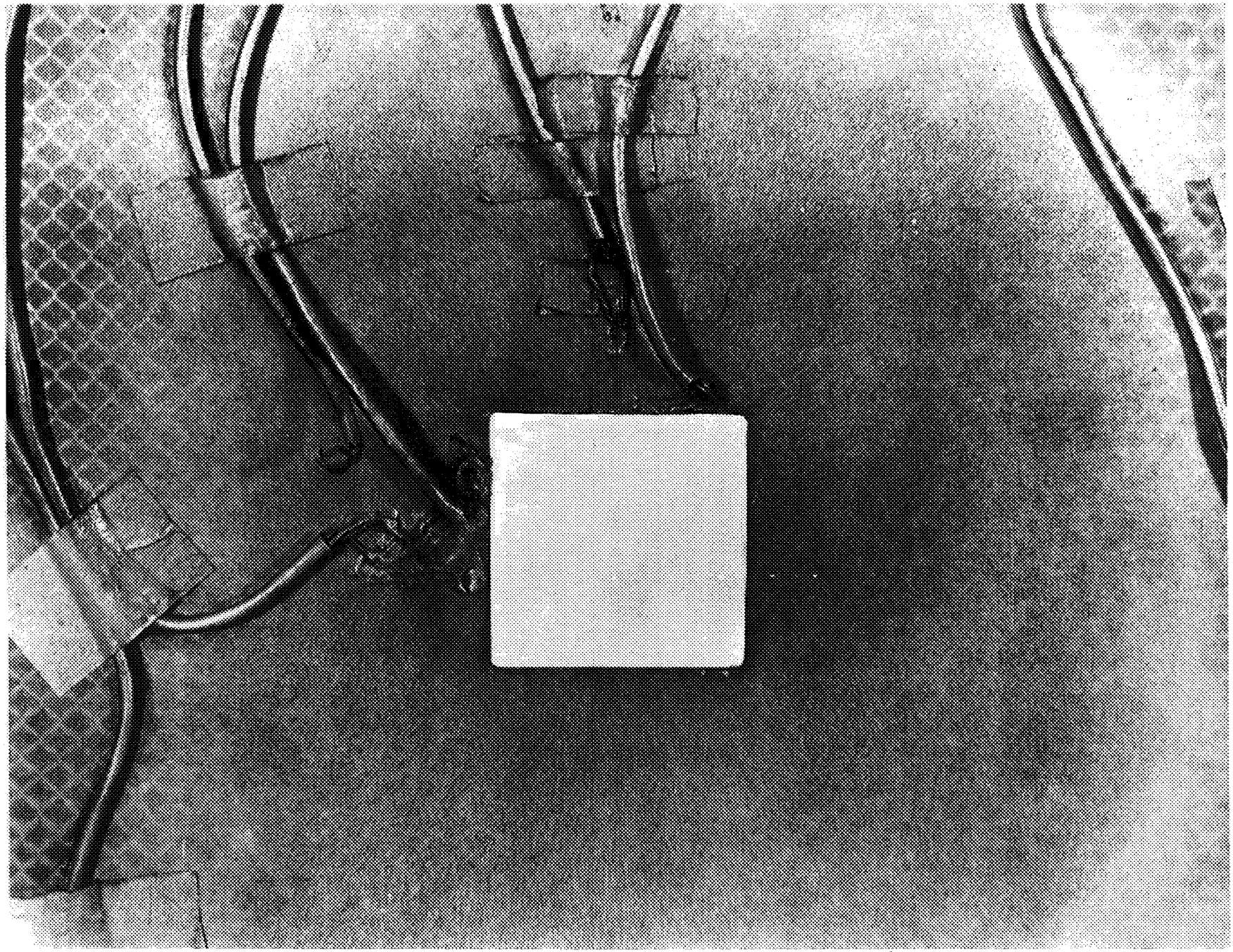

Figure 53 Center Hole Stress Coat Close-up, Panel #1 Modified Hole Pattern

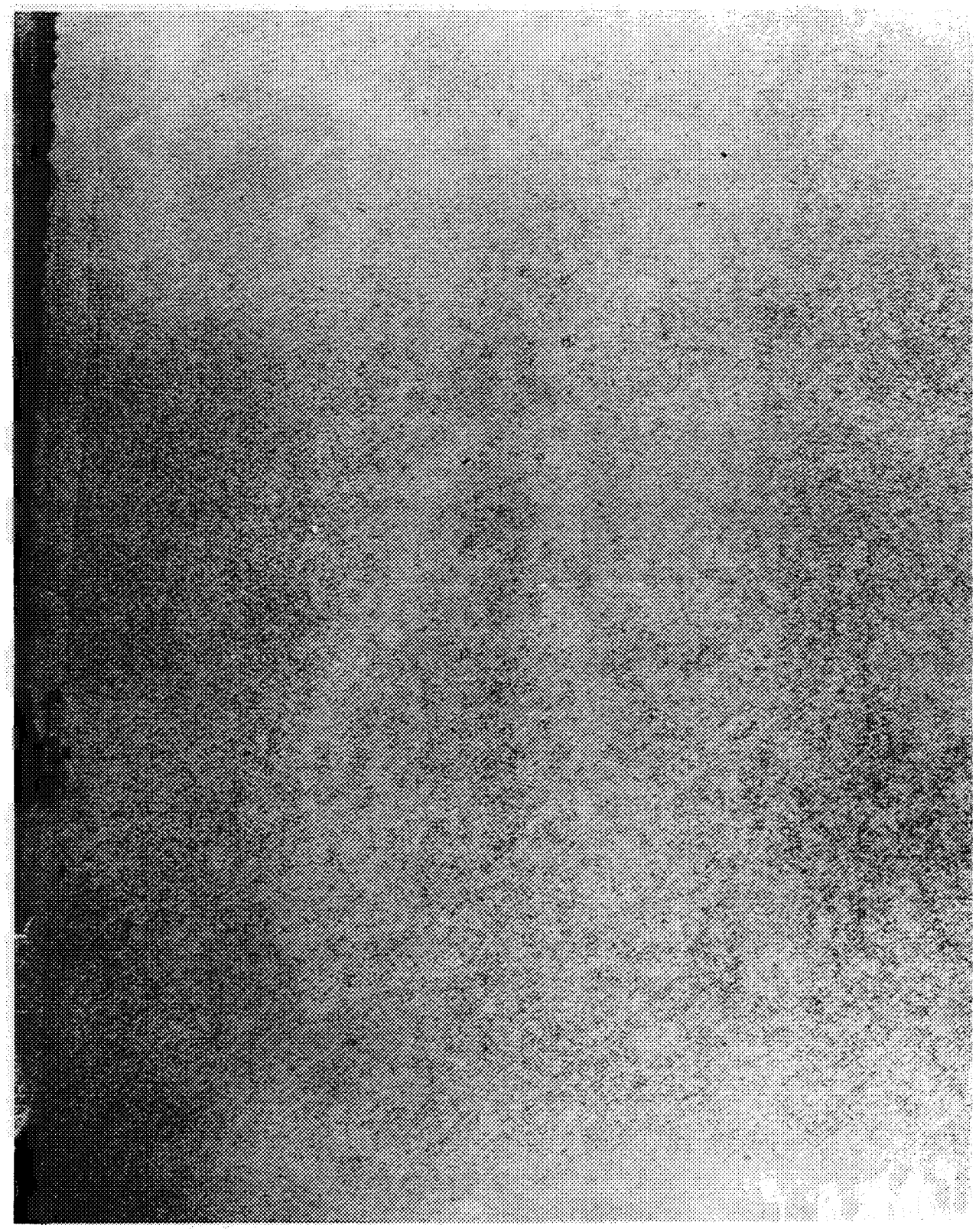

Figure 54 Panel No. 2, Stresscoat Pattern, Quarter Section View

to no hole strain at the hole boundary gives the observed stress concentration factors for biaxial loading. Theoretical values for the same hole conditions were obtained from published data. The observed and theoretical values are given in Table 23 and the agreement appears satisfactory. The desirability of round holes versus square holes is clearly shown.

Since only steady state loading conditions were evaluated while practical application includes a sizeable thermal and acoustic load, the addition of a doubler equal in thickness to the facing is recommended for all instrumentation holes. Simulated environmental testing under combined air, thermal and noise loads of a full size heat shield panel having multiple hole patterns accomplished after panel fabrication is recommended.

TABLE 23

SUMMARY OF EXPERIMENTAL AND THEORETICAL VALUES OF STRESS CONCENTRATION FACTOR K FOR BIAXIAL LOADING

Strain Gage Position**	First Test, Panel No. 1 Two Round Holes		Second Test, Panel No. 1 Square Center Hole Round Corner Hole	
	K_{theory}*	$K_{obs.}$	K_{theory}*	$K_{obs.}$
A	2.4	2.38C 2.41T	.9	.69C .85T
B	3.9	4.1 T	2.4	2.34T
C			4.5	4.7 T
D			4.5	4.25T
E			6.0	6.20T
F	3.8	3.66T		
G	3.8	3.25T		
H	2.3	1.9T	2.3	2.13T
J	3.4	3.13T	3.4	3.25T

T, Tension Side of Panel

C, Compression Side of Panel

* Theoretical values for biaxial loading from Stresses Around Holes, W. Griffel, Product Engineering 11/11/63, based on Stress Concentration Around Holes, G. N. Savin.

** See Figure 55 for locations A through J.

▭ Strain Gage Position and Direction on Face Sheet in Tension

▬ Strain Gage Position and Direction on Both Face Sheets
One in Tension and One in Compression (2 gages(

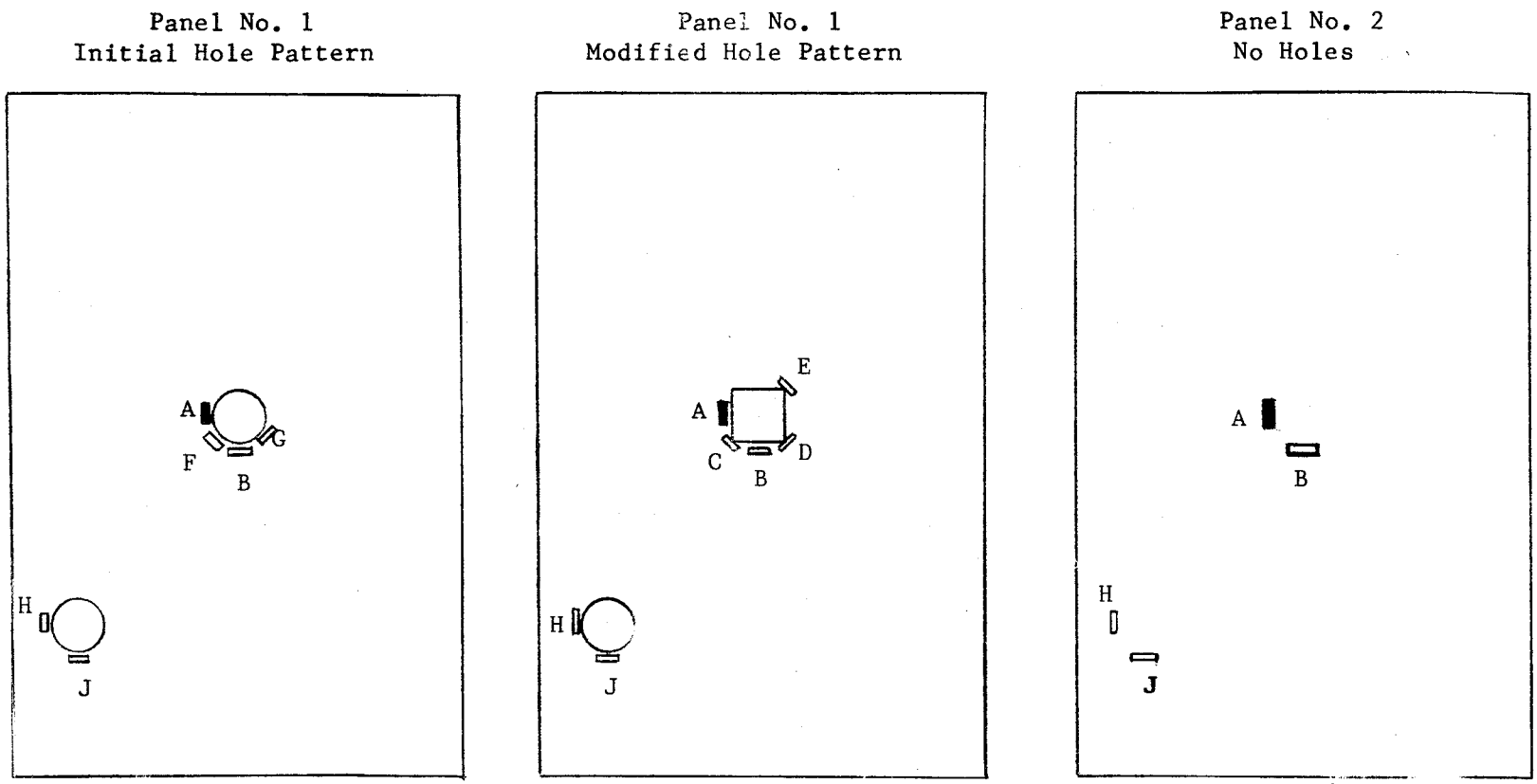

Figure 55 Strain Gage Locations on Test Panels Used for Experimental Determi[illegible] of Stress Concentration Factor, K

SECTION VIII

DESIGN RECOMMENDATIONS FOR S-1C HEAT SHIELD PANELS

The following recommended design changes for current heat shield panel designs are based on the structural analysis developed on this program and on the heat shield panel fabrication experience on Contract NAS8-6976.

1. Honeycomb Reinforcement for M-31 Insulation

Presently specified core configuration for the M-31 insulation reinforcement is Type 8-15 (½" cell size - 0.0015" foil gage). A slightly heavier core, Type 8-20 (½" cell size - 0.002" foil gage) is preferred for increased stability in the actual panel brazing as well as the core machining and panel layup operations. The greater stability of the Type 8-20 core during the brazing process will allow the use of a higher vacuum desirable to insure the fit of the panel details than the presently used 3" mercury or 1.5 psi. Likewise both the core machining and panel layup operations will benefit from the increased stability provided by the Type 8-20 core in:

a. Improving the resistance to deformation caused by shop handling

b. Reducing the time required for panel layup.

The difference in weight for the Type 8-20 versus 8-15 core (1/8" in thickness) is very slight, amounting to 0.011 lbs. per square foot or 0.21 lbs. for the 30M12571 panel.

2. Brazing Alloy Thickness for Open Faced Honeycomb Core

The 30M12571 panels produced on Contract NAS8-6976 utilized 0.002" thick brazing alloy (silver-copper-lithium) for the Type 8-15 open face core to facing attachment because of availability and prior experience on other open face honeycomb brazing applications. A thinner gage of brazing alloy, namely 0.0015", would be advantageous from a weight viewpoint (0.078 lbs/ft^2 versus 0.104 lbs/ft^2 for 0.002" braze alloy) and would provide comparable size braze fillets.

3. Welded Zee Edge Member Frame

The 30M12571 panel utilizes a one piece edge member frame fabricated as a subassembly by fusion welding four (4) zee sections at the corners followed by radiographic inspection of the welds and grinding the weld bead flush with the surface. As a consequence of the welded edge member frame, the completed panel is "sealed" with respect to the structural honeycomb core.

4. Brazed Zee Edge Member Assembly

The one piece welded edge member frame has many advantages. However, it involves expense and fabrication operations that could be eliminated by using the fully brazed edge member assembly shown in Figure 56. This arrangement, made up of four zee sections brazed together, is also fully sealed by use of a small piece of facing integrally brazed as a doubler at each corner to provide additional strength and close off the corner gap from the core. This is the assembly that is recommended.

5. Core Sealed Edge Member Assembly

For minimum cost the corner joint sealing can be accomplished with a cost savings by using the corner configuration shown in Figure 57 with a high temperature elastomeric sealer such as Coast Pro Seal 700 applied to the corner opening. This type corner joint uses four (4) separate zee sections brazed to the panel facings and eliminates the welding operation, weld fixture, radiographic inspection and weld bead machining.--It has likewise been extensively used in brazed panels for airframe application.

6. Gage Reduction for Zee Section Edge Member

An 0.030" thick zee section edge member will satisfy the design conditions and afford weight savings of approximately 5 lbs. for the 30M12571 panel configuration. The analysis for the 0.030" edge member and a comparison with the present 0.050" edge member appears in Section II, Stress Analysis.

7. Treatment of the panel edges for the cup type attachment heat shield panels, particularly for exposed panel edges such as the outboard fairing panels, will be required to protect the structural honeycomb core from thermal and mechanical damage. Presumably, this will be accomplished by completely machining out the honeycomb core approximately 1/8" from the edge of the panel facings and filling the resulting slot with M-31 insulation. It appears unlikely that the unreinforced M-31 edge fill will be retained under the severe noise and vibration environment sustained during ignition and flight. A better edge treatment would be to leave a minimum of 0.25" honeycomb on each panel face in the slot area to provide a more positive attachment for the M-31 insulation. The best edge treatment is a complete insulated metal seal.

8. The necessity for deformed or crushed open faced honeycomb core to insure the adherence of the M-31 insulation under acoustic and thermal loads was established by the NASA S-1C Heat Shield Panel Test Program. Since the initial core height on both the 30M12571 and 60B20210 panel designs was 0.125" and then further reduced by deformation or crushing to about 0.075", a thicker open faced core is clearly indicated. A thickness of 0.250" deformed to 0.180" is recommended.

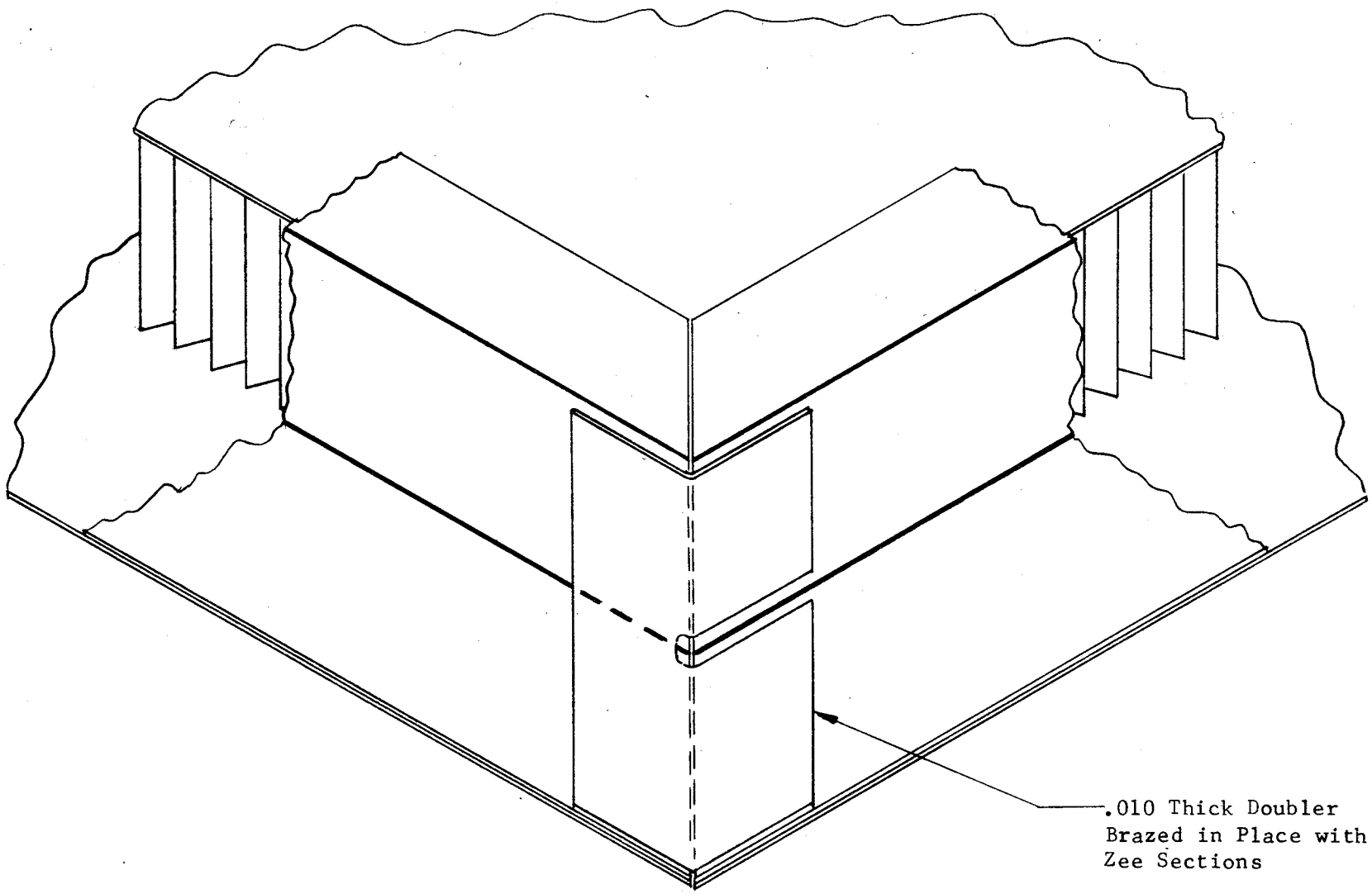

Figure 56 Recommended Zee Section Corner Joint Assembly

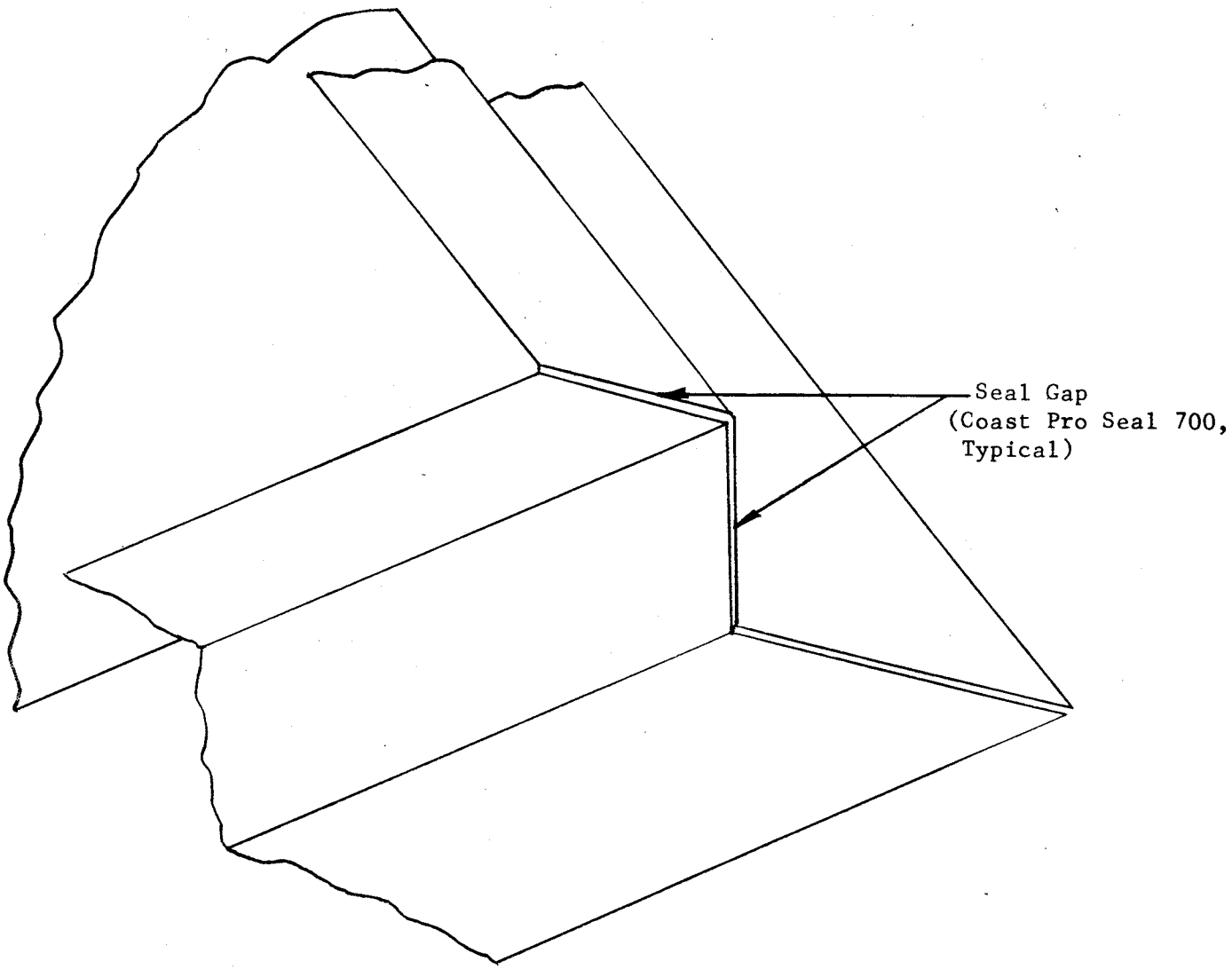

Figure 57 Economical Zee Section Corner Joint Assembly